Dissertation zur Erlangung des Doktorgrades
der Fakultät für Chemie und Pharmazie
der Ludwig-Maximilians-Universität München

A channel independent function of connexin 43 in cell migration

Juliane Viktoria Behrens

aus Wesel

2011

Erklärung

Diese Dissertation wurde im Sinne von § 13 Abs. 3 bzw. 4 der Promotionsordnung vom 29. Januar 1998 (in der Fassung der sechsten Änderungssatzung vom 16. August 2010) von Herrn Professor Dr. Ulrich Pohl betreut und von Herrn Professor Dr. Stefan Zahler von der Fakultät für Chemie und Pharmazie vertreten.

Ehrenwörtliche Versicherung

Diese Dissertation wurde selbstständig, ohne unerlaubte Hilfe erarbeitet.

München, 07.10.2011

Juliane Behrens

Dissertation eingereicht am: 07.10.2011

1. Gutachter: Prof. Dr. Stefan Zahler
2. Gutachter: Prof. Dr. Ulrich Pohl

Mündliche Prüfung am: 14.11.2011

Success in science is about combining ambition, imagination and knowledge

Table of Contents

I Introduction ... 1
1 Gap Junctions ... 1
2 Cx43 ... 4
2.1 Cx43: function as a channel and as an adapter ... 4
2.2 Proteins interacting with the C-terminal part of Cx43 ... 6
2.2.1 Cortactin ... 7
2.2.2 The nephroblastoma-overexpressed protein (NOV; CCN3) ... 8
3 Cell migration ... 9
3.1 Cell migration and actin dynamics ... 9
3.2 Role of Cx43 in cell migration ... 13
4 Aim of the study ... 15
II Materials and Methods ... 16
1 Materials ... 16
1.1 Chemicals ... 16
1.2 Cell culture ... 17
1.3 Fluorescent activated cell sorting ... 19
1.4 Migration ... 19
1.5 Cloning ... 19
1.6 Western blotting ... 21
1.7 Immunoprecipitation ... 23
1.8 Immunofluorescence ... 23
1.9 Staining of the actin cytoskeleton ... 24
1.10 Lab Equipment ... 24
2 Methods ... 26
2.1 Cell biological methods ... 26
2.1.1 Cell culture ... 26
2.1.1.1 Cell lines ... 26
2.1.1.2 Cell passaging ... 27
2.1.1.3 Cell freezing ... 27
2.1.1.4 Cell thawing ... 27
2.1.2 Lethality curve ... 28
2.1.3 Transfection of HeLa wt cells ... 28
2.1.3.1 Transient transfection of HeLa wt cells ... 28
2.1.3.2 Stable transfection of HeLa wt cells ... 29
2.1.4 Analysis of cell coupling using fluorescent activated cell sorting (FACS) ... 30
2.1.5 Analysis of cell migration ... 32
2.2 Cloning of cDNAs encoding truncated Cx43 proteins ... 34
2.2.1 Preparation of plasmid DNA ... 35
2.2.2 Polymerase chain reaction (PCR) ... 35
2.2.3 Agarose gel electrophoresis ... 37
2.2.4 Purification of the PCR product ... 38
2.2.5 Digestion of DNA with restriction enzymes ... 38
2.2.6 Isolation of DNA from agarose gels ... 39
2.2.7 DNA ligation ... 39
2.2.8 Transformation of DNA in bacteria ... 39
2.3 Protein biochemistry ... 41
2.3.1 Western blot analysis ... 41
2.3.1.1 SDS-Polyacrylamid gel electrophoresis (SDS-PAGE) ... 41
2.3.1.2 Semi-dry blotting ... 42

2.3.1.3 Protein detection by western blot analysis ... 42
2.3.1.4 Membrane stripping ... 43
2.3.2 Immunoprecipitation ... 43
2.4 Confocal laser scanning microscopy ... 45
2.4.1 Immunofluorescence staining ... 45
2.4.2 Staining of the actin cytoskeleton ... 46
2.4.2.1 Staining of migrating HeLa cells ... 47
2.4.2.2 Staining of HeLa cells after inhibition of p38 MAPK ... 47
3 Statistics ... 48
III Results ... 49
1 Generation and functional analysis of truncated Cx43 proteins ... 49
1.1 Generation and separate expression of the N-terminal and the C-terminal part of Cx43 in HeLa cells ... 49
1.2 HeLa 43NT-GFP cells were functionally coupled via gap junctions ... 52
1.3 The C-terminal part of Cx43 increases cell migration of HeLa cells ... 53
2 Generation of further truncated Cx43 proteins: ... 54
Cx43(tr298)-GFP and Cx43(tr336)-GFP ... 54
2.1 Expression of Cx43(tr298)-GFP and Cx43(tr336)-GFP in HeLa cells ... 54
2.2 Cx43(tr336)-GFP increases cell migration of HeLa cells ... 55
3 Further restriction of the migration mediating part of Cx43 ... 56
3.1 Generation and expression of a small part of the cytoplasmic tail of Cx43: Cx43(299-336)-GFP ... 56
3.2 Cx43(299-336)-GFP increases cell migration of HeLa cells ... 57
4 Analysis of protein-protein interactions of Cx43 with cortactin and NOV ... 58
4.1 Colocalization of cortactin and the C-terminal part of Cx43 in HeLa cells ... 59
4.2 The C-terminal part of Cx43 and cortactin are part of a complex ... 61
4.3 The C-terminal part of Cx43 and NOV are part of a complex ... 62
5 Influence of Cx43 on the actin cytoskeleton ... 63
5.1 Cx43 and Cx43CT-GFP increase filopodia formation in migrating cells ... 63
5.2 Inhibition of p38 MAPK decreases filopodia formation in HeLa 43 cells ... 66
5.3 Cx43(tr336)-GFP and Cx43(299-336)-GFP increase filopodia formation in migrating cells ... 67
5.4 Cx43 is localized in filopodia ... 69
IV Discussion ... 70
1 Cx43 enhances cell migration in a gap junction independent manner ... 70
2 Influences of the GFP-tag on Cx43 expression pattern, cell coupling and migration ... 73
3 Cx43 interacts with cortactin ... 74
4 Cx43 interacts with NOV ... 75
5 Cx43 influences the actin cytoskeleton ... 76
6 Inhibition of p38 MAPK influences the actin cytoskeleton ... 77
7 Future prospects ... 77
V Summary ... 80
VI References ... 81
VII Appendix ... 92
1 Abbreviations ... 92
2 Curriculum vitae ... 96
3 Acknowledgements ... 97

Index of Figures

Figure I.1: Structure of Cx43 ... 2
Figure I.2: Model of gap junction assembly ... 3
Figure I.3: Phosphorylation sites of the C-terminal part of Cx43 ... 5
Figure I.4: Process of cell migration ... 10
Figure I.5: Model of actin assembly and disassembly at the leading edge of motile cells ... 11
Figure I.6: Model of filopodia formation ... 12
Figure II.1: Principle of fluorescent activated cell sorting ... 31
Figure II.2: Hydrolysis of calcein-AM ... 31
Figure II.3: Schematic illustration of cell culture inserts (Ibidi) ... 33
Figure II.4: Experimental settings for live cell imaging ... 33
Figure II.5: Modified vector map of pcDNA4-myc-His Version B (Invitrogen) ... 34
Figure II.6: Principle of a confocal laser scanning microscope ... 45
Figure III.1: Expression of single cell clones of truncated Cx43 proteins ... 49
Figure III.2: Expression of Cx43 and truncated proteins in HeLa cells ... 50
Figure III.3: Localization of Cx43 and truncated proteins ... 51
Figure III.4: Gap junctional cell coupling of Cx43 and truncated Cx43 proteins ... 52
Figure III.5: Analysis of accumulated distance of transfected HeLa cells ... 53
Figure III.6: Expression of Cx43(tr298)-GFP and Cx43(tr336)-GFP ... 54
Figure III.7: Cx43(tr298)-GFP and Cx43(tr336)-GFP are localized in the membrane ... 55
Figure III.8: HeLa 43(tr336)-GFP cells showed increased accumulated migration distance ... 56
Figure III.9: Expression of Cx43(299-336)-GFP in HeLa cells ... 57
Figure III.10: Cx43(299-336)-GFP is localized in the cytosol ... 57
Figure III.11: HeLa 43(299-336)-GFP cells showed increased accumulated migration distances ... 58
Figure III.12: Colocalization of cortactin and Cx43 in migrating HeLa 43-GFP cells ... 59
Figure III.13: Colocalization of cortactin and the N-terminal or the C-terminal part of Cx43 in migrating HeLa cells ... 60
Figure III.14: The C-terminal part of Cx43 interacts with cortactin ... 61
Figure III.15: Both C-terminus truncated Cx43 proteins interact with cortactin ... 62
Figure III.16: Interaction of the C-terminal part of Cx43 with NOV ... 62
Figure III.17: Filopodia formation of migrating HeLa cells expressing Cx43 and truncated Cx43 proteins ... 64
Figure III.18: Length of filopodia of migrating HeLa cells expressing Cx43 and truncated Cx43 proteins ... 65
Figure III.19: Quantity of filopodia of migrating HeLa cells expressing Cx43 and truncated Cx43 proteins ... 65
Figure III.20: Filopodia formation of HeLa cells with and without addition of p38 MAPK inhibitor ... 66
Figure III.21: Quantity of filopodia of HeLa cells with and without addition of p38 MAPK inhibitor ... 67
Figure III.22: Filopodia formation of migrating HeLa cells expressing C-terminus truncated Cx43 proteins ... 68
Figure III.23: Quantity of filopodia of migrating HeLa cells expressing Cx43(tr298)-GFP, Cx43(tr336)-GFP and Cx43(299-336)-GFP ... 69
Figure III.24: Cx43 is localized in filopodia of HeLa 43 cells ... 69

Index of Tables

Table II.1: In the present study generated HeLa cell lines by stable transfection 26
Table II.2: Transfection protocol for transient transfection 29
Table II.3: Transfection protocol for stable transfection 30
Table II.4: Created cDNAs and primer pairs used for PCR; restriction enzymes for cloning; expected protein mass and number of base pairs of the cDNAs is displayed 36
Table II.5: PCR protocol 37
Table II.6: PCR settings 37
Table II.7: Protocol for digestion of the PCR product 38
Table II.8: Protocol for digestion of the pcDNA4-GFP vector 39
Table II.9: Antibodies used for western blot analysis and their dilution factors 43
Table II.10: Antibodies and appropriate protein beads used for immunoprecipitation 44
Table II.11: Antibodies used for immunofluorescence stainings and their dilution factors 46

I Introduction

The gap junction protein connexin 43 (Cx43) is one of the most ubiquitously expressed connexins in the human body [191 199 83 101]. It is important for the formation of intercellular channels to achieve communication among cells [37 199] which for example is essential for myocardial contractions. Moreover, Cx43 influences different cellular processes including cell migration [68 204 4 38] and proliferation [30 80]. Additionally, expression of Cx43 has been shown to be altered in certain processes that are associated with enhanced cell migration such as wound healing [95] or atherosclerosis [94 98 23].

1 Gap Junctions

Communication among cells in a cell assembly is essential for development, tissue repair and maintaining tissue homeostasis. Cell to cell communication can either be straight via agonists and receptors fixed at adjacent cells (juxtacrine signaling), or over short distances by growth factors or hormones (paracrine signaling), or over larger distances via neurotransmitters that are sent by nerves or via hormones (endocrine signaling). One type of direct cell to cell signaling is communication through intercellular channels, named gap junctions. Except for erythrocytes, platelets, sperms, and differentiated skeletal muscle cells, all cells show gap junctional communication (GJC) [199]. They are important for cell to cell communication in various tissues including musculature [2 180], vasculature [161 58 72 15], central nervous system [134 133] and in the kidney [60 92] and they are required for the electrical conduction in the myocard [26 162 55]. Moreover, they are involved in proliferation and differentiation, especially during embryonic development [172 16 54]. They also play a role in the immune system, as many immune and haematopoietic cells express connexin proteins and are thus able to exchange immunological information such as the presentation of antigens [139 135]. Gap junctions are clusters of channels which connect the cytoplasms of adjacent cells with each other enabling the direct exchange of ions (Na^+, K^+), metabolites (glucose, amino acids, nucleotides), second messengers (Ca^{2+}, cAMP, IP_3) and dyes (calcein) up to a molecular mass of 1.8 kilodalton (kDa) [91 83]. Larger molecules, for example siRNA with a molecular weight of 2 – 4 kDa, have also been shown to be transferred via certain gap junction channels [183]. Permeability and junctional conductance differ between gap junction channels containing various connexin proteins, for example cardiac gap junction channels composed of connexin 43 (Cx43) show five times higher permeability for the transfer of Lucifer Yellow compared to those composed of Cx40 [182]. The structure of gap junctions was first described in 1977 by Makowski using X-ray diffraction data, electron microscopy and chemical data [120]. One gap junction channel

consists of two hemichannels, named connexons, from adjacent cells [22 120]. The hemichannel in turn is composed of six connexins [22 120] and can either be assembled by only one type of connexin proteins (homomeric) or by different types of connexins (heteromeric). Moreover, the gap junction channel can either be homotypic (if the two connexons are identical) or heterotypic (if the two connexons are different) [208 199]. A certain amount of gap junction channels accumulate and constitute a gap junction plaque. Up to now 21 different connexins have been analyzed in humans [83]. They are different in protein size and are named with suffixes according to their molecular mass in kDa, which ranges from 25 to 62 kDa [40 166]. For example, Cx43 has a molecular mass of 43 kDa. The general structure is identical among all connexins. They are membrane spanning proteins containing four transmembrane domains, forming two extracellular and one intracellular loop. Both, the N-terminus and the C-terminus are intracellular [120 90 54 91]. The C-terminus differs in length and amino acid (aa) composition among the connexins [199]. As an example the structure of Cx43 is displayed in figure I.1.

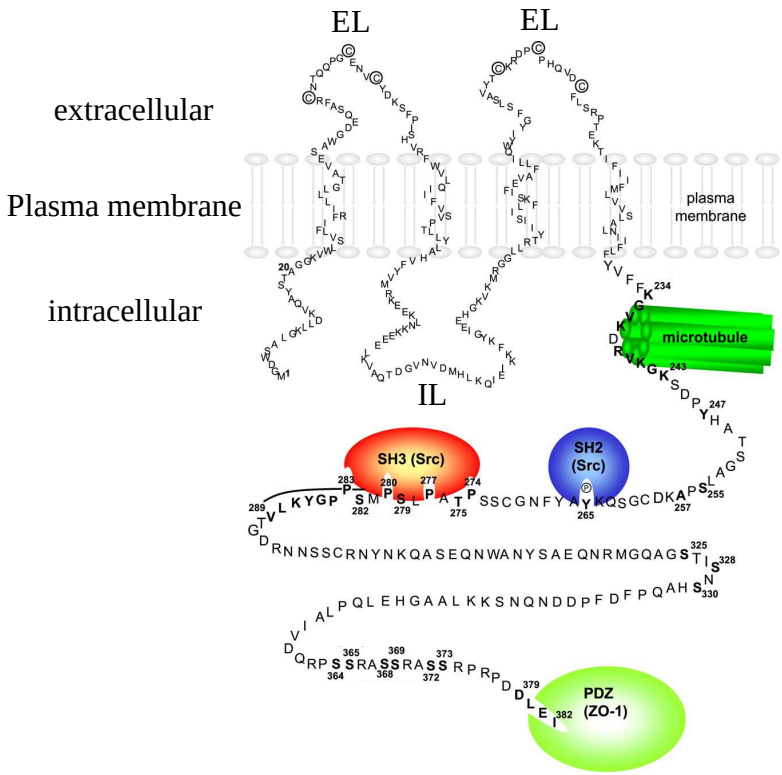

Figure I.1: Structure of Cx43
Cx43 consists of an intracellular N-terminus, four transmembrane domains, two extracellular (EL) and one intracellular loop (IL), which together represent the channel building part, and a long cytoplasmic C-terminal part (modified after [50]).

After protein synthesis, six connexins oligomerize to one connexon in the *trans*-golgi apparatus [132 91]. Afterwards, the connexons are transported via vesicles to peripheral areas of existing gap junction plaques at the plasma membrane, where they dock with connexons in the cell membrane of an adjacent cell to constitute gap junction channels. The already

assembled connexons then leave the center of the plaque via vesicles followed by proteosomal ubiquitination, whereas the newly arrived connexons are assembled in the periphery of the plaque [77 40] (Figure I.2). At the gap junction sites, the cells are only about 3.5 nm apart [120 91 208 199]. The docking between the connexons involves non-covalent interactions between their extracellular loops, which show the highest similarity in sequence among all the connexins. Nevertheless, they are able to influence the selectivity of docking between different connexons [37 198].

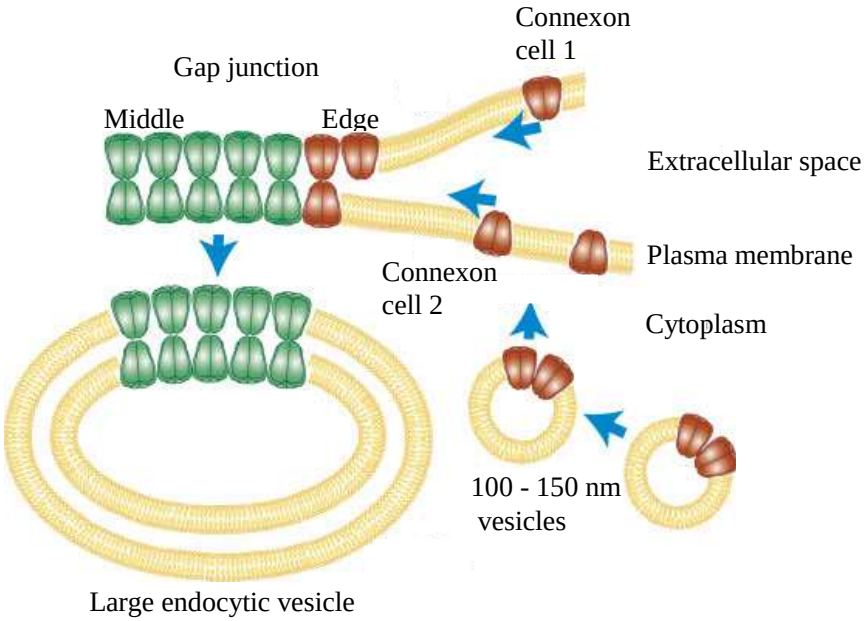

Figure I.2: Model of gap junction assembly
Connexons are transported via vesicles to the plasma membrane, where they dock with counterparts in the plasma membrane of an adjacent cell. In this process already assembled gap junction units (green) are removed from the middle of the plaque into large phagocytic vesicles and new connexons (red) are assembled in the periphery of the plaque (modified after [40]).

Gap junction channels can be regulated acutely in response to various stimuli such as changes in voltage, pH (acidification-induced closure of cardiac gap junction channels [173 33 66]) and connexin phosphorylation [106 107]. Cell coupling is also influenced by ion concentrations, as high extracellular calcium concentrations cause increased gap junctional communication [76]. There exist two models concerning the mechanisms for opening and closure of gap junction channels. Closure might either be achieved by a twist of the connexins [16] or by a blockade of the channel via the C-terminal part of the connexin, according to a ball-and-chain model [128 34]. The first model predicts that sliding of the six connexin subunits against each other in one hemichannel and tilting at one end causes a rotation at the base in a clockwise direction and consequently closure of the channel [181 199]. In the ball-and-chain model, the C-terminal part of the connexin protein moves toward the channel pore and binds to specific aa residues thereby closing it. In this context, the presence of a histidine residue at position 95 is essential, which

may be part of the receptor to which the C-terminus binds, presumably after protonation of the histidine [128].

Mutations of connexins play a role in several diseases [197]. For example, mutations in the Cx43 gene in humans are associated with oculodentodigital dysplasia, which is an autosomal dominant syndrome and exhibits craniofacial (ocular, nasal, and dental) as well as limb dysmorphisms, spastic paraplegia, and neurodegeneration [141].

2 Cx43

One of the most ubiquitously expressed connexins in mammalian and non-mammalian cells is Cx43 with a molecular mass of 43 kDa [191 199 83 101]. The protein consists of 382 aa [10] and the structure is analogous to the other connexin proteins [104]. However, the cytoplasmic C-terminus is longer than in most other connexins [106]. The sequence homology of Cx43 between the different species is very high. Thus, it only differs in six aa between mammals and non-mammals [185] and Cx43 of human, rat and mouse are completely homologous [10 44 200 199]. In mammalian species it is highly expressed in the ventricular myocardium, where it is responsible for the synchronization of myocardial contractions [26 162 55]. Consequently, specific deletion of Cx43 in mouse myocardium results in arrhythmia [57 166]. The half-life of Cx43 in the plasma membrane is very short, about 1 – 3 h [129 103], required for a dynamic regulation of GJC. Besides being important for intercellular communication, Cx43 also influences different cellular processes such as cell migration [68 204 4 38], which will be described in detail in chapter I.3.2, and proliferation [30 80]. Several studies indicate that Cx43 decreases cell proliferation. Thus, overexpression of Cx43 reduces the proliferation rate in several tumor cells, for example in Neuro2A [126], in C6 glioma [210], and in mouse MCA-10 cells [159].

As Cx43 is an essential protein, Cx43 knockout (KO) mice die at birth due to conotruncal heart malformations that lead to obstruction of the right ventricular outflow tract of the heart and consequently prevents the regular blood flow into the lungs, which in turn causes right ventricular failure [154 69 212]. These malformations may be due to a reduced migration of cardiac neural crest cells observed in embryogenesis [116]. On the contrary, overexpression of Cx43 in neural crest cells causes embryonic cranial neural tube defects and heart malformations which are different from those in Cx43-deficient mice [115 41 207].

2.1 Cx43: function as a channel and as an adapter

Cx43 is important for the formation of gap junction channels to achieve GJC. The dynamic GJC is regulated by changes in voltage, ion concentrations and pH, which have been

mentioned above. Moreover, phosphorylation of the connexins by several protein kinases [93 96 97 106 107 108 167] are important for the regulation of GJC. These phosphorylation events can increase or decrease the permeability of gap junction channels or affect their assembly and disassembly. Phosphorylation of Cx43 seems to occur only at the cytoplasmic C-terminus as the intracellular loop region does not contain any known sequences, which could be phosphorylated, and phosphorylation of the N-terminal region of connexins has also not yet been reported [106 107]. Phosphorylation of Cx43 differs through its life cycle [152 167]. Cx43 is translated as a non-phosphorylated 42 kDa protein (Cx43-NP), which is then posttranslationally phosphorylated primarily resulting in a 44 kDa protein (Cx43-P1) and subsequently in a 46 kDa protein (Cx43-P2) [129]. Cx43-P2 is exclusively found in gap junction plaques, whereas Cx43-NP is predominantly localized in the cytosol [131]. In western blot analysis the Cx43 protein appears as a triple band, which results in one band after alkaline phosphatase treatment, suggesting that phosphorylation of Cx43 is one reason for these different Cx43 forms [130]. However, 2 – 4 kDa (2000 – 4000 Da) shifts cannot appear only due to phosphorylation (mass of phosphate 80 Da), but rather seem to be specific phosphorylation events, which lead to conformational changes [105 169]. Mainly serine, tyrosine, proline and threonine residues get phosphorylated [106 107] and known phosphorylation sites exist for various kinases, including v-Src, mitogen-activated protein kinases (MAPKs), protein kinase C (PKC), protein kinase A (PKA) and casein kinase 1 (CK1) (Figure I.3) [106 107]. For example, phosphorylation by PKA increases GJC by upregulating connexon trafficking and assembly into the membrane, whereas PKC decreases GJC by phosphorylation of Ser368 and consequent channel closure [108 156].

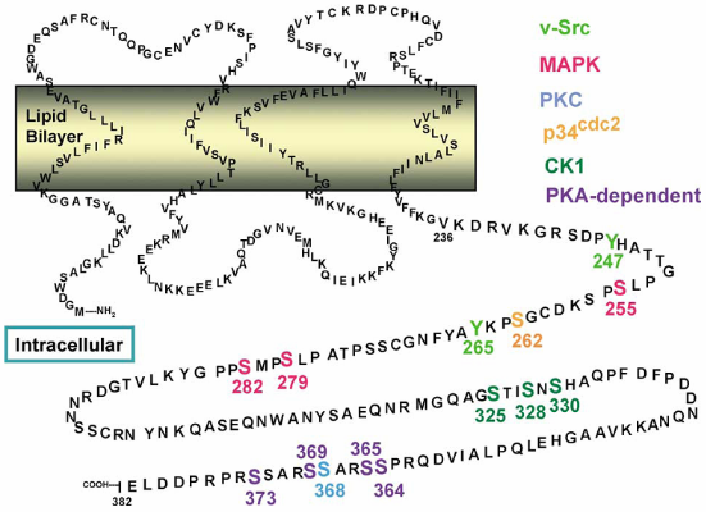

Figure I.3: Phosphorylation sites of the C-terminal part of Cx43
The C-terminal part of Cx43 is phosphorylated at several serine and threonine residues by various protein kinases, including v-Src, mitogen-activated protein kinase (MAPK), protein kinase C (PKC) and casein kinase 1 (CK1) (from [107]).

Among all connexins Cx26 is the only one which has not been shown to be phosphorylated presumably due to its short cytoplasmic tail [179]. This fact shows that phosphorylation is not principally required for the formation of functional gap junction channels, but rather can improve or decrease channel opening dependent on the specific phosphorylation site. Dunham et al. analyzed the functional channel forming capacity of truncated Cx43 variants, lacking the C-terminal part, by dual voltage-clamp technique in oocytes and showed that at least aa 1 – 257 of Cx43 are required for the formation of functional gap junction channels [35]. Thus, truncated Cx43 variants are able to form functional channels, but permeability and electrophysiological properties differ from those formed by full length Cx43. This is confirmed by the fact that truncation of the C-terminal part of Cx43 after aa 257 leads to a loss of pH sensitive channel gating [128]. Interestingly, the pH sensitivity can be restored by an additional expression of the C-terminus alone [128].

Besides its channel forming capacity, Cx43 also seems to have an important role as an adapter protein as there are several known protein-protein interaction domains on the C-terminal part that lead to further regulatory events [106 108 107 50 51]. Structural models of Cx43 revealed that the fourth transmembrane domain ends at about aa 230 and consequently the cytosolic C-terminal part consists of nearly 150 aa [168]. It contains two α-helical structures at Ala311 – Ser325 and at Asp339 – Lys345 [170 171].

Concerning the growth inhibition effect of Cx43 mentioned above, several studies aimed to identify whether this is dependent on the channel forming capacity of Cx43 or on its function as an adapter protein. In this context, Moorby and Patel could show that blocking of Cx43 gap junction channels by 1-heptanol in 3T3 cells resulted in similar inhibition of cell growth compared to expression of non-blocked Cx43 gap junction channels [126], indicating that a functional channel is not required for this effect. Further on, expression of the C-terminal part alone in Neuro2A cells [126] and in HeLa cells [30], which both do not express Cx43 in their wild-type forms, revealed the same growth inhibition compared to expression of the full length Cx43. This effect might be caused by nuclear localization of the C-terminus [30]. Those studies demonstrate that Cx43 has gap junction independent effects on cell growth [126]. Whether the influences on cell migration by Cx43 are gap junction dependent or independent will be explained in chapter I.3.2 and is part of the present study.

2.2 Proteins interacting with the C-terminal part of Cx43

Several proteins have been shown to interact with the C-terminal part of Cx43 [50], including actin-binding proteins, such as α-actinin and drebrin [20 204]; adhesion proteins, such as E-

cadherin [46], N-cadherin [64] or Zonula occludens-1 (ZO-1) [70]; and proteins that influence cell proliferation and migration such as cortactin [174] and the nephroblastoma overexpressed protein (NOV) [123 45 48]. In the present study we focused on the two proteins cortactin and NOV, which both on the one hand show interaction with Cx43 and on the other hand interact with the actin cytoskeleton, consequently influencing cell migration and thus represent a potential link between Cx43 and increased cell migration.

2.2.1 Cortactin

The actin binding protein cortactin (previously termed p80/p85 protein) is a 65 kDa protein and was originally characterized as a tyrosine phosphorylated substrate in v-Src-transformed chicken embryo fibroblast [79 203]. In SDS-PAGE it migrates as an 80/85 kDa doublet. The reason for the discrepancy between calculated mass and observed molecular mass in SDS-PAGE is unclear [202]. Cortactin is present in multiple cell types and its expression is enhanced in actin-rich cellular protrusions, namely lamellipodia, of migrating cells and cell-substratum adhesion sites of adherent cells [202 194]. Co-staining studies using Alexa Fluor-coupled phalloidin, which stains F-actin filaments, and cortactin antibody revealed colocalization of cortactin and F-actin in the peripheral cortical region [202]. Further experiments showed that cortactin binds efficiently to F-actin due to direct interaction between its fourth tandem repeat region and actin [1].

In unstimulated cells, cortactin is present in the cytoplasm as a non-phosphorylated protein [62], whereas in response to growth factor stimulation (EGF, FGF or PDGF), it is phosphorylated at tyrosine residues and translocates to the cell membrane [203 36 201 62].

Cortactin consists of several distinct domains including an N-terminal acidic domain (NTA) and a series of six complete and one partially repeated segments (called the repeat region) [1]. At the end of the C-terminus there is a Src homology 3 (SH3) domain, which interacts with proline-rich regions of several cortactin-interacting proteins [202 1], including neuronal Wiscott-Aldrich syndrome protein (N-WASP) [192], WASP-interacting protein (WIP) [84], and dynamin 2 [124]. Thus, at the SH3 domain cortactin binds to and activates N-WASP [87] and at the NTA region (aa 1 – 84) it binds to the actin-related protein 3 (Arp3) and subsequently activates the Arp2/3 complex [194 192]. The Arp2/3 complex is important for the nucleation of new actin filaments [11 196 86] and leads to the formation of actin-rich protrusions, including invadopodia and lamellipodia at the leading edge of migrating cells [28]. As formation of these actin protrusions is the initial step of directional cell migration, cortactin also enhances cell migration [17 65]. Moreover, it has been described as a regulator for tumor cell invasion [28],

which depends on the formation of invadopodia and is associated with extracellular matrix (ECM) degradation. In this context matrix metalloproteinases (MMPs) play a crucial role [113] [53], as they can degrade components of the ECM, including collagen, laminin, fibronectin, vitronectin, elastin, and proteoglycans [158]. By regulating the secretion of several MMPs, such as MMP-2, MMP-9, and membrane type-1 matrix metalloproteinase (MT1-MMP), cortactin is involved in cancer cell invasion [28]. MMP-2 and MMP-9 are type IV collagenases [158] and are also expressed in HeLa cells [209], which were used in the present study.
Furthermore, cortactin interacts with Cx43 [174] and might therefore be a link between Cx43 and the cytoskeleton. However, which part of Cx43 interacts with cortactin is not known yet. In the present study we therefore wanted to observe the part of Cx43 binding to cortactin and whether this influences cell migration in HeLa cells.

2.2.2 The nephroblastoma-overexpressed protein (NOV; CCN3)

The 48 kDa nephroblastoma-overexpressed protein (NOV; CCN3) is one member of the CCN protein family. The name CCN originates from the first three identified members of this family namely connective tissue growth factor (CTGF), cysteine-rich (CYR61) and NOV. Therefore, NOV is also named CCN3 [13] [109]. The CCN protein family consists of six members, which are involved in cell proliferation, migration, and differentiation. Moreover, they are important for angiogenesis, chondrogenesis, and wound healing [14] [109] [146] [148]. NOV is expressed in a wide variety of tissues including lung, heart, liver, endothelium, and muscle [146]. NOV was discovered as an overexpressed gene in nephroblastomas induced by the myeloblastosis-associated virus type 1 (MAV-1) in one day old chickens [121] [75]. However, it was also the first CCN protein, shown to exhibit antiproliferative activity in tumors due to aberrant expression [146]. An N-terminal truncated 31/32 kDa isoform of NOV was detected in the nucleus of HeLa cells and osteosarcoma cells and showed interaction with RNA polymerase II [145] [146], thus it might modulate gene expression during normal development, but can as well function as a growth suppressor gene by blocking cells in the cell cycle [145] [146]. Moreover, NOV is involved in cell migration and remodeling of the actin cytoskeleton. It promotes cell migration by different mechanisms which seem to be cell-type specific. Thus, in sarcoma cells enhanced cell migration by NOV is associated with increased expression of MMP-9 at the cell surface [7], whereas in glioblastoma cells expression of MMP-3 is increased [110]. In the breast cancer cell line MDA-MB-231 NOV enhances cell migration by reorganization of the actin cytoskeleton with formation of cortical actin-rich membrane protrusions, namely lamellipodia, which might be due to activation of the small GTPase Rac1,

that is increased in these membrane protrusions [165]. Besides intracellular localization, NOV can also be found extracellularly due to a signal peptide allowing secretion of the protein [148]. Thereby, it binds directly to specific integrin receptors and can influence cell adhesion e.g. via the integrins $\alpha_6\beta_1$, $\alpha_v\beta_3$, and $\alpha_5\beta_1$ in human venous endothelial cells (HUVEC) as well as cell migration e.g. via the integrins $\alpha_v\beta_3$ and $\alpha_5\beta_1$ in endothelial cells [112].

It has been assumed that NOV interacts with Cx43, as overexpression of NOV in certain tumors is associated with a growth inhibitory effect [146] and, likewise, overexpression of Cx43 reduces the proliferation rate in several tumor cells as mentioned above. Indeed, confocal microscopy studies revealed that NOV colocalizes with Cx43 at the cell membrane [123]. Later on, glutathione S-transferase pull-down assays and co-immunoprecipitation studies showed that NOV directly interacts with Cx43, namely at its C-terminal part observed with differently truncated Cx43 proteins in C6 glioma cells (aa 244 – 382) [45] and in Jeg3 cells (aa 257 – 382) [48]. In this context it was also shown that Cx43 recruits NOV to gap junctional plaques, where they interact with each other [45]. In addition, expression and also secretion of NOV is increased in the carcinoma cell lines C6 glioma [45] and Jeg3 [48] after transfection with Cx43. This increase might either be due to enhanced transcription or prevented degradation of NOV [45]. Thus, it has been supposed that the tumor-suppressive and antiproliferative effects of Cx43 are associated with the increased expression of NOV [45] [48]. Recently, another group created different deletion mutants of the C-terminal part of Cx43 and could further specify the NOV binding sequence on the C-terminus of Cx43 to aa 260 – 340 [165]. In addition, this study revealed that NOV links Cx43 to the actin cytoskeleton, which might cause the influence of Cx43 on cell migration [165]. Therefore, we wanted to clearly specify the sequence on the C-terminus at which NOV binds to and analyze whether this interaction could influence cell migration in HeLa cells.

3 Cell migration

Cell motility and directional cell migration are essential for various physiological processes including embryonic morphogenesis, tissue repair as well as regeneration and immune surveillance [157]. Moreover, they play a role in disease states, such as tumor invasion and metastasis [157].

3.1 Cell migration and actin dynamics

Cell migration is a complex process starting with cell polarization and followed by formation of membranous protrusions at the leading edge, which can either be broad lamellipodia or

spike-like filopodia or a combination of both. These protrusions are driven by actin polymerization. In lamellipodia the actin filaments form a branched network, whereas in filopodia they show long parallel bundles [157]. Cell migration continues with attachment of the lamella to the substratum, followed by forward translocation of the cell body and detachment of adhesions and subsequent retraction of the cell rear [157] (Figure I.4).

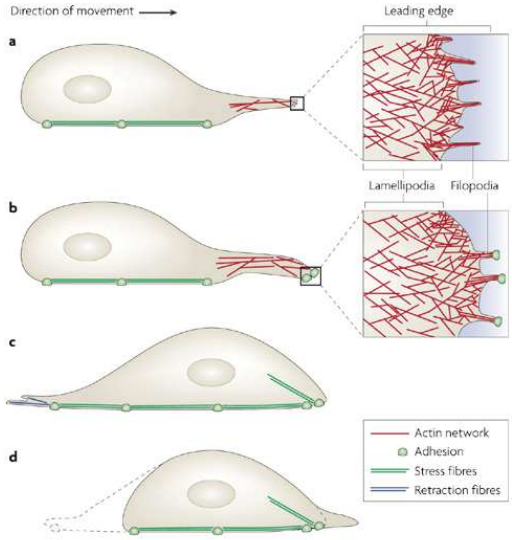

Figure I.4: Process of cell migration
(a) Cell migration starts with cell polarization and formation of actin-dependent protrusions, namely broad lamellipodia and finger-like filopodia, at the leading edge. (b) The cell extends and forms new adhesions with the substratum under the leading edge and (c) consequently the cell body translocates forward through actomyosin-based contraction forces. (d) Retraction fibers pull the rear of the cell forward leading to disassembly of adhesions at the cell rear and retracting of the trailing edge (from [122]).

The cytoskeleton of cells consists mainly of actin and plays the major role during cell migration. Two forms of actin exist in the cell, on the one hand monomeric, globular actin (G-actin) and, on the other hand, filamentous actin (F-actin). G-actin polymerizes by the hydrolysis of ATP and release of inorganic phosphate (P_i) to F-actin. Actin filaments are polarized and consist of a fast-growing (barbed) and a slow-growing (pointed) end. Polymerization mainly takes place at the fast-growing end [196]. The protein profilin binds ATP-actin monomers and thus maintains a pool of G-actin within the cell. Moreover, it inhibits spontaneous actin nucleation and secures that the actin monomers associate only with barbed ends but not with pointed ends of existing actin filaments [11]. Free barbed ends are required for actin assembly, which can either be created by uncapping or cutting of pre-existing filaments or by de novo filament nucleation [150 196]. The protein complex, which is responsible for this nucleation process, is the Arp2/3 complex. It consists of seven subunits including the actin-related proteins Arp2 and Arp3 [11 150 151]. The process of actin assembly and disassembly is displayed in figure I.5. In response to extracellular stimuli, such as chemotactic factors, the Rho family of small GTP-binding proteins (GTPases) is activated,

which subsequently leads to an activation of the Wiscott Aldrich syndrome protein/Suppressor of cAMP-receptor (WASP/Scar) family proteins. These in turn activate the Arp2/3 complex, which initiates assembly of a new actin filament by nucleation. The new barbed end is elongated using the profilin bound ATP-actin pool. The growing filament then pushes forward the plasma membrane until elongation is stopped by binding of capping protein. This process of actin assembly results in a branched actin network, which is seen in lamellipodia [21 12 11 151]. Disassembly of the actin filament is initiated by the actin depolymerization factor (ADF)/cofilin complex, which catalyzes the hydrolysis of ATP and release of phosphate. Consequently, the actin branch dissociates from the existing actin filament. To decelerate the disassembly of actin filaments, the GTPase Rac1 can also activate p21-activated protein kinase (PAK), which consequently leads to phosphorylation and inactivation of ADF/cofilin [21 12 11 151].

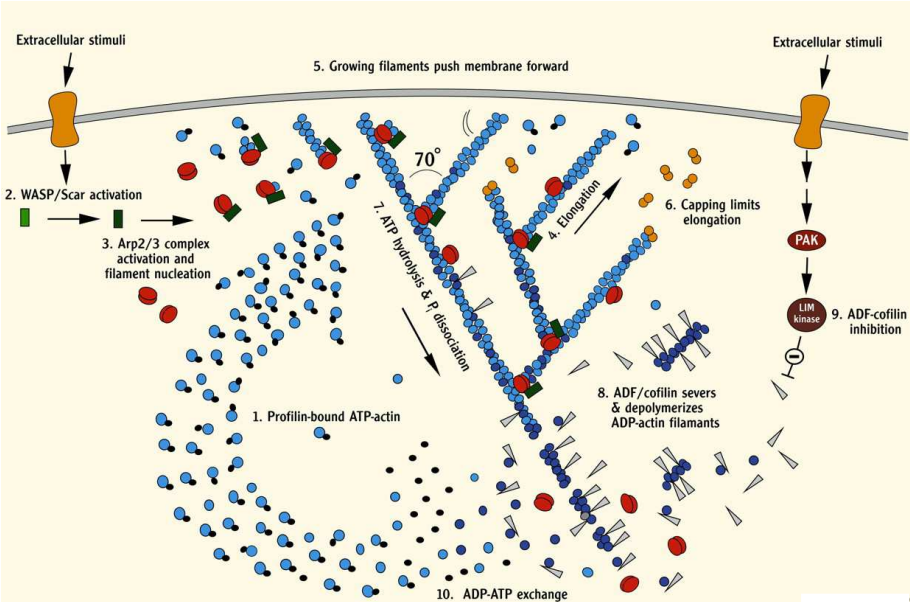

Figure I.5: Model of actin assembly and disassembly at the leading edge of motile cells
The Rho family of GTPases activate WASP/Scar family proteins, which consequently activate the Arp2/3 complex. This complex initiates nucleation of a new actin filament that is elongated using the profilin-bound ATP-actin pool until binding of capping protein. Disassembly of the actin branch is initiated by the ADF/cofilin complex, which catalyzes the hydrolysis of ATP leading to dissociation of the actin branch (from [151]).

In contrast to lamellipodia, which contain branched actin filaments, filopodia are thin (0.1 – 0.3 µm) structures and show parallel actin filament bundles. Moreover, filopodia are processed differently [122]. They are either embedded in or protruding from the lamellipodia [177]. Filopodia are involved in several cellular processes including wound healing, migration and adhesion, the latter due to expression of integrins and cadherins at the filopodioal tips [140 47]. Moreover, filopodia are important for the guidance towards chemoattractants, as they contain

receptors for several signaling molecules, and also for the neuronal growth-cone development [42 56 122]. Furthermore, they are associated with cancer cell invasion, for example in colon cancer [186]. In macrophages filopodia act as tentacles, which can bind particles and pull them to the cell body, where they form a so called phagocytic cup together with the underlying lamellipodia [136 88 188]. The process of filopodia formation is discussed controversially. Currently, three different models exist: the convergent elongation model, the de novo nucleation model and a combination of both, which are all adequately documented and might therefore depend on the different cell types that were investigated. According to the convergent elongation model, filopodia emanate from an existing lamellipodial actin network and are mediated by a tip complex that contains the enabled/vasodilator-stimulated phosphoprotein (Ena/VASP) in the filopodial tip [177 125 56]. The de novo filament nucleation model indicates that actin filaments in filopodia are nucleated at filopodial tips by formins, instead of deriving from an existing lamellipodial network [176]. The protein mammalian diaphanous-related formin 2 (mDia2) as well as the Ena/VASP proteins are essential for filopodia formation and may play synergistic roles as they both prevent capping of barbed ends and thus initiate filopodia formation [160]. The combination of both models leads to the following model for filopodia formation, which is displayed in figure I.6.

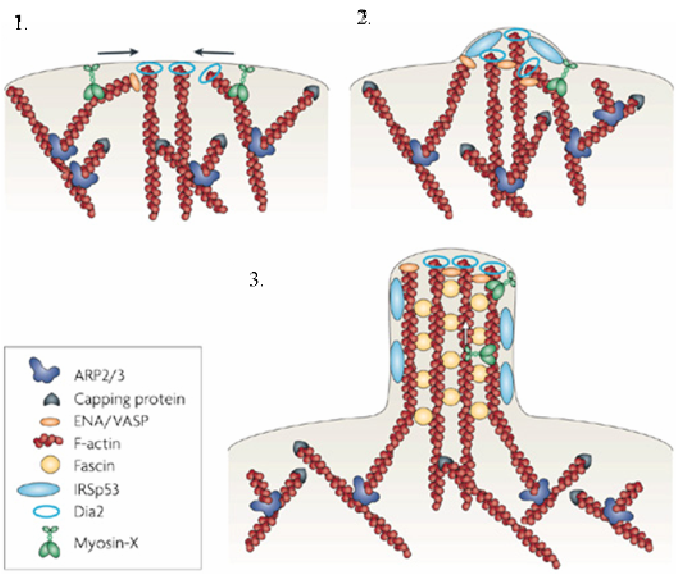

Figure I.6: Model of filopodia formation

1. Starting from the lamellipodial network, some actin filaments are prevented from capping by Ena/VASP and/or by mDia2 and therefore elongate further on. MDia2 is also able to generate new, unbranched actin filaments. 2. Myosin-X connects the parallel elongated actin filaments initiating a filopodium, which then pushes forward the cell membrane. IRSp53 might play a supporting role by deforming the membrane. 3. Fascin then incorporates into the shaft of the filopodium generating a stiff actin filament bundle. Adhesion molecules might be localized to the filopodial tip by myosin-X (arrow) (modified after [122]).

Some actin filaments from the lamellipodial network are prevented from capping by Ena/VASP and/or by mDia2 and elongate continuously. The latter is also able to nucleate new, unbranched actin filaments. Myosin-X connects the parallel elongated actin filaments initiating a filopodium, which then pushes forward the cell membrane. The protein insulin-receptor substrate p53 (IRSp53) might support this by deforming the membrane. The protein fascin then incorporates into the shaft of the filopodium generating a stiff actin filament bundle. Adhesion molecules might be transported to the filopodial tip by myosin-X. Ena/VASP and mDia2 are localized in the filopodial tip complex [122].

The Rho family of GTPases, namely RhoA, Rac1, and Cdc42 play important roles in regulating the actin cytoskeleton. RhoA is involved in the formation of stress fibers and focal adhesions, whereas Rac1 promotes lamellipodia and Cdc42 filopodia formation [122].

Recently, it has been shown that MAPKs are also involved in cell migration [67]. The p38 MAPKs are a subfamily of these kinases [73] and are activated by growth factors [67]. They influence growth factor- and cytokine-stimulated cell migration in various cell types [67]. Thus, inhibition of p38 MAPK by the specific inhibitors SB203580 or SB202190 decreases growth factor-stimulated cell migration of several cell types. This was observed for example in smooth muscle cells stimulated with PDGF, TGF-β and IL-1β [63] and in corneal epithelial cells treated with HGF [164]. Likewise, EGF or TGF-β stimulated mouse mammary epithelial cells (NMuMG) [85 3] and TGF-β induced human breast cancer cells (MDA-MB-231) [3] exhibited diminished cell migration after inhibition of p38 MAPK. We, therefore, wanted to test whether the p38 MAPK pathway plays a role in Cx43 mediated cell migration.

3.2 Role of Cx43 in cell migration

It has been shown that Cx43 is involved in cell migration in several cell lines. For example, Cx43 is highly expressed in migrating neural crest cells during embryogenesis [68 116] and overexpression of Cx43 increases cell motility and directionality in these cells [204] as well as in C6 glioma cells [4]. Likewise, downregulation of Cx43 leads to decelerated cell migration in neural crest cells [68 116], in mouse embryonic fibroblasts (NIH3T3) [195], and in C6 glioma cells [4]. However, the mechanism by which Cx43 modulates cell migration and whether it is a gap junction dependent or independent effect remained unclear. Expression of truncated Cx43, lacking the C-terminal part, resulted in decreased cell migration compared to the full length protein in C6 glioma cells [4] and in 3T3 fibroblasts [127]. The same was observed for neuronal migration during brain development in mice [27]. These studies indicated that not the channel building part of Cx43 but rather the C-terminus is essential to enhance cell migration.

However, there exist studies showing a gap junction dependent effect of Cx43 on cell migration. Thus, expression of a truncated Cx43 protein, lacking the C-terminal part, increased migration of radial glia cells [38]. Adhesive properties of the gap junction channel may play a role in this context because a mutated Cx43 gap junction channel, which exhibits a closed channel but enables adhesion, also showed enhanced radial glia migration comparable to wild-type Cx43 [5 38]. Likewise, glioblastoma cells showed decreased cell migration and invasion after blocking gap junctional communication with carbenoxolone (CBX) [137].

Conversely, there are a few studies, which indicate that Cx43 decreases cell migration. For example, transient downregulation of Cx43 has been reported to result in an enlarged rate of wound closure in skin lesions [153] as well as in enhanced cell growth and migration in the breast carcinoma cell line Hs578T [163].

Thus, it is evident that Cx43 influences cell migration either by increasing or decreasing, which may be dependent on the studied cell type.

There are several aspects to be kept in mind, which can lead to modified cell motility. One aspect is the reorganization of the actin cytoskeleton and there are some hints that Cx43 interacts with the actin cytoskeleton. Thus, neural crest cells show a parallel alignment of actin stress fibers, whereas downregulation of Cx43 in these cells leads to a polygonal array of stress fiber bundles being associated with less expression of β1 integrin and vinculin [204]. Moreover, Cx43 colocalizes with the actin cytoskeleton itself and also with several actin-binding proteins, including α-actinin, ezrin, IQGAP, drebrin [204], NOV [45 48], and cortactin [174]. Thereby, it might directly or indirectly influence the actin cytoskeleton. Furthermore, it has been assumed that enhanced cell migration due to Cx43 expression could be associated with expression of N-cadherin that by itself increases cell migration, for example in the breast cancer cell line MCF7 [61], in NIH3T3 cells [195] and in mouse neural crest cells [206], indicating a link between gap junction and adherens junction formation. Likewise, p38 MAPK, which is involved in cell migration [61], could play a role in Cx43 mediated cell migration.

Eventually, it still has to be clarified, whether Cx43 increases or decreases cell migration and whether this influence depends on the channel forming part of Cx43 or its C-terminal tail. Moreover, the associated mechanisms remain to be elucidated.

4 Aim of the study

Several physiological and pathophysiological processes, which are characterized by enhanced cell migration such as wound healing or atherosclerosis, are linked with increased expression of Cx43, for example in endothelial [95 94] and smooth muscle cells [149]. Since Cx43 has been shown to modulate migration processes, a better understanding of the mechanisms by which Cx43 can affect cell migration may be helpful in developing effective therapeutic control of such processes. However, up to now there exist controversial data how Cx43 is affecting migration and, in particular, whether the migration modulating effect of Cx43 is gap junction dependent [137 38] or independent [127 4].

We therefore aimed to study three aspects of Cx43 mediated modulation of cell migration:

I. Does Cx43 exhibit stimulatory effects on cell migration and are they channel dependent or independent?

II. Do interactions of Cx43 with other proteins play a role in this context?

III. Does Cx43 influence cell migration by modulating the actin cytoskeleton and/or by activation of p38 MAPK?

To clarify the role of Cx43 during cell migration we studied the effects of an isolated expression of either the channel forming part or the C-terminal part of Cx43 in HeLa cells. These cells were chosen as they do not express connexins in their wild-type form [82 81], but can be stably transfected with those. Using HeLa cells is clearly an advantage compared to other cell types, which endogenously express several connexins, as it has been shown that the knockdown of one connexin affects the expression of other connexins in the same cell [89].

II Materials and Methods

1 Materials

1.1 Chemicals

Substance	Catalog number	Company
Acrylamide 4K-Solution (30 %), Mix 37.5:1	A1672	AppliChem GmbH, Darmstadt, Germany
Agar	A0949	AppliChem GmbH, Darmstadt, Germany
Agarose low EEO	A2114	AppliChem GmbH, Darmstadt, Germany
Albumin fraction V	A1391	AppliChem GmbH, Darmstadt, Germany
Ammoniumpersulfat	A2941	AppliChem GmbH, Darmstadt, Germany
Aqua ad iniectabilia	3703452	B. Braun Melsungen AG, Melsungen Germany
Boric acid	A2318	AppliChem GmbH, Darmstadt, Germany
Chemiluminescent Detection Kit for Horseradish peroxidase, Solution A and Solution B	A3417, 1200A and 1200B	AppliChem GmbH, Darmstadt, Germany
Ethanol absolut	A3678	AppliChem GmbH, Darmstadt, Germany
Ethidium bromide	E7637	Sigma-Aldrich GmbH, Steinheim, Germany
Formaldehyd 37 %	A0877	AppliChem GmbH, Darmstadt, Germany
Glycerin waterfree	A2364	AppliChem GmbH, Darmstadt, Germany
Glycine	A1067	AppliChem GmbH, Darmstadt, Germany
Isopropanol	A3928	AppliChem GmbH, Darmstadt, Germany
KCl	A2939	AppliChem GmbH, Darmstadt, Germany
KH_2PO_4	A591973	Merck, Darmstadt, Germany
β-Mercaptoethanol	A1108	AppliChem GmbH, Darmstadt, Germany
Methanol	A0688	AppliChem GmbH, Darmstadt, Germany

Na_2HPO_4	A3905	AppliChem GmbH, Darmstadt, Germany
NaCl	A4661	AppliChem GmbH, Darmstadt, Germany
Nonfat dried milk powder	A0830	AppliChem GmbH, Darmstadt, Germany
SB203580 (in solution)	559398	Calbiochem, Merck kGaA, Darmstadt, Germany
SDS ultrapure	A1112	AppliChem GmbH, Darmstadt, Germany
TEMED	A1148	AppliChem GmbH, Darmstadt, Germany
Tris	A1379	AppliChem GmbH, Darmstadt, Germany
Triton X-100	789704	Boehringer, Mannheim, Germany
Trypton (Pepton from Casein)	A2208	AppliChem GmbH, Darmstadt, Germany
Tween® 20	A1389	BioChemica, AppliChem GmbH, Darmstadt, Germany
Western Blocking Reagent	13702000	Roche Diagnostics GmbH, Mannheim, Germany
Yeast extract	A1552	AppliChem GmbH, Darmstadt, Germany

1.2 Cell culture

Material	**Catalog number**	**Company**
Cell counting: Fast-Read 102 For standardized Urine analysis	BVS100H	Biosigma S.r.l., Hycor Biomedical Inc., Cona, Italy
DMEM (Dulbecco's modified eagle medium) 1x cell growth medium	31885	Invitrogen, Eugene, Oregon, USA
DMSO	D2650	Sigma-Aldrich GmbH, Steinheim, Germany
Fetal bovine serum	S0115	Biochrom AG, Berlin, Germany
Micro Tube 1.5 ml	72.690	Sarstedt, Nürnbrecht, Germany
Newborn calf serum	S0125	Biochrom AG, Berlin, Germany
Penicillin (10,000 units/ml)/Streptomycin (10 mg/ml) in 0.9 % NaCl solution	P0781	Sigma-Aldrich GmbH, Steinheim, Germany
Pipette, 5 ml, sterile	606180	Greiner bio-one GmbH, Solingen-Wald, Germany
Pipette, 10 ml, sterile	607180	Greiner bio-one GmbH, Solingen-Wald, Germany
Polypropylene Conical tube,	352070	Falcon, Becton Dickinson Labware,

Blue Max™, 50 ml, sterile		Franklin Lakes, NJ, USA
Polypropylene Conical tube 15 ml, high clarity	352096	Falcon, Becton Dickinson Labware, Franklin Lakes, NJ, USA
Puromycin-Dihydrochlorid	A2856	AppliChem GmbH, Darmstadt, Germany
Reaction tube 2.0 ml	710220	Biozym Scientific GmbH, Hess. Oldendorf, Germany
Tissue culture dish, 60 x 20 mm Style	353004	Falcon, Becton Dickinson Labware, Franklin Lakes, NJ, USA
Tissue culture dish, 100 x 20 mm Style	353003	Falcon, Becton Dickinson Labware, Franklin Lakes, NJ, USA
Tissue Culture Plate, 6-Well, Flat Bottom with low evaporation lid	353224	Becton Dickinson Labware, Franklin Lakes, NJ, USA
Tissue Culture Plate, 12-Well, Flat Bottom with low evaporation lid	353225	Becton Dickinson Labware, Franklin Lakes, NJ, USA
Tissue Culture Plate, 24-Well, Flat Bottom with low evaporation lid	353226	Becton Dickinson Labware, Franklin Lakes, NJ, USA
Trypsin-EDTA 1x	T3924	Sigma-Aldrich GmbH, Steinheim, Germany
Zeocin®	R25001	Invitrogen, Carlsbad, CA, USA

Solutions

PBS- (Sodiumchloride solution 0.81 % in phosphate buffer 0.0067 mol/l pH 7.2)

NaCl	8.1 g
Na_2HPO_4	0.862 g
KH_2PO_4	0.248 g
Aqua ad iniectabilia	ad 1.0 ml

Puromycin 10 mg/ml Hepes buffer (sterile filtrated), 50 µl/500 ml DMEM medium

Hepes buffer pH 7.4

NaCl	8.473 g
KCl	0.224 g
Na_2HPO_4 x 2 H_2O	0.215 g
$CaCl_2$ x 2 H_2O	0.487 g
MgCl x 6 H_2O	0.651 g
Hepes 1M solution	10.0 g
Aqua ad iniectabilia	ad 1000.0 g

1.3 Fluorescent activated cell sorting

Material	Catalog number	Company
Accutase	L11-007	PAA Laboratories, Pasching, Austria
Calcein-AM	C1430	Invitrogen, Carlsbad, CA, USA
FACS Clean	340345	Becton Dickinson, BD Biosciences, San Jose, California, USA
FACS Flow	342003	Becton Dickinson, BD Biosciences, San Jose, California, USA
FACS Rinse	340346	Becton Dickinson, BD Biosciences, San Jose, California, USA
FACS test tubes: Polystyrene round-bottom tube	352052	Falcon, Becton Dickinson Labware, Franklin Lakes, NJ, USA
PKH-26 Red Fluorescent Cell Linker Kit for general cell membrane labeling (PKH26 GL-1KT)	039K0781	Sigma-Aldrich GmbH, Steinheim, Germany

Solutions

Calcein-AM 1mg/ml in DMSO

1.4 Migration

Material	Catalog number	Company
Culture Insert, for self insertion	80209	Ibidi, Martinsried, Germany
µ-Dish low with culture insert, ibiTreat	80206	Ibidi, Martinsried, Germany
µ-Slide 8 well, ibiTreat	80826	Ibidi, Martinsried, Germany

1.5 Cloning

Vector	Catalog number	Company
pcDNA4-myc-His Version B	V863-20	Invitrogen, Eugene, Oregon, USA
pcDNA3.1-TOPO	K4900-01	Invitrogen, Eugene, Oregon, USA

Restriction enzyme	Catalog number	Company
BamHI, Source: purified from *Bacillus amyloliquefaciens* H (20,000 U/ml)	15201023	Invitrogen, Eugene, Oregon, USA
PmeI, Source: purified from *Pseudomonas mendocina* (10,000 U/ml)	R0560L	New England Biolabs (NEB) GmbH, Frankfurt, Germany
XbaI, Source: purified from *Xanthomonas campestris (Xanthomonas badrii)* (20,000 U/ml)	15226012	Invitrogen, Eugene, Oregon, USA
XhoI, Source: purified from *Xanthomonas campestris (Xanthomonas holcicola)* (20,000 U/ml)	15231012	Invitrogen, Eugene, Oregon, USA

Polymerase	Catalog number	Company
Herculase II Fusion DNA Polymerase	600675	Stratagene, Agilent Technologies, USA
Taq polymerase, 5 U/µl supplied: PCR Grade Nucleotide Mix, premixed 10 mM deoxynucleotide triphosphate (dATP, dCTP, dGTP, dTTP) solution	04728866001	Roche Applied Science, Mannheim, Germany

Gel electrophoresis

TBE 10x

Tris HCl	890 mM
Boric acid	890 mM
EDTA	20 mM
Aqua dem.	ad 1000 ml
pH 8.5	

Gene Ruler 1 kb DNA ladder, Cat.No. SM0311, Fermentas, St. Leon-Rot, Germany
Gene Ruler 100 bp DNA ladder plus, Cat.No. SM0321, Fermentas GmbH, St. Leon-Rot, Germany
6x loading dye, Cat.No. R0611, Fermentas, St. Leon-Rot, Germany

Bacteria
XL1-Blue supercompetent cells, Cat.No. 200236, Stratagene, Agilent Technologies, USA
Plates: Petri Dish, Cat.No. 663102, Greiner Bio-One, Frickenhausen, Germany

LB medium

Trypton (Pepton from Casein)	10.0 g
Yeast extract	5.0 g
NaCl	5.0 g
Aqua dem.	ad 1000.0 ml

LB agar

Trypton (Pepton from Casein)	10.0 g
Yeast extract	5.0 g
NaCl	5.0 g
Aqua dem.	ad 1000.0 ml
Agar	12.0 g

Kits for cloning	Catalog number	Company
HiSpeed® Plasmid Maxi Kit	12663	Qiagen GmbH, Hilden, Germany
QIAquick® Gel Extraction Kit	28706	Qiagen GmbH, Hilden, Germany
QIAquick® PCR Purification Kit	28106	Qiagen GmbH, Hilden, Germany
QIAprep® Spin Miniprep Kit	27106	Qiagen GmbH, Hilden, Germany
Rapid DNA Ligation Kit	11635379001	Roche Diagnostics GmbH, Mannheim, Germany

Transfection
SuperFect Transfection Reagent, Cat.No. 301305, Qiagen GmbH, Hilden, Germany

1.6 Western blotting

Separating gel 10 %

Aqua dem.	4.0 ml
Tris/HCl 1.5 M pH 8.8	2.5 ml
SDS 10 %	100.0 µl
Polyacrylamid 30 %	3.3 ml
APS 10 %	50.0 µl
TEMED	5.0 µl

Stacking gel 4 %

Aqua dem.	6.0 ml
Tris/HCl 0.5 M pH 6.8	2.5 ml
SDS 10 %	100.0 µl
Polyacrylamid 30 %	1.3 ml
APS 10 %	65.0 µl
TEMED	5.0 µl

Tris 1.5 M pH 8.8
Tris 90.8 g in 500 ml Aqua dem.

Tris 0.5 M pH 6.8
Tris 30.2 g in 500 ml Aqua dem.

Electrophoresis buffer 5x

Tris	75.0 g
Glycine	360.0 g
SDS	25.0 g
Aqua dem.	ad 5000 ml

Western transfer buffer

Tris	5.8 g
Glycine	2.9 g
SDS 10 %	3.7 ml
Methanol	200 ml

Aqua dem. ad 1000 ml

Washing buffer
PBS 1x
Tween 0.1 %

Stripping buffer (pH 2.8)

Glycine	15.01 g
NaCl	29.22 g

Aqua dem. ad 1000 ml

PBS 10x (pH 7.4)

NaCl	80.0 g
KCl	2.0 g
Na_2HPO_4	11.5 g
KH_2PO_4	2.0 g

Aqua dem. ad 1000 ml

Laemmli sample buffer

Tris	62.5 mM
SDS	2 %
Glycerol	25 %
Bromphenolblau	0.01 %

(before use add 0.5 % β-Mercaptoethanol)

Material	Catalog number	Company
Amersham Hypond-P, PVDF membrane	RPN303F	GE Healthcare, Buckinghamshire, UK
Gel blotting paper GB003	10426892	Whatman GmbH, Dassel, Germany
Mighty Small II for 8 x 9 cm gels	80614935	Amersham Biosciences, Minnesota, San Franscisco, USA
Page ruler prestained, protein ladder	SM0671	Fermentas, St. Leon-Rot, Germany

Antibodies

Primary antibodies

Antibody	**Isotype**	**Catalog number**	**Company**
Calnexin	Rabbit polyclonal	2433	Cell Signaling Technology, Danvers, USA
Cx43	Rabbit polyclonal	C 6219	Sigma Alldrich, St. Louis, USA
Cortactin (p80/85), clone 4F11	Mouse monoclonal IgG_1	05-180	Upstate/Millipore, Temecula, California, USA
GAPDH (Glyceraldehyde-3-phosphate dehydrogenase) clone 6C5	Mouse monoclonal IgG_1	MAB 374	Chemicon International/Millipore, Temecula, California, USA
GFP	Rabbit polyclonal IgG	Ab 290	Abcam, Cambridge, United Kingdom
NOV (CCN3)	Goat polyclonal IgG	AF 1640	R&D Systems, Minneapolis, USA
Phospho-p38 MAP kinase (Thr180/Tyr182) (28B10)	Mouse monoclonal IgG_1	9216	Cell Signaling Technology, Danvers, USA

Secondary antibodies

Antibody	**Isotype**	**Catalog Number**	**Company**
Anti-mouse IgG H&L Chain specific Peroxidase conjugate	Goat	401253	Calbiochem, Merck kGaA, Darmstadt, Germany
Anti-rabbit IgG, H&L Chain specific Peroxidase conjugate	Goat	401353	Calbiochem, Merck kGaA, Darmstadt, Germany
Anti-goat IgG, H&L Chain specific Peroxidase conjugate	Rabbit	401515	Calbiochem, Merck kGaA, Darmstadt, Germany

1.7 Immunoprecipitation

Material	Catalog number	Company
µ Columns MACS	130-042-701	Miltenyl Biotec, Auburn CA, USA
µMACS Micro Beads, Protein A	120-000-396	Miltenyl Biotec, Auburn CA, USA
µMACS Micro Beads, Protein G	120-000-397	Miltenyl Biotec, Auburn CA, USA
µMACS Separation Unit	426-03	Miltenyl Biotec, Aubum CA, USA

Primary antibodies

Antibody	Isotype	Catalog number	Company
Cx43	Rabbit polyclonal	C 6219	Sigma Alldrich, St. Louis, USA
Cortactin (p80/85), clone 4F11	Mouse monoclonal IgG_1	05-180	Upstate/Millipore, Temecula, California, USA
GFP	Rabbit polyclonal IgG	Ab 290	Abcam, Cambridge, United Kingdom
NOV (CCN3)	Goat polyclonal IgG	AF 1640	R&D Systems, Minneapolis, USA

Solutions

Triton X-100 lysis buffer (pH 8.0)
NaCl 150 mM (0.87 g)
Triton X-100 1 % (1 ml)
Tris HCl 50 mM (0.60 g)
Aqua dem. ad 100 ml

Low salt buffer
Tris HCl 20 mM (0.24 g)
Aqua dem. ad 100 ml

1.8 Immunofluorescence

Solutions

Phosphate buffered saline (PBS+): Hank's solution without phenol red
NaCl 8.0 g
KCl 0.4 g
Mg_2SO_4 x 7 H_2O 0.074 g
MgCl x 6 H_2O 0.074 g
$CaCl_2$ 0.138 g
Na_2HPO_4 x 2 H_2O 0.15 g
KH_2PO_4 0.06 g
Glucose 1.0 g
$NaHCO_3$ 0.3 g
Aqua ad iniectabilia ad 1000.0 g

Formaldehyde 3.7 % in PBS+
Triton X-100 0.1 % in PBS+
Immu-Mount, Cat.No. 9990402, Shandon, Pittsburgh, USA

Antibodies

Primary antibodies

The same antibodies were used as for western blotting (chapter II.1.6).

Secondary antibodies

Antibody	Source	Catalog number	Company
Alexa Fluor 488 anti-rabbit IgG	Chicken	A21441	Invitrogen, Eugene, Oregon, USA
Alexa Fluor 546 anti-mouse IgG	Goat	A11030	Invitrogen, Eugene, Oregon, USA

1.9 Staining of the actin cytoskeleton

Antibody	Source	Catalog number	Company
Alexa Fluor 488 phalloidin	Amanita phalloides mushroom	A-12379	Molecular Probes, Invitrogen, Eugene, Oregon, USA
Alexa Fluor 546 phalloidin	Amanita phalloides mushroom	A-22283	Molecular Probes, Invitrogen, Eugene, Oregon, USA

1.10 Lab Equipment

Equipment	Company
BioPhotometer 6131	Eppendorf AG, Hamburg, Germany
Block thermostat HLC BT1301	Scientific Plastics (Europe), Great Britain
Cell incubator	Binder GmbH, Tuttlingen, Germany
Centrifuges Eppendorf centrifuge 5410 Biofuge primo R Megafuge 1.OR	 Eppendorf AG, Hamburg, Germany Heraeus, Osterode, Germany Heraeus, Osterode, Germany
FACSort	Becton Dickinson, BD Biosciences, San Jose, California, USA
Gel documentation system: Gel Doc 1000 Single wavelength mini-transilluminator	BIO-RAD Laboratories, München, Germany

Laminar flow bench: Steril VBH	REWA, Reichertshausen, Germany
Live cell imaging Heating system 6: HT200 temperature controller, heated lid with gas incubation, heated plate with multi-well format, Cat.No. 10918 Insert for µ-Dish 35 mm low, Cat.No. 10932 Insert for various µ-slides, Cat.No. 10933 Gas incubation system: Unit I for CO_2 and pressurized air, Cat.No. 10920	Ibidi, Martinsried, Germany
Microscopes Migration microscope: Axio Observer Z1 Cell culture microscope: Leitz Fluovert FU Confocal laser scanning microsope: Leica TCS SP5	 Carl Zeiss GmbH, Jena, Germany Leica Microsystems, Wetzlar, Germany Leica Microsystems, Wetzlar, Germany
PCR thermal cycler, V2.600	Eppendorf, Hamburg, Germany
pH meter: S20-SevenEasy™ pH	Mettler Toledo, Giessen, Germany
Power Supply SDS gel electrophoresis: Standard Power Pack P25 Agarose gel electrophoresis: Gibco BRL PS305	 Biometra GmbH, Göttinge, Germany Life technologies, Darmstadt, Germany
Sonicator Ultrasonic processor XL	Heat Systems, Reichshof/Wenrath, Germany
UV surface emitting diode	H. Faust GmbH, Meckenheim, Germany
Waterbath SWB 25	Thermo Haake GmbH, Karlsruhe, Germany
Westernblot Detector: Camera Controller Orca ER	Hamamatsu Photonics, Hamamatsu City, Shizuoka Pref, Japan

2 Methods

2.1 Cell biological methods

2.1.1 Cell culture

2.1.1.1 Cell lines

In this work HeLa wild-type (wt) cells were used, which are immortal cervix carcinoma cells originally isolated from the patient Henrietta Lacks in 1951. They do not express any connexins, but can be stably transfected with those. HeLa wt cells and HeLa cells stably expressing Cx43 (HeLa 43) were a kind gift from Dr. Klaus Willecke (University of Bonn, Germany). Furthermore, various HeLa cell lines, stably expressing the full length Cx43 protein tagged with GFP or differently truncated Cx43 proteins, tagged with GFP, were generated in the present study (Table II.1). As controls, cells were transfected with the empty vector pcDNA4-myc-His Version B (Invitrogen) (HeLa CTL) or with a cDNA encoding GFP alone (HeLa GFP).

Table II.1: In the present study generated HeLa cell lines by stable transfection

Cell line	**Transfected plasmid**
HeLa CTL	pcDNA4-myc-His Version B (Invitrogen)
HeLa GFP	pcDNA4-GFP
HeLa 43-GFP	pcDNA4-rCx43-GFP (full length rat Cx43, aa 1 – 382, GFP-tagged)
HeLa 43NT-GFP	pcDNA4-rCx43NT-GFP (N-terminal part of rat Cx43, aa 1 – 257, GFP-tagged)
HeLa 43CT-GFP	pcDNA4-rCx43CT-GFP (C-terminal part of rat Cx43, aa 257 – 382, GFP-tagged)
HeLa 43(tr298)-GFP	pcDNA4-rCx43(tr298)-GFP (truncated rat Cx43, aa 1 – 298, GFP-tagged)
HeLa 43(tr336)-GFP	pcDNA4-rCx43(tr336)-GFP (truncated rat Cx43, aa 1 – 336, GFP-tagged)
HeLa 43(299 – 336)-GFP	pcDNA4-rCx43(299 – 336)-GFP (truncated rat Cx43, aa 299 – 336, GFP-tagged)

2.1.1.2 Cell passaging

Cells were cultivated in an incubator with a humidified atmosphere at 37 °C and 5 % CO_2. All workflows in the cell culture were done in a laminar flow bench under sterile conditions.

HeLa wt cells were maintained in Dulbecco's modified Eagle medium (DMEM) supplemented with 10 % new born calf serum (NBCS) and the antibiotics penicillin (100 U/ml) and streptomycin (100 µg/ml). Culture medium of HeLa 43 cells additionally contained puromycin (1 µg/ml) due to a vector encoded puromycin resistance. Cells, which were generated in the present study, were cultivated in culture medium for HeLa wt cells supplemented with Zeocin (200 µg/ml) due to an encoded Zeocin resistance on the vector pcDNA4.

Cells were grown in cell culture dishes (100 mm in diameter) and split twice a week after reaching confluence. For that purpose they were washed with phosphate buffered saline without magnesium and calcium ions (PBS-). Subsequently, to detach cells from the bottom of the culture dish, a solution containing 0.5 % trypsin and 0.2 % EDTA was added. To deactivate the trypsin, cell culture medium was added and the cells were resuspended. According to the required amount of cells, the cell suspension was transferred to new cell culture dishes and diluted to the desired concentration with fresh cell culture medium.

<u>PBS-</u>

NaCl	8.1 g
Na_2HPO_4	0.862 g
KH_2PO_4	0.248 g
Aqua ad iniectabilia	ad 1.0 ml

2.1.1.3 Cell freezing

Cells were grown until confluence, washed with PBS- and were detached by adding 1 ml trypsin/EDTA solution. The cells were resuspended in an appropriate amount of freezing medium (cell culture medium supplemented with 20 % NBCS and 10 % DMSO) and the cell suspension was added to cryovials. The cryovials were frozen at -80 °C for 24 h and afterwards placed in a liquid nitrogen tank (-196 °C) for long time storage.

2.1.1.4 Cell thawing

The frozen cells were thawed quickly in a 37 °C water bath. The cell suspension was mixed with fresh cell culture medium, centrifuged at 1200 rpm for 5 min and the cell pellet was resuspended in fresh cell culture medium to remove the DMSO. The cell suspension was transferred into a new cell culture dish and fresh cell culture medium was added.

2.1.2 Lethality curve

To determine the optimal concentration of Zeocin in the cell culture medium for generation of stably transfected cells, a lethality curve was performed. HeLa wt cells were seeded in a 6-well-plate at a dilution of 4 x 10^5 cells/ml. After appropriate attachment of the cells, the following Zeocin concentrations were added: 0, 100, 150, 200, 250 and 300 µg/ml. Cells were cultivated for 10 days and the media were changed every two days. The lowest Zeocin concentration, sufficient to kill all cells after 10 days, was used to produce stably transfected cell lines. In the present study a Zeocin concentration of 200 µg/ml was used.

2.1.3 Transfection of HeLa wt cells

Transfection of cells is a powerful tool to study and control gene expression. During the process of transfection, foreign DNA is delivered into eukaryotic cells. Two transfection techniques can be distinguished: transient and stable transfection. Using transient transfection, the DNA is introduced into the nucleus of the cell, but does not integrate into the chromosomal DNA. Consequently, a lot of copies of the transfected gene are present leading to high levels of expressed protein, which can be observed within 24 – 96 h after introduction of the DNA.

Using stable transfection, the DNA is either integrated into the chromosomal DNA or maintained as an episome. Cells which have integrated the transfected DNA or have generated episomal plasmid DNA can be selected as single cell clones using a vector encoded resistance against a specific antibiotic. In the present study SuperFect transfection reagent (Qiagen) was used, which optimizes the entry of DNA into the cell (first described by [178]). Preparation of DNA and SuperFect transfection reagent should be done in serum-free medium because serum may inhibit complex formation.

2.1.3.1 Transient transfection of HeLa wt cells

Transient transfection was performed to observe whether the constructed plasmid leads to expression of the respective protein within the cell. Expression of GFP-tagged proteins was either visually monitored in living cells by fluorescence of the GFP-tag using laser scanning microscopy (LSM; Leica) or cell extracts were investigated by western blot analysis (WB).

HeLa wt cells were seeded on glass cover slips (15 mm diameter) in a 12-well-plate, reaching 50 % confluence the next day (for observation by LSM) or they were seeded in a 6-well-plate, reaching 60 – 70 % confluence the next day (for observation by WB). The respective

transfection protocols according to the manufacturer's instructions and own experiences are listed in table II.2.

Table II.2: Transfection protocol for transient transfection

Substance	**Amount for transient transfection and observation using LSM**	**Amount for transient transfection and observation using WB**
Plasmid DNA	1.0 µg	2.0 µg
DMEM medium without serum and antibiotics	ad 75.0 µl	ad 100.0 µl
SuperFect transfection reagent	7.5 µl	10.0 µl
Cell culture medium for HeLa wt cells	400.0 µl	600.0 µl

For transfection, the plasmid DNA was diluted in DMEM medium without serum and antibiotics in a 1.5 ml tube, vortexed and shortly centrifuged. SuperFect transfection reagent was added, mixed by pipetting up and down and incubated for 10 min at room temperature to allow transfection complex formation. In the meantime the medium of the cells was removed and they were washed twice with PBS-. The required amount of cell culture medium for HeLa wt cells was added to the mixture and the whole solution was transferred to the cells.

After incubation for 24 h at 37 °C and 5 % CO_2, the medium was removed and the cells were washed three times with PBS-. Protein expression of the transfected plasmid DNA was observed either by fluorescence of the GFP-tag using LSM by placing the glass cover slips in a special fitting for the microscope or cells were lysed in 100 µl Laemmli sample buffer [99] and expression of the proteins was detected using WB.

2.1.3.2 Stable transfection of HeLa wt cells

Stable transfection was performed to reach a permanent expression of the respective protein in all transfected cells as a necessary prerequisite for long term investigations and functional analyses.

For stable transfection, HeLa wt cells were seeded in a 60 mm cell culture plate, reaching 50 % confluence the next day (transfection protocol is listed in table II.3) and cells were transfected as described in chapter II.2.1.3.1

Table II.3: Transfection protocol for stable transfection

Substance	**Amount**
Plasmid DNA	5.0 µg
DMEM medium without serum and antibiotics	ad 150.0 µl
SuperFect transfection reagent	50.0 µl
Cell culture medium for HeLa wt cells	1000.0 µl

After further incubation for 24 h, cells were detached with 500 µl trypsin/EDTA solution and transferred to a new 100 mm cell culture plate in 12 ml of fresh cell culture medium supplemented with 200 µg/ml Zeocin. Cells got fresh cell culture medium twice a week until single cell clones were visible. Approximately 12 single cell clones per culture dish were picked using a 1000 µl sterile pipet tip and grown separately in a 24-well-plate until confluence. Single cell clones were expanded and investigated for their protein expression using western blot. Localization of the protein was analyzed by fluorescence of the GFP-tag using LSM.

2.1.4 Analysis of cell coupling using fluorescent activated cell sorting (FACS)

To analyze cell coupling, fluorescent activated cell sorting (FACS) was used. With this method, it is possible to measure fluorescent labeled single cells in a focused stream of fluid that pass a laser beam. Additional detectors measuring in line with the light beam (forward scatter, FSC) reveal the cell volume and detectors measuring perpendicular to it (side scatter, SSC) reveal the inner constitution of the cell, such as amount and type of cytoplasmic granules (Figure II.1). Therefore, it is possible to characterize different cell populations and sort them according to specific characteristics. In this study the FACSort (Becton Dickinson) was used, equipped with an argon laser, exhibiting an excitation wavelength of 488 nm, and able to measure green (FL-1) and red (FL-2) fluorescence at emission wavelengths of 530 and 585 nm, respectively. It was connected to a computer and data was analyzed using the CellQuest software (Becton Dickinson).

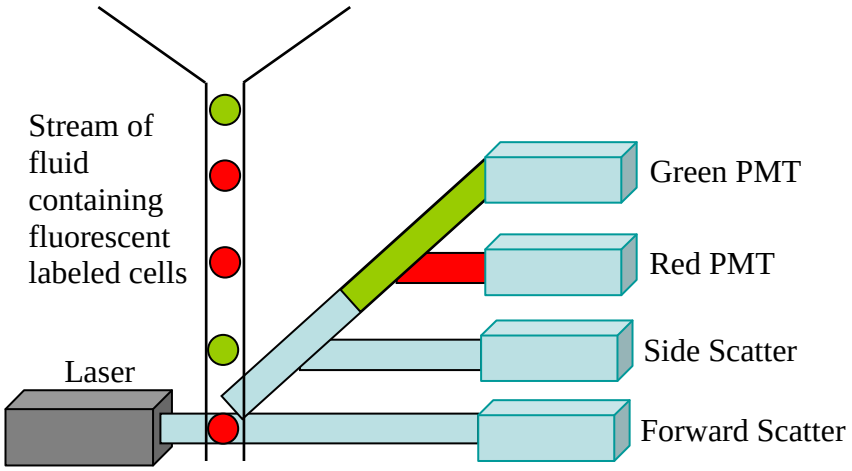

Figure II.1: Principle of fluorescent activated cell sorting
Fluorescence of single cells in a focused stream of fluid can be excited by a laser and emission can be detected by photomultiplier tubes (PMT) for green and red fluorescence. Additional detectors measuring volume (forward scatter, FSC) and inner constitution of the cell (side scatter, SSC), respectively, allow sorting of the cells according to specific characteristics.

For analysis of cell coupling, HeLa CTL, HeLa 43, HeLa 43-GFP, HeLa 43NT-GFP and HeLa 43CT-GFP cells (dye donor cells) were seeded in 6-well-plates. The next day, these cells were washed twice with PBS- and stained with calcein-AM (final concentration: 0.2 µM; Invitrogen) for 30 min at 37 °C and 5 % CO_2. Calcein-AM is a membrane permeant nonfluorescent molecule. After diffusion into the cell, it is hydrolyzed by esterases (Figure II.2) and cannot further permeate the cell membrane except when it is transferred by gap junctions. Calcein binding to intracellular calcium ions results in a fluorescent complex with an excitation wavelength of 495 nm and an emission wavelength of 515 nm.

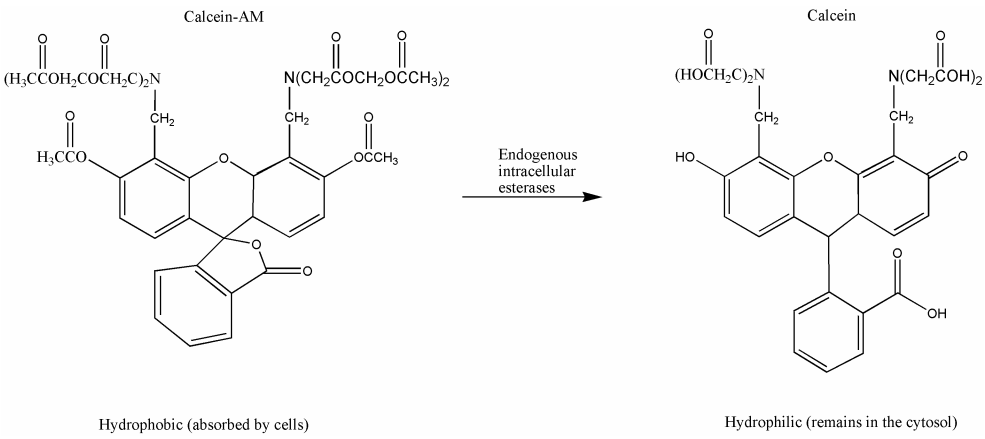

Figure II.2: Hydrolysis of calcein-AM
Calcein-AM is able to penetrate the cell membrane and, after hydrolysis by intracellular esterases to calcein, remains in the cytosol of the cell and can be detected by excitation at 495 nm.

After staining, the cells were washed four times with PBS- and incubated for 2 h at 37 °C and 5 % CO_2. A second cell population (dye acceptor cells), HeLa 43 cells, cultivated in a 100 mm culture dish, was stained with PKH26 Red Fluorescent Cell Linker Kit (Sigma). PKH26

is a fluorescent dye, which is incorporated into lipid regions of the cell membrane and can therefore not be transferred through gap junction channels. Its excitation maximum is at 551 nm, but it can also be excited at 488 nm, and its emission maximum is at 567 nm. Cells were washed with PBS- and 500 µl of Diluent C were added. 500 µl Diluent C and 3 µl PKH26 were mixed and transferred dropwise to the cells. After incubation for 3 min at 37 °C and 5 % CO_2, the staining reaction was stopped by adding 1 ml fetal calf serum (FCS). Subsequently, the cells were incubated in 10 ml cell culture medium for 2 h at 37 °C and 5 % CO_2. The cells were then trypsinized and resuspended in cell culture medium and a cell suspension of 140,000 cells/ml was prepared. 2 ml of this suspension were added to each well of calcein stained cells and cocultured for 3 h at 37 °C and 5 % CO_2. As controls, the calcein stained cells alone (0 h of coculture) and PKH26 stained HeLa 43 cells alone were used.

After coculture, the supernatants of each well were transferred to 15 ml Falcon tubes. The adherent cells were washed with PBS- and detached with 500 µl accutase. Accutase instead of trypsin was used, as it causes single isolated cells, which is important for the FACS measurement. The detached cells were resuspended in 5 ml cell culture medium and transferred to the supernatants in the appropriate Falcon tube. After centrifugation (1200 rpm; 5 min), the pellets were resuspended in 500 µl cell culture medium and transferred to FACS test tubes. 10,000 cells of each sample were analyzed by measuring the fluorescence of calcein stained (dye donor) cells as well as of PKH26 stained (dye acceptor) HeLa 43 cells at an excitation wavelength of 488 nm. Emission light of calcein and PKH26 was determined at 530 (FL-1) and 585 nm (FL-2), respectively.

The red stained HeLa 43 cells were selected and the fraction of double stained (red and green) cells, representing the amount of cells which were functionally coupled via gap junctions, was calculated.

2.1.5 Analysis of cell migration

Cell migration was analyzed using cell culture inserts for wound healing (Ibidi). A cell suspension of 9 x 10^5 cells/ml was prepared in cell culture medium containing only 0.5 % NBCS. 70 µl of this cell suspension were transferred into both wells of a silicone insert (growth area 0.22 cm^2 per well; Figure II.3), which was placed in a 35 mm culture dish. The next day, after appropriate cell attachment, the insert was removed using sterile tweezers, creating a defined cell free gap of approximately 500 (± 50) µm between both cell populations. Cell migration into the cell free gap was started by adding cell culture medium

containing 10 % NBCS and observed for 24 h by live cell imaging using time lapse microscopy.

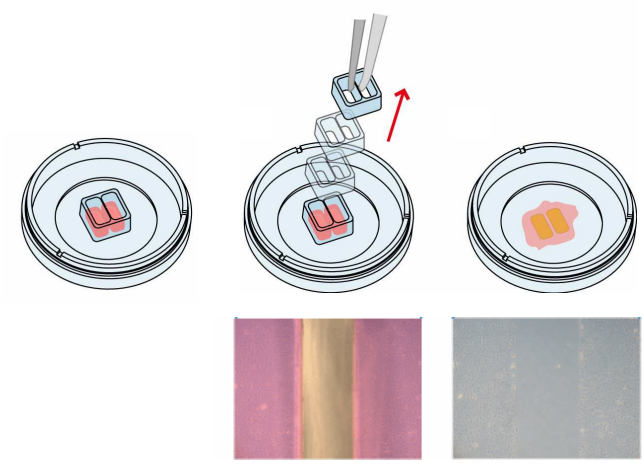

Figure II.3: Schematic illustration of cell culture inserts (Ibidi)
Cells were plated in the two wells of the insert. After cell adhesion, the insert was removed using sterile tweezers and the cells migrated into the defined cell free gap (modified after Ibidi manual for culture inserts: http://www.ibidi.com/products/disposables/E_8XXXX_CultureInsert/IN_8XXXX_CI.pdf).

For that purpose, a microscope (Zeiss Axio observer) was equipped with a life cell imaging system (Ibidi) composed of a heating system and a gas mixer, which allowed controlled culture conditions with a humidified atmosphere at 37 °C and 5 % CO_2 (Figure II.4).

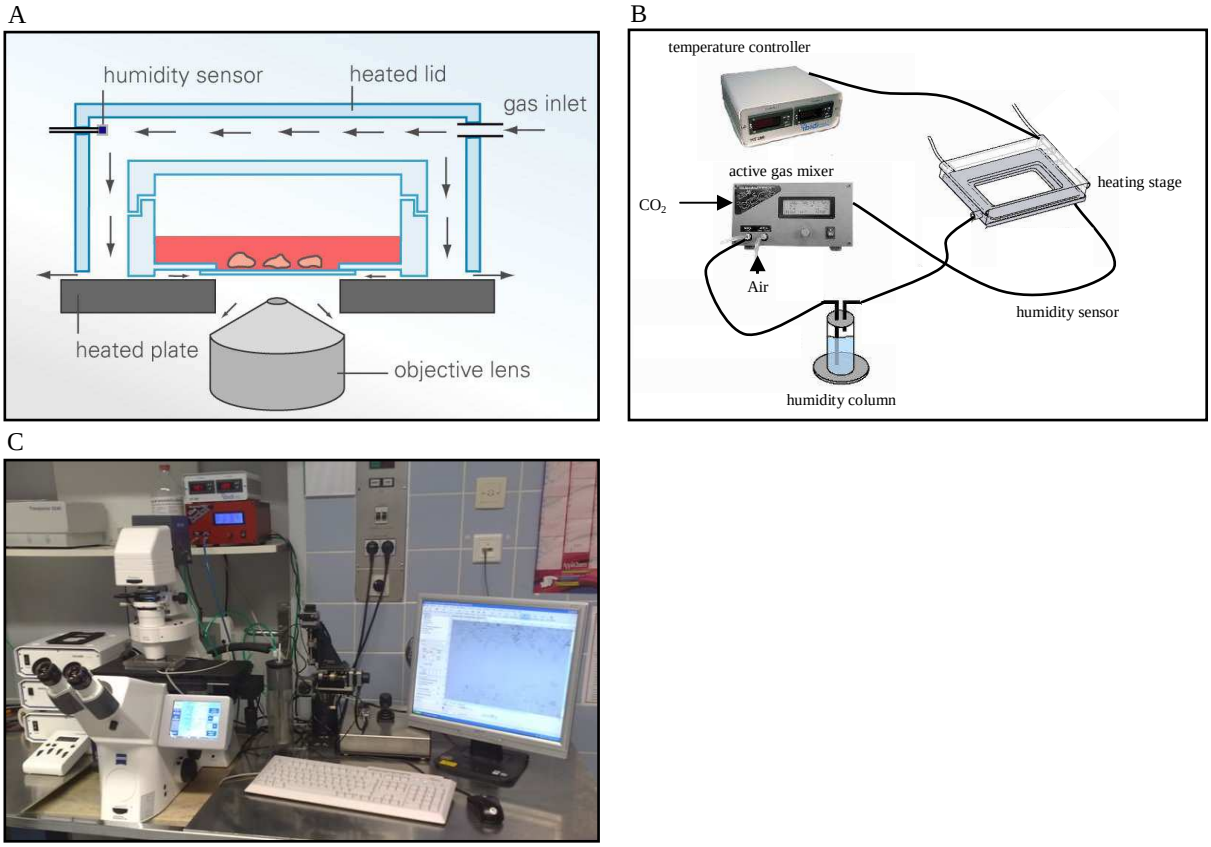

Figure II.4: Experimental settings for live cell imaging
A: Schematic illustration of the gas flow in the heated stage (Ibidi application manual), B: Schematic illustration of the experimental settings (modified after Ibidi application manual), C: Image of the experimental settings.

The microscope was connected to a computer equipped with the AxioVision software (Zeiss) and images were taken with an AxioCam camera (Zeiss) every 10 min for 24 h. For assay analysis, cells were tracked using the manual tracking software component of the ImageJ programme. After tracking, the cell paths were analyzed using the *Chemotaxis and Migration tool*, a free ImageJ plugin provided by Ibidi to compute the following parameters: center of mass (center of mass of all endpoints), accumulated distance (mean distance of all cell paths), euclidian distance (direct connection from starting point to end point), directionality, and velocity. Directionality was calculated by dividing euclidian distance by accumulated distance. The closer this value was towards 1, the higher directionality the cells had shown during migration. Velocity of the cells was calculated by dividing accumulated distance (in µm) by migration time (in sec).

2.2 Cloning of cDNAs encoding truncated Cx43 proteins

For cloning of cDNAs encoding truncated Cx43 proteins, the vector pcDNA4-myc-His Version B (Invitrogen) or the plasmid pcDNA4-GFP was used (Figure II.5).

The GFP plasmid pcDNA4-GFP was generated by amplification and subcloning of the open reading frame of the green fluorescent protein (GFP; variant sg143GFP) by PCR from the plasmid pFred143, which has been published previously [175] [117], into the vector pcDNA4-myc-His Version B using the restriction enzymes XbaI and PmeI. Consequently, the myc-His-tag was no longer expressed. For the plasmids Cx43(tr299)-GFP, Cx43(tr336)-GFP, and Cx43(299-336)-GFP, GFP was amplified and subcloned without the first ATG start-codon. The cDNAs encoding truncated Cx43 proteins without a stop-codon were cloned into the pcDNA4-GFP vector using the restriction enzymes BamHI and XhoI to ensure a continuous transcription of Cx43 fragments coupled with GFP.

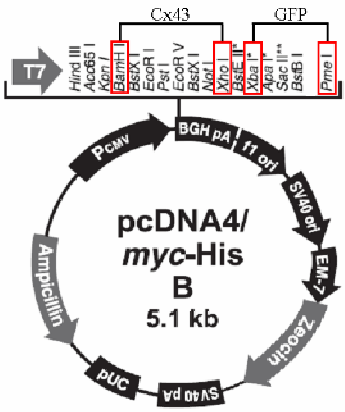

Figure II.5: Modified vector map of pcDNA4-myc-His Version B (Invitrogen)
Unique restriction sites, used for insertion of DNA fragments encoding Cx43 or truncated Cx43 proteins (BamHI; XhoI) and GFP (XbaI; PmeI), are displayed (red boxes).

2.2.1 Preparation of plasmid DNA

The plasmid DNA was augmented by bacterial transformation using LB agar plates containing 100 µg/ml ampicillin and one bacterial colony was incubated in LB medium [8], supplemented with 100 µg/ml ampicillin, overnight for amplification. Plasmid DNA was isolated from bacterial cells using either Qiaprep Spin Miniprep (15 – 20 µg DNA) or Hispeed Plasmid Maxi Kit (400 – 500 µg DNA) according to the manufacturer's protocol (Qiagen). In both isolation methods the plasmid DNA is, after alkaline lysis, bound to an anion-exchange resin in a column and impurities such as RNA and proteins are removed by several washing steps.

2.2.2 Polymerase chain reaction (PCR)

The polymerase chain reaction (PCR) allows amplification of a specific target DNA out of a pool of DNA. Two specific primers, complementary to the 3´ ends of sense and anti-sense strands of the target DNA, bind to the DNA strands and are elongated by a DNA polymerase in repeated cycles of three major steps: DNA denaturation, primer annealing and primer elongation.

The cDNAs, encoding the truncated proteins of Cx43, were all synthesized by PCR using rat Cx43 cDNA as template and self-designed primer pairs (Table II.4). Unique restriction sites are underlined and the start-codon ATG is in bold.

Table II.4: Created cDNAs and primer pairs used for PCR; restriction enzymes for cloning; expected protein mass and number of base pairs of the cDNAs is displayed

cDNA	**Forward primer 5´ → 3´**	**Revers primer 5´ → 3´**	**Restriction enzymes**	**Protein mass [kDa]**	**Number of base pairs [bp]**
rCx43 (aa 1 – 382)	CTC GGA TCC **ATG** GGT GAC TGG AGT	CGA CTC GAG CGA ATC TCC AGG TCA TC	BamH1; XhoI	69.9 (with GFP-tag)	1146
rCx43NT (aa 1 – 257)	CTC GGA TCC **ATG** GGT GAC TGG AGT	GCT CTC GAG TGA TGG GCT CAG TGG	BamH1; XhoI	55.4 (with GFP-tag)	771
rCx43CT (aa 257 – 382)	GCC **ATG** TCA AAA GAC TGC GGA	AAT CTC CAG GTC ATC AGG CCG	BamH1; XhoI	40.8 (with GFP-tag)	375
rCx43(tr298) (aa 1 – 298)	CTC GGA TCC **ATG** GGT GAC TGG AGT	GCT CTC GAG CGG CAC GAG GAA TTG TT	BamH1; XhoI	60.0 (with GFP-tag)	894
rCx43(tr336) (aa 1 – 336)	CTC GGA TCC **ATG** GGT GAC TGG AGT	AAT CTC GAG CGA TCG AAC GGC TGG GC	BamH1; XhoI	64.2 (with GFP-tag)	1008
rCx43(299–336) (aa 299 – 336)	GCT GGA TCC **ATG** CGC AAT TAC AAC AAG	AAT CTC GAG CG ATC GAA CGG CTG GGC	BamH1; XhoI	30.1 (with GFP-tag)	111
GFP	GAC GA TCT AGA G **ATG** GCT AGT TCC GGA GGT	CGA G GT TTA AAC TCA ACC GTA CAG CTC GTC	Xba1; Pme1	26.9	741
GFP without start-codon ATG	GAC GA TCT AGA G GCT AGT TCC GGA GGT	CGA G GT TTA AAC TCA ACC GTA CAG CTC GTC	Xba1; Pme1	26.8	738

PCR was performed using standard protocols (PCR protocol is listed in table II.5, PCR settings are listed in table II.6. Herculase was used as DNA polymerase because of its proof-reading capability.

Table II.5: PCR protocol

Substance	**Amount [µl]**
Template DNA rCx43 (1µg/µl)	1.0
Primer forward (100 pm/µl)	2.0
Primer revers (100 pm/µl)	2.0
dNTPs (10 mM)	1.5
Herculase buffer (5x)	10.0
Herculase	1.0
Aqua ad iniectabilia	32.5

Table II.6: PCR settings

Step	**Temperature [°C]**	**Duration**	**Number of cycles**
Initial denaturation of the DNA template	95	2 min	1
Denaturation of synthesized DNA strands	95	20 sec	30
Primer annealing	60	15 sec	
Primer elongation	72	30 sec	
Final elongation	72	3 min	1

The optimal temperature for primer annealing was adjusted to the appropriate primer pairs by performing a gradient PCR with different temperatures in the range of 55 – 65 °C. Elongation time of 30 sec was sufficient for all cDNA constructs.

2.2.3 Agarose gel electrophoresis

The PCR product was determined by agarose gel electrophoresis, which reveals a single band due to amplification of a single segment of the target DNA. 1 % agarose was dissolved in TBE 1x buffer by heating the solution in a microwave for about 2 – 3 min until the agarose was completely solved. Subsequently, the solution was cooled down to 40 – 50 °C and, after addition of ethidium bromide (0.05 µg/ml), filled in a gel electrophoresis chamber. After gel

polymerization, 5 µl of the PCR product was mixed with 1 µl of 6x sample buffer and loaded onto the gel together with a 1 kb gene ruler and, for the analysis of small PCR products, with a 100 bp gene ruler. Electrophoresis was performed at 90 volts (1.1 V/cm^2) for 45 min and the separated DNA was observed under UV light and pictures were taken with the gel documentation system (Gel Doc 1000; BIO-RAD Laboratories).

TBE 10x
Tris HCl 890 mM
Boric acid 890 mM
EDTA 20 mM
Aqua dem. ad 1000 ml
pH 8.5

2.2.4 Purification of the PCR product

The PCR product was purified using the Qiaquick PCR purification kit (Qiagen) according to the manufacturer's protocol. Briefly, the DNA is bound to a silica membrane and primers, nucleotides, salt and other impurities are removed by several washing steps. Subsequently, the DNA is eluted from the membrane.

2.2.5 Digestion of DNA with restriction enzymes

The purified PCR product and also the vector pcDNA4-GFP were both digested overnight at 37 °C using the restriction enzymes BamHI and XhoI as specified in tables II.7 and II.8.

Table II.7: Protocol for digestion of the PCR product

Substance	**Amount**
PCR product	4.0 µg
BamHI (20,000 U/ml)	0.5 µl
XhoI (20,000 U/ml)	0.5 µl
Enzyme buffer 10x (NEB buffer 3)	6.0 µl
BSA 10x	6.0 µl
Aqua ad iniectabilia	ad 60.0 µl

Table II.8: Protocol for digestion of the pcDNA4-GFP vector

Substance	**Amount**
Vector pcDNA4-GFP	1.0 µg
BamHI (20,000 U/ml)	0.5 µl
XhoI (20,000 U/ml)	0.5 µl
Enzyme buffer 10x (NEB buffer 3)	2.0 µl
BSA 10x	2.0 µl
Aqua ad iniectabilia	ad 20.0 µl

2.2.6 Isolation of DNA from agarose gels

Digested DNA of PCR product and vector were separated by agarose gel electrophoresis (1 % agarose gel). Extraction and purification of DNA fragments from the agarose gel were performed using the Qiaquick gel extraction kit (Qiagen) according to the manufacturer's protocol. DNA concentration was measured photometrically at 260 nm due to emission maximum of the DNA bases at this wavelength. Additional measurement at 280 nm allowed evaluation of the purity, as for example proteins which could remain after DNA purification show an emission maximum at this wavelength. The quotient of the value at 260 nm/value at 280 nm had to be in the range of 1.8 – 2.0 to consider the DNA as sufficiently pure.

2.2.7 DNA ligation

DNA ligation was used to insert DNA fragments of Cx43 into the vector pcDNA4-GFP. The mechanism of a DNA ligase is to form phosphodiester bonds between the 3´ hydroxyl ends of one nucleotide with the 5´ phosphate ends of another. This results in covalent binding of vector and DNA fragment. To ligate vector and DNA, both were digested with the same restriction enzymes to generate compatible DNA overhangs. For DNA ligation the rapid DNA ligation kit (Roche) including a T4 DNA ligase was used according to the manufacturer's protocol. The molar ratio of vector DNA to insert DNA was 1:5 and usually 50 ng of linearized dephosphorylated vector DNA was used.

2.2.8 Transformation of DNA in bacteria

The recombinant plasmids were transferred and amplified in bacterial strains by bacterial transformation. In this technique the plasmid is introduced into bacteria and replicated by the bacterial DNA polymerases independently of the host cell chromosomes. In the present study XL1-Blue supercompetent cells (Stratagene) were used. For heat shock transformation 40 µl

XL1-Blue supercompetent cells were thawed on ice in a 1.5 ml tube, mixed with 0.8 µl β-mercaptoethanol for increasing the transformation efficiency, and incubated for 10 min on ice with gentle shaking every 2 min. Subsequently, 7 µl of the ligation mixture were added and the tube was incubated on ice for 30 min. As negative control one tube was left without ligation mixture. The tube was heat-pulsed in a 42 °C water bath for 45 sec and subsequently incubated on ice for 2 min. 450 µl LB medium [8], preheated to 37 °C, were added and the tube was incubated at 37 °C for 1 h with shaking at 350 rpm. This step allows bacteria to recover from the heat shock and to express the antibiotic resistance gene.

LB-Amp agar plates were prepared using 15 ml liquefied LB agar, supplemented with 100 µg/ml ampicillin, due to an ampicillin resistance on the vector, which were poured into bacterial plates (100 mm diameter). One plate without addition of ampicillin was used as positive control for bacterial growth. The transformation reaction was plated on the LB-Amp agar plates (50 and 200 µl transformation reaction, respectively) and the plates were incubated bottom-up at 37 °C overnight for bacterial colony formation.

In order to screen for positive E. coli transformants, carrying the desired plasmid DNA, bacterial colonies were picked using autoclaved toothpicks and incubated in 15 ml Falcon tubes in 5 ml LB-Amp medium, supplemented with 100 µg/ml ampicillin, at 37 °C overnight with shaking for amplification. Mini preparations of plasmid DNA were performed using Qiaprep Spin Miniprep (Qiagen) according to the manufacturer's protocol as described above (chapter II.2.2.1), followed by restriction analysis (chapter II.2.2.5) to determine the correct size of the DNA insert. Finally the authenticity of the DNA sequence was verified by sequencing, which was carried out using commercial services (MWG Eurofins).

<u>LB medium</u>

Trypton (Pepton from Casein)	10.0 g
Yeast extract	5.0 g
NaCl	5.0 g
Aqua dem.	ad 1000.0 ml

<u>LB agar</u>

Trypton (Pepton from Casein)	10.0 g
Yeast extract	5.0 g
NaCl	5.0 g
Aqua dem.	ad 1000.0 ml
Agar	12.0 g

2.3 Protein biochemistry

2.3.1 Western blot analysis

2.3.1.1 SDS-Polyacrylamid gel electrophoresis (SDS-PAGE)

The expression of proteins of interest was investigated with SDS-PAGE followed by western blot analysis. For SDS-PAGE the Laemmli sample buffer [99] was used for sample preparation. This buffer contains β-mercaptoethanol, which reduces disulfide bonds, and sodium dodecylsulfate (SDS) that destroys the secondary and tertiary protein structure and therefore leads to negatively charged SDS-protein complexes in a way that a negative charge is applied to each protein in proportion to its mass. The negatively charged protein complexes can be separated in a polyacrylamide gel as the small proteins migrate faster towards the anode than the bigger proteins.

The polyacrylamide gel was composed of a separating and a stacking gel. First the separating gel was prepared containing 10 % polyacrylamide. Ammonium persulfate (APS) functioned as initiator for gel polymerization and N,N,N´,N´-tetramethylethylenediamine (TEMED) as catalyst. After gel polymerization the stacking gel was prepared containing 4 % polyacrylamide.

Sample preparation for SDS-PAGE: cell lysates were prepared by washing confluent cell monolayers with PBS- and subsequent cell lysis with an appropriate amount of Laemmli sample buffer (e.g. cell amount of one 6-well: 6 x 10^5 cells/100 µl). The cell lysates were kept on ice for 10 min and could be stored at -20 °C. For electrophoresis the samples were thawed on ice, heated at 100 °C for 5 min for protein denaturation and size-separated by SDS-PAGE at 0.3 mA/cm^2 using the Mighty Small II unit for 8 x 9 cm gels (Amersham Biosciences), filled with 1x electrophoresis buffer. A protein standard (Fermentas) was used for size determination.

<u>Separating gel 10 %</u>

Aqua dem.	4.0 ml
Tris/HCl 1.5 M pH 8.8	2.5 ml
SDS 10 %	100.0 µl
Polyacrylamid 30 %	3.3 ml
APS 10 %	50.0 µl
TEMED	5.0 µl

<u>Stacking gel 4 %</u>

Aqua dem.	6.0 ml
Tris/HCl 0.5 M pH 6.8	2.5 ml
SDS 10 %	100.0 µl
Polyacrylamid 30 %	1.3 ml
APS 10 %	65.0 µl
TEMED	5.0 µl

<u>Laemmli sample buffer</u>

Tris	62.5 mM
SDS	2 %
Glycerol	25 %
Bromphenolblau	0.01 %

(before use add 0.5 % β-Mercaptoethanol)

<u>Electrophoresis buffer 5x</u>

Tris	75.0 g
Glycine	360.0 g
SDS	25.0 g
Aqua dem.	ad 5000 ml

2.3.1.2 Semi-dry blotting

The separated proteins were transferred from the polyacrylamide gel to a PVDF-membrane by semi-dry blotting. The PVDF-membrane (Amersham Hypond-P; GE Healthcare) and two pieces of blotting paper (Gel blotting paper GB003; Whatman) were cut according to the size of the gel. The PVDF-membrane was soaked in methanol for 5 sec and subsequently in western transfer buffer; the pieces of blotting paper were soaked only in western transfer buffer. The following setup was prepared on the blotting unit: blotting paper, membrane, gel, blotting paper. The blotting unit was connected to anode and cathode and the proteins were electrotransferred from the gel onto the membrane (from negative to positive pole) at 1.1 mA/cm^2 for 90 min. After protein transfer the membrane was washed in washing buffer for 10 min and then blocked in 1x blocking reagent (Roche) in washing buffer for 1 h.

Western transfer buffer	
Tris	5.8 g
Glycine	2.9 g
SDS 10 %	3.7 ml
Methanol	200 ml
Aqua dem. ad 1000 ml	

Washing buffer
PBS 1x
Tween 0.1 %

2.3.1.3 Protein detection by western blot analysis

The membrane was incubated overnight at 4 °C with the primary antibody diluted in 0.5x blocking reagent (Roche) in washing buffer under gentle agitation. After washing three times for 10 min with washing buffer, the membrane was incubated with the horseradish peroxidase-labeled secondary antibody, diluted in 0.5x blocking reagent (Roche) in washing buffer for 1.5 h, at room temperature under gentle agitation. Afterwards, the membrane was washed three times for 10 min with washing buffer. Detection of the proteins was performed using the enhanced chemiluminescence (ECL) detection system kit (Applichem), which is based on the emission of light during the oxidation of luminol by hydrogen peroxide, catalyzed by the enzyme horseradish peroxidase (HRP). The kit contains two solutions, luminol substrate and peroxide solution, which were mixed in a 1:1 ratio. The membrane was incubated in this mixture and proteins were observed using a Digital CCD Camera that was connected to a computer with the Wasabi imaging software (Hamamatsu Photonics).

Used antibodies and their dilution factors are specified in table II.9.

Table II.9: Antibodies used for western blot analysis and their dilution factors

Primary antibody	**Dilution**	**Secondary antibody**	**Dilution**
Cx43 (polyclonal)	1:1000	Anti-rabbit	1:2000
Cortactin (monoclonal)	1:500	Anti-mouse	1:2000
GAPDH (monoclonal)	1:5000	Anti-mouse	1:5000
GFP (polyclonal)	1:2000	Anti-rabbit	1:3000
NOV (CCN3) (polyclonal)	1:500	Anti-goat	1:2000

2.3.1.4 Membrane stripping

The primary and secondary antibodies can be removed from a western blot membrane by stripping. This is recommendable when detecting several antigens on one western blot. For stripping the antibodies, the membrane was incubated in stripping buffer for 1 h at room temperature under gentle agitation. After blocking for 1 h in 1x blocking reagent (Roche) in washing buffer, the blot could be incubated with the next desired primary antibody.

Stripping buffer (pH 2.8)
Glycine 15.01 g
NaCl 29.22 g
Aqua dem. ad 1000 ml

2.3.2 Immunoprecipitation

Immunoprecipitation is a method for identifying complexes of interacting proteins in cell extracts by using an antibody specific for one of the proteins to precipitate the complex. Affinity reagents that bind to the antibody are coupled to a solid matrix and are then used to drag the complex out of solution. If the protein is associated tightly enough with another protein, while captured by the antibody, the partner precipitates as well. Cell lysates were prepared by washing a confluent cell monolayer (culture plate 10 mm diameter; about 5 x 10^6 cells) with ice-cold PBS-, subsequent adding of 1 ml ice-cold Triton X-100 lysis buffer and incubation on ice for 10 min. Cells were scraped off the plate using a cell scraper, transferred into a 1.5 ml tube, and incubated on ice for additional 20 min. Afterwards, they were centrifuged for 10 min at 10,000 rpm and 4 °C. The supernatant was transferred to a fresh 1.5 ml tube and the pellet consisting of unsolved cell particles and membranes, was solved in the remaining supernatant by sonication (one pulse for 2 sec at 10 % output power, level 3.5). The samples were reunited and again centrifuged for 10 min at 10,000 rpm and 4 °C. The cell lysates (500 µl) were then incubated with the appropriate magnetic protein beads (50 µl; µMACS Micro beads, Miltenyl Biotec) and the specific antibody (5 µg) on ice for 30 min,

followed by an additional incubation step at 4 °C overnight to allow the formation of a protein-antibody-beads-complex. Immunoprecipitation was performed using a magnetic separation unit (µMACS Separation unit, Miltenyl Biotec) and µ Columns (MACS, Miltenyl Biotec). The columns were washed with 200 µl Triton X-100 lysis buffer and subsequently the samples were loaded on the columns. The magnetic beads and bound proteins attached to the magnetic column, while the rest of the sample flowed through. The columns were washed four times with 200 µl Triton X-100 lysis buffer and once with 100 µl low salt buffer. The specific bound proteins were solved from the column by adding 20 µl Laemmli sample buffer, pre-heated to 100 °C, and incubation for 5 min. Afterwards, 50 µl Laemmli sample buffer, pre-heated to 100 °C, were added and the sample was completely eluted from the column. The samples were boiled again at 100 °C for 5 min and immediately investigated by SDS-PAGE and western blot analysis (chapter II.2.3.1). Antibodies, used for immunoprecipitation, and appropriate protein beads are specified in table II.10.

Table II.10: Antibodies and appropriate protein beads used for immunoprecipitation

Antibody	**Protein beads**
Cx43 (polyclonal)	Protein A
Cortactin (monoclonal)	Protein G
GFP (polyclonal)	Protein A
NOV (polyclonal)	Protein G

<u>Triton X-100 lysis buffer</u> (pH 8.0)

NaCl	150 mM (0.87 g)
Triton X-100	1 %
Tris HCl	50 mM (0.60 g)
Aqua dem.	ad 100 ml

<u>Low salt buffer</u>

Tris HCl	20 mM (0.24 g)
Aqua dem.	ad 100 ml

2.4 Confocal laser scanning microscopy

In this study a confocal laser scanning microscope (TCS SP5; Leica) was used, which was equipped with one argon (488 nm) and two helium-neon (543 and 633 nm) lasers. A confocal laser scanning microscope uses point illumination by a laser, thus only one specific plane of the sample is in focus (focal plane). Additionally, a pinhole arranged in front of the detector eliminates out of focus signals, resulting in an increased optical resolution of the image. The emitted fluorescence from the focal plane is detected by a photomultiplier tube (PMT) (Figure II.6). Confocal scanning of sequential levels of the sample allows reconstruction of a three-dimensional image.

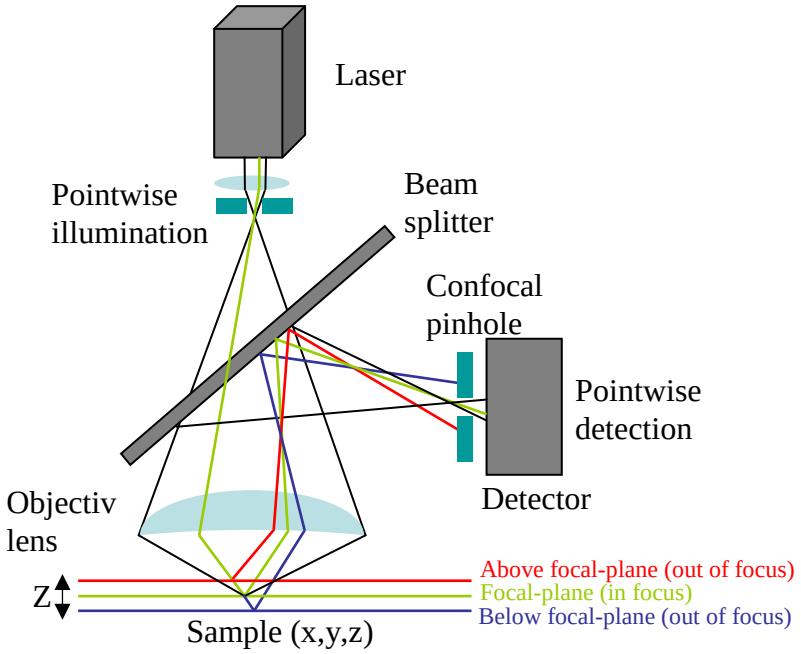

Figure II.6: Principle of a confocal laser scanning microscope
The sample is illuminated pointwise by a laser and, additionally, a pinhole in front of the detector allows detection of only signals of the sample in focus (focal plane) and eliminates out of focus signals thus increasing the optical resolution of the image.

2.4.1 Immunofluorescence staining

Besides detection by western blot analysis, proteins can also be determined by immunofluorescence. This technique offers the advantage to visualize localization of the proteins and also colocalization with other proteins within the cell. Specific secondary antibodies are used, labeled with a fluorophore (e.g. Alexa Fluor), which can be detected by excitation at a specific wavelength using a laser.

For immunofluorescence stainings, HeLa cells were seeded in cell culture medium on glass cover slips (15 mm diameter). The next day the medium was removed and the cells were washed twice with PBS supplemented with magnesium and calcium ions (PBS+). The cells

were fixed with 3.5 % formaldehyde solution in PBS+ for 20 min. After washing twice with PBS+, the cells were permeabilized with 0.1 % TritonX-100 in PBS+ for 5 min. Subsequently, the cells were washed twice with PBS+ and then incubated with 1 % BSA in PBS+ for 1 h at room temperature to block unspecific protein bindings. Afterwards, the cells were incubated with the primary antibody diluted in 0.2 % BSA in PBS+ overnight at 4 °C (except for the cortactin antibody, which was incubated with the cells at 37 °C and 5 % CO_2). After washing three times with PBS+, the cells were incubated with either an Alexa Fluor 488-coupled or an Alexa Fluor 546-coupled secondary antibody, diluted 1:200 in 0.2 % BSA in PBS+, for 45 min at room temperature. As negative control only secondary antibody was added to one glass cover slip. Afterwards, the cells were washed three times with PBS+ and the glass cover slips were placed cell-side down in a drop of Immu-Mount mounting solution on a microscope slide. After drying, the glass cover slips were sealed with nail polish. The cells were observed by LSM using a 63-fold oil objective and different zoom factors. Used antibodies and their dilution factors are specified in table II.11.

Table II.11: Antibodies used for immunofluorescence stainings and their dilution factors

Primary antibody	**Dilution**	**Secondary antibody**	**Dilution**
Cx43 (polyclonal)	1:100	Anti-rabbit-Alexa Fluor 488	1:200
Cortactin (monoclonal)	1:50	Anti-mouse-Alexa Fluor 546	1:200
GFP (polyclonal)	1:100	Anti-rabbit-Alexa Fluor 488	1:200

<u>Phosphate buffered saline (PBS+)</u>

NaCl	8.0 g
KCl	0.4 g
Mg_2SO_4 x 7 H_2O	0.074 g
MgCl x 6 H_2O	0.074 g
$CaCl_2$	0.138 g
Na_2HPO_4 x 2 H_2O	0.15 g
KH_2PO_4	0.06 g
Glucose	1.0 g
$NaHCO_3$	0.3 g
Aqua ad iniectabilia	ad 1000.0 g

2.4.2 Staining of the actin cytoskeleton

The actin cytoskeleton can be stained using phallotoxins. These phallotoxins were isolated from the deadly *Amanita phalloides* mushroom and are bicyclic peptides, which bind to F-actin. In this study Alexa Fluor 488-coupled phalloidin with an excitation wavelength of 495

nm and Alexa Fluor 546-coupled phalloidin with an excitation wavelength of 556 nm were used.

2.4.2.1 Staining of migrating HeLa cells

Cells were plated in cell culture inserts for wound healing (chapter II.2.1.5) in an 8-well µ-slide (Ibidi). After migration for 24 h, the medium was removed and the cells were washed twice with PBS+ and subsequently fixed with 3.5 % formaldehyde in PBS+ for 20 min. After washing twice with PBS+, the cells were permeabilized with 0.1 % TritonX-100 in PBS+ for 5 min. Unspecific bindings were blocked with 1 % BSA in PBS+ for 30 min. Subsequently, the cells were stained with 5 µl Alexa Fluor-coupled phalloidin diluted in 200 µl 1 % BSA in PBS+ for 30 min at room temperature. Afterwards, the cells were washed three times with PBS+. After the last washing step 200 µl PBS+ were left on the cells and they were observed by LSM. The length of individual filopodia of a single cell was determined using the Zeiss Axiovision software and the distance from the filopodium starting point at the cell membrane to its tip was measured. The amount of the measured values equates the quantity of filopodia per single cell. 14 cells in four independent experiments were analyzed for each transfected HeLa cell population.

2.4.2.2 Staining of HeLa cells after inhibition of p38 MAPK

HeLa 43 and HeLa CTL cells were seeded on glass cover slips (15 mm diameter) in a 24-well-plate, in a way that they are about 50 % confluent the next day. Then they were incubated overnight with cell culture medium containing only 0.5 % NBCS. The next day, half of the cells were incubated for 1 h with the specific p38 MAPK inhibitor SB203580 with a final concentration of 25 µM, whereas the other half was left without addition of SB as controls. Afterwards, the medium was replaced with cell culture medium containing 10 % NBCS and the cells were incubated for further 4 h, half of the cells again after addition of SB203580 (25 µM). Subsequently, the cells were fixed and stained as described in chapter II.2.4.2.1 and the glass cover slips were placed cell-side down in a drop of Immu-Mount mounting solution on a microscope slide. After drying, the glass cover slips were sealed with nail polish. Cells were observed by LSM. Analysis of filopodia formation was performed as described in chapter II.2.4.2.1

3 Statistics

Each experiment was repeated at least four times and the data of each series is displayed as mean values + SEM. For statistical analysis, the software SigmaStat for windows version 2.0 (Jandel Corporation) was used. The samples were compared with each other by one way analysis of variance (ANOVA) followed by the Student-Newman-Keuls test. P-values less than 0.05 were considered to be significant.

III Results

1 Generation and functional analysis of truncated Cx43 proteins

1.1 Generation and separate expression of the N-terminal and the C-terminal part of Cx43 in HeLa cells

To analyze which part of Cx43 influences cell migration, cDNAs were created encoding either the N-terminal part (aa 1 – 257), which represented the channel building part of Cx43 (Cx43NT-GFP), or the C-terminal part (aa 257 – 382), representing the cytoplasmic adapter part of Cx43 (Cx43CT-GFP). Both truncated proteins were tagged with the green fluorescent protein (GFP) in order to detect their localization by fluorescence microscopy and their expression by western blot analysis. As controls a cDNA encoding full length Cx43 protein tagged with GFP (aa 1 – 382, Cx43-GFP), and also a cDNA encoding only GFP were created. HeLa wild-type cells, which do not express connexins and therefore lack gap junctional communication, were stably transfected with Cx43NT-GFP (HeLa 43NT-GFP cells), Cx43CT-GFP (HeLa 43CT-GFP), Cx43-GFP (HeLa 43-GFP), GFP (HeLa GFP) and the empty vector pcDNA4 (HeLa CTL), respectively. Single cell clones were investigated for their expression of the appropriate proteins by western blot using a polyclonal antibody against GFP. HeLa 43NT-GFP cells showed a protein band at the predicted molecular mass of 55 kDa (29 kDa 43NT + 26 kDa GFP), HeLa 43CT-GFP at 41 kDa (15 kDa 43CT + 26 kDa GFP) and HeLa GFP at 26 kDa. GAPDH was used as loading control (Figure III.1).

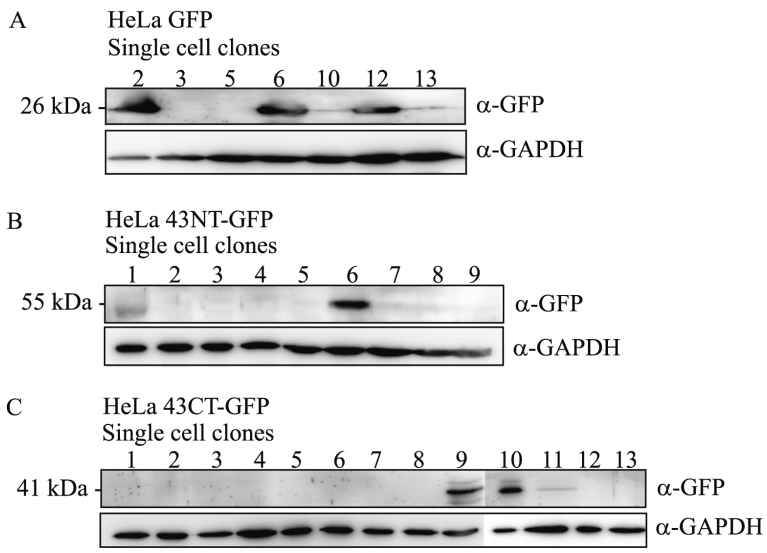

Figure III.1: Expression of single cell clones of truncated Cx43 proteins
Single cell clones of stably transfected HeLa cells were investigated for the expression of (A) GFP, (B) Cx43NT-GFP, and (C) Cx43CT-GFP by western blot analysis using a polyclonal antibody against GFP. GAPDH was used as loading control.

The cell clones 2, 6 and 12 of HeLa GFP cells showed a strong expression of GFP. Clone 2 was selected for further investigations. Since clone 6 of HeLa 43NT-GFP cells was the only one (out of 10 selected) expressing the protein with the expected molecular mass, this clone was taken for further experiments. Two clones of HeLa 43CT-GFP cells (clone 9 and 10) displayed expression of the protein with the expected molecular mass and clone 10 was used in further experiments. The expression of the selected cell clones of HeLa 43NT-GFP and HeLa 43CT-GFP cells compared to full length Cx43 (without GFP-tag; HeLa 43) and HeLa CTL is shown in figure III.2. HeLa 43 cells showed a triple band at the expected protein size of 43 kDa which is presumably due to phosphorylation events and conformational changes of the protein. HeLa CTL cells showed neither Cx43 nor GFP expression as expected. HeLa 43NT-GFP and HeLa 43CT-GFP cells showed protein bands at 55 and 41 kDa, respectively (Figure III.2).

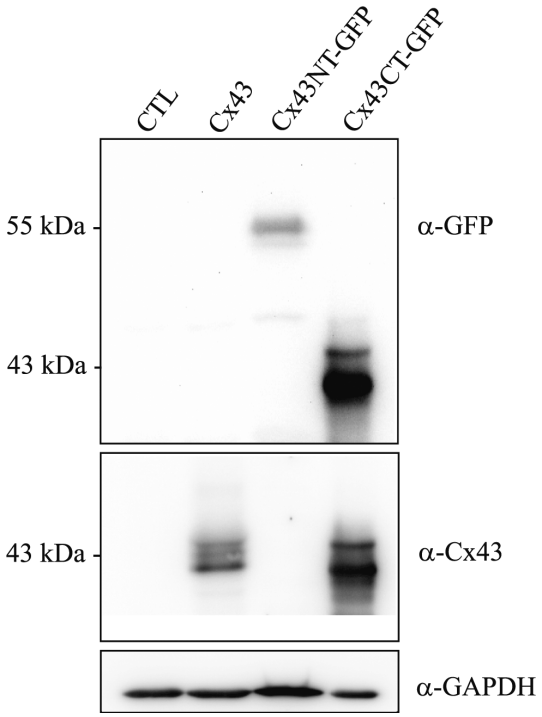

Figure III.2: Expression of Cx43 and truncated proteins in HeLa cells
Expression of the selected cell clones of HeLa 43NT-GFP (clone 6) and HeLa 43CT-GFP (clone 10) cells was analyzed by western blot using a polyclonal antibody against GFP. Subsequent incubation of the membrane with a polyclonal antibody against Cx43 revealed expression of Cx43 in HeLa 43 cells. HeLa CTL cells showed neither expression of GFP nor Cx43. GAPDH was used as loading control.

Expression of HeLa 43-GFP cell clones was observed by LSM using fluorescence of the GFP-tag. One clone out of ten selected single cell clones (clone 8) exhibited expression of the GFP-tagged protein and thus these cells were used for further experiments (Figure III.3).

Localization of the truncated proteins was analyzed using LSM and compared to the localization of the full length Cx43 without GFP-tag, which was detected by immunofluorescence staining with a polyclonal antibody against Cx43 (Figure III.3).

Cx43 in HeLa 43 cells was localized at the membrane mainly at cell-cell contacts and at perinuclear regions. Cx43-GFP and Cx43NT-GFP were both also localized at the membrane. However, compared to the punctate pattern of Cx43, the expression of the GFP-tagged proteins looked differently as they were localized in the whole membrane and not exclusively at cell-cell contacts. In contrast, Cx43CT-GFP and GFP were localized in the cytosol and partly in the nucleus (Figure III.3).

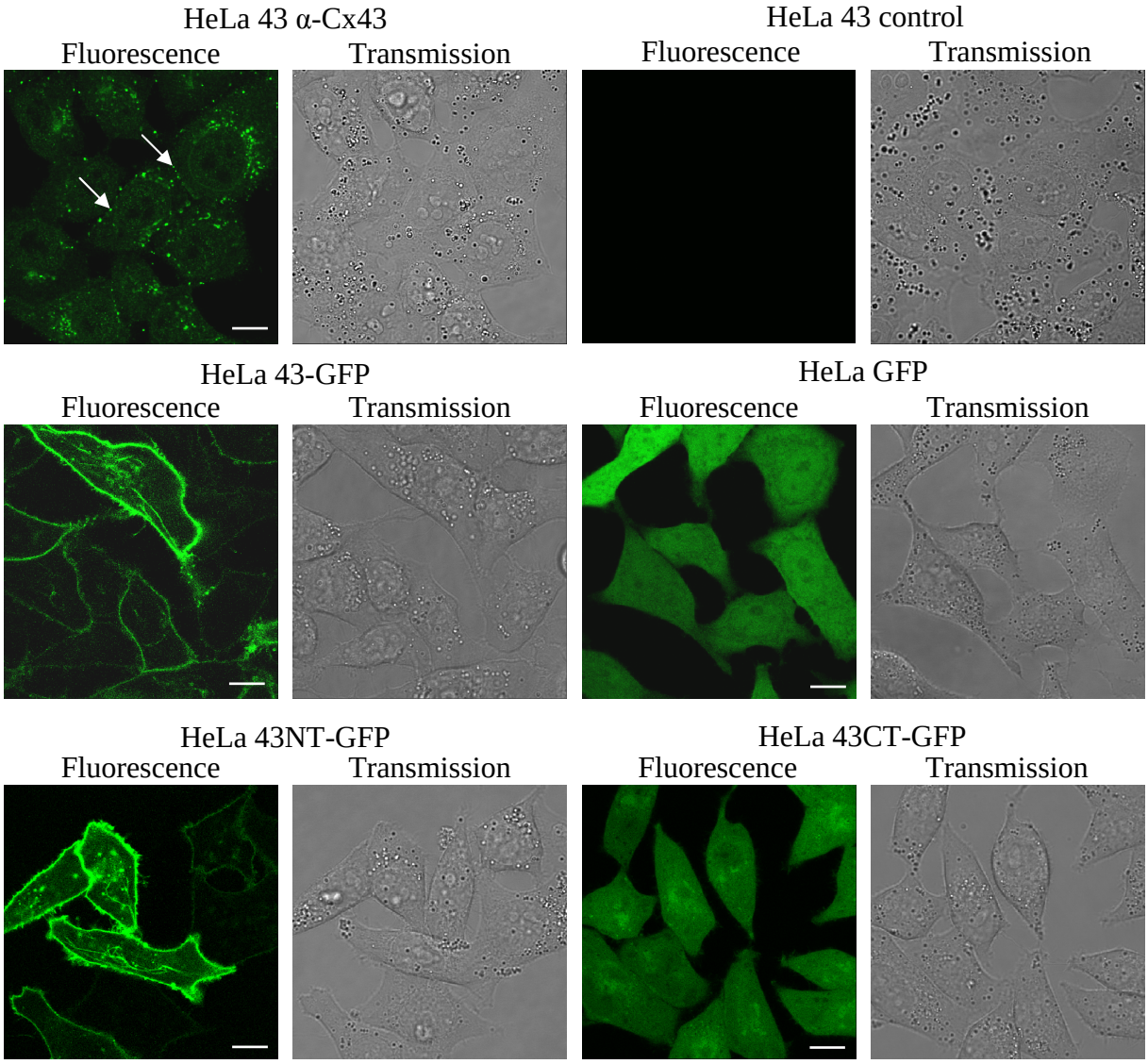

Figure III.3: Localization of Cx43 and truncated proteins

Immunofluorescence staining of Cx43 in HeLa 43 cells with a polyclonal antibody against Cx43 and subsequent confocal microscopy revealed the typical punctate pattern of Cx43, especially at cell-cell contacts (arrows) and at perinuclear regions. No staining was observed using the secondary antibody only (control). GFP fluorescence showed membranous localization of Cx43-GFP and of Cx43NT-GFP, whereas Cx43CT-GFP as well as GFP alone were localized in the cytosol and partly in the nucleus (scale bars 10 µm).

These results indicated that the N-terminal part of Cx43 (aa 1 – 257) containing the four transmembrane domains of Cx43 was indeed localized in the cell membrane, required for functional gap junction formation. The C-terminal part comprising the cytoplasmic tail of Cx43 was localized in the cytosol as expected.

1.2 HeLa 43NT-GFP cells were functionally coupled via gap junctions

As the channel building part of Cx43 (Cx43NT-GFP) was localized in the cell membrane, cell coupling experiments were performed to investigate whether this part of Cx43 is sufficient to form functional gap junctions.

Cell coupling was verified using fluorescent activated cell sorting (FACS). Calcein stained donor cells (green), expressing Cx43, Cx43-GFP, Cx43NT-GFP and Cx43CT-GFP, respectively, or empty vector transfected cells (CTL) as a control were cocultured for 3 h with PKH-26 stained HeLa 43 dye acceptor cells (red). The amount of double stained HeLa 43 acceptor cells (red and green) was calculated, representing the cell population that have coupled with the respective donor cells (Figure III.4).

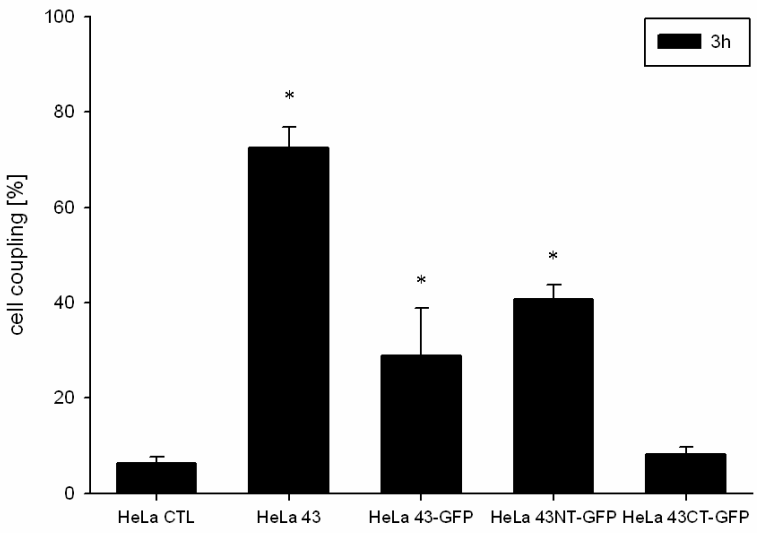

Figure III.4: Gap junctional cell coupling of Cx43 and truncated Cx43 proteins
FACS analysis indicated functional cell coupling in HeLa 43, HeLa 43-GFP and HeLa 43NT-GFP cells. In contrast, HeLa 43CT-GFP and HeLa CTL cells showed no functional cell coupling. Data are represented as percentage of cell coupling, mean + SEM (n = 4 independent cell cultures), (*) $p < 0.001$ vs. HeLa CTL and HeLa 43CT-GFP.

After 3 h of coculture, HeLa 43 cells coupled by 73 ± 4 % with HeLa 43 cells. HeLa 43NT-GFP showed 41 ± 3 % and HeLa 43-GFP cells 29 ± 10 % functional cell coupling with HeLa 43, both coupling levels lower compared to HeLa 43/HeLa 43. Neither HeLa CTL nor HeLa

43CT-GFP cells showed functional cell coupling (HeLa CTL: 6 ± 1 %, HeLa 43CT-GFP: 8 ± 2 % double stained cells).

1.3 The C-terminal part of Cx43 increases cell migration of HeLa cells

To analyze whether the migration enhancing effect of Cx43 is a channel dependent or independent effect, cell migration of HeLa cells expressing Cx43 or truncated Cx43 proteins was analyzed. Life cell migration was observed for 24 h using an in vitro wound healing model and time lapse microscopy. Cell paths of all tracked cell cultures were evaluated regarding accumulated and euclidian migration distance, shift of the center of mass, migration velocity and directionality. HeLa 43, HeLa 43-GFP and HeLa 43CT-GFP cells showed significantly higher accumulated distances (mean ± SEM: Cx43: 252.4 ± 10.3 µm, Cx43-GFP: 191.1 ± 7.6 µm or Cx43CT-GFP: 212.0 ± 15.8 µm) compared to HeLa 43NT-GFP (156.7 ± 16.5 µm) or HeLa CTL (142.4 ± 7.1 µm) cells (Figure III.5).

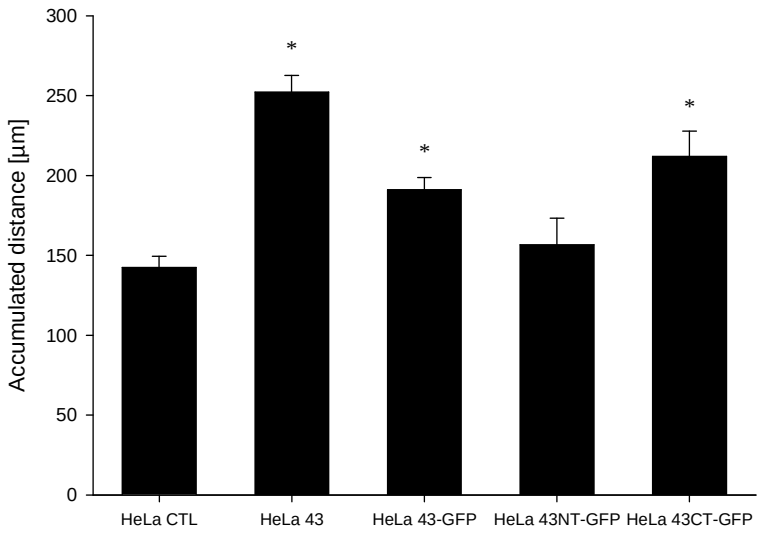

Figure III.5: Analysis of accumulated distance of transfected HeLa cells
HeLa 43, HeLa 43-GFP and HeLa 43CT-GFP cells showed higher accumulated distances compared to HeLa 43NT-GFP and HeLa CTL cells. Data are represented as means + SEM (n = 5 independent cell cultures), (*) $p < 0.001$ vs. HeLa CTL and HeLa 43NT-GFP.

Similarly, regarding the euclidian distances, which is the shortest distance from the start to the end point, HeLa 43 and HeLa 43CT-GFP cells showed significantly higher values compared to HeLa 43NT-GFP and HeLa CTL (mean ± SEM: HeLa 43: 219.8 ± 11.9; HeLa 43CT-GFP: 156.3 ± 10.2 µm; HeLa 43NT-GFP: 109.6 ± 12.9 µm; HeLa CTL: 114.5 ± 7.9 µm). Evaluation of the directionality revealed similar results as the euclidian distance: HeLa 43 had significantly higher directionality (0.97 ± 0.01) during migration compared to HeLa CTL cells (0.80 ± 0.02). HeLa 43CT-GFP cells exhibited significantly higher directionality (0.77 ± 0.02)

compared to HeLa 43NT-GFP cells (0.70 ± 0.03). HeLa 43-GFP (0.73 ± 0.01) also showed a tendency towards increased directionality compared to HeLa 43NT-GFP but the difference was not significant (p = 1.0). The migration velocity as well as the shift of center of mass of HeLa 43, HeLa 43-GFP and HeLa 43CT-GFP cells was higher compared to HeLa CTL or HeLa 43NT-GFP cells. These results were comparable to the results of the accumulated migration distances (data not shown).

Taken together all numerical migration parameters (accumulated and euclidian distance, velocity, directionality and center of mass) were significantly increased in HeLa 43CT-GFP cells compared to HeLa 43NT-GFP cells.

2 Generation of further truncated Cx43 proteins: Cx43(tr298)-GFP and Cx43(tr336)-GFP

Migration analysis had shown that the C-terminal part of Cx43 is mediating the migration enhancing effect of Cx43. To specify which sequence on the C-terminus is required for this effect, cDNAs for two further truncated proteins of Cx43 were constructed, which contained either aa 1 – 298 (Cx43(tr298)-GFP) or aa 1 – 336 (Cx43(tr336)-GFP), and cloned into the plasmid pcDNA4-GFP.

2.1 Expression of Cx43(tr298)-GFP and Cx43(tr336)-GFP in HeLa cells

HeLa cells were stably transfected with cDNAs encoding either Cx43(tr298)-GFP or Cx43(tr336)-GFP. Single cell clones were investigated for their protein expression by western blot analysis using a polyclonal antibody against GFP.

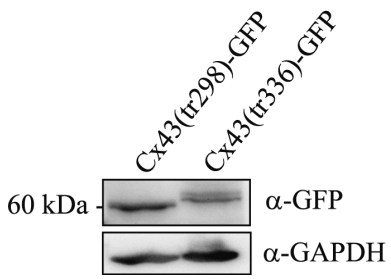

Figure III.6: Expression of Cx43(tr298)-GFP and Cx43(tr336)-GFP
HeLa cells were stably transfected with Cx43(tr298)-GFP or Cx43(tr336)-GFP and protein expression was analyzed by western blot using a polyclonal antibody against GFP. GAPDH was used as loading control.

HeLa cells expressing Cx43(tr298)-GFP showed a single band at the predicted molecular weight of 60 kDa (34 kDa Cx43(tr298) + 26 kDa GFP) and HeLa cells expressing

Cx43(tr336)-GFP showed a double band at 64 kDa (38 kDa Cx43(tr336) + 26 kDa GFP), which might occur due to phosphorylation events (Figure III.6).

Subcellular localization of Cx43(tr298)-GFP and Cx43(tr336)-GFP was studied using LSM (Figure III.7).

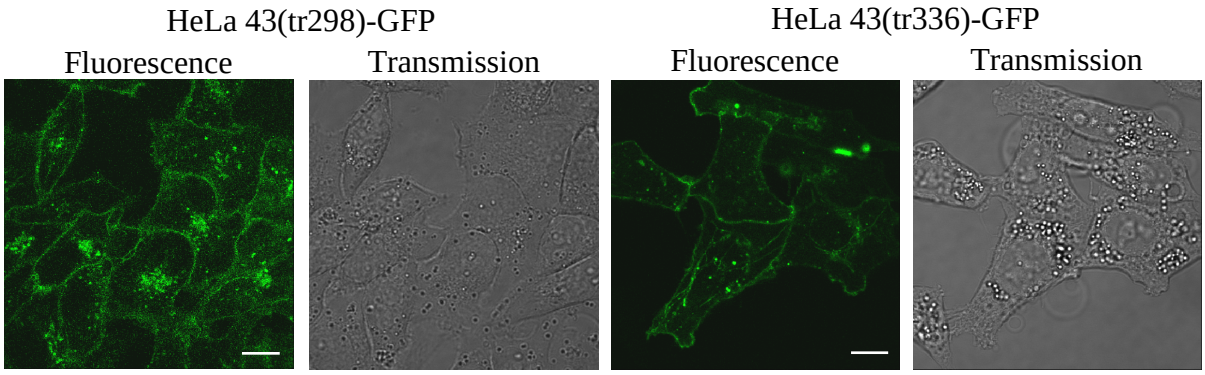

Figure III.7: Cx43(tr298)-GFP and Cx43(tr336)-GFP are localized in the membrane
Fluorescence of the GFP-tag using confocal microscopy at an excitation wavelength of 488 nm revealed membranous localization of Cx43(tr298)-GFP as well as of Cx43(tr336)-GFP in stably transfected HeLa cells (scale bars 10 µm).

Since both proteins contained the four transmembrane domains like the full length Cx43 and Cx43NT-GFP, their localization was expected in the cell membrane. Indeed, confocal microscopy revealed cytosolic and membranous localization of Cx43(tr298)-GFP and Cx43(tr336)-GFP in stably transfected HeLa cells (Figure III.7). Like in HeLa 43-GFP and HeLa 43NT-GFP cells, the proteins were localized in the whole cell membrane in contrast to the punctate pattern in the cell membrane only at cell-cell contacts of Cx43.

2.2 Cx43(tr336)-GFP increases cell migration of HeLa cells

Cell migration was analyzed as described above. HeLa 43(tr336)-GFP cells showed significantly increased accumulated migration distances (186.07 ± 9.16 µm) compared to HeLa 43(tr298)-GFP cells (108.68 ± 6.06 µm) as well as compared to HeLa 43NT-GFP cells and HeLa CTL cells (Figure III.8).

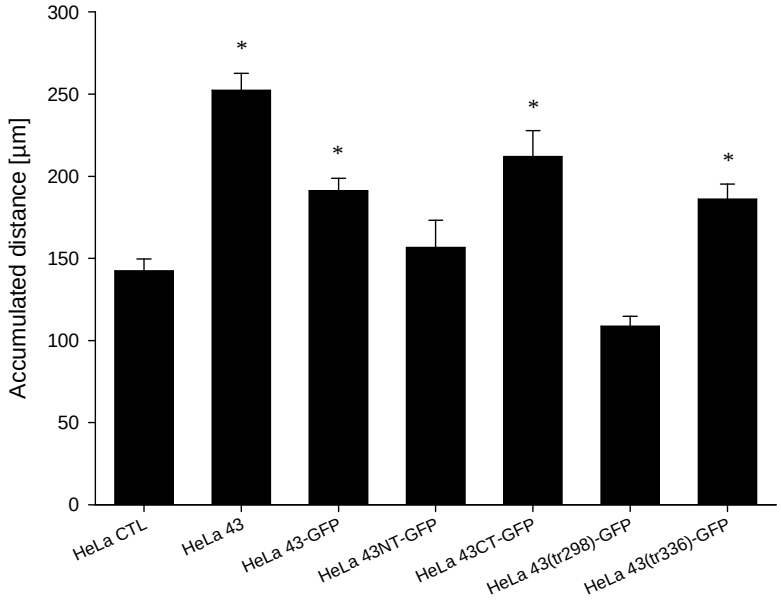

Figure III.8: HeLa 43(tr336)-GFP cells showed increased accumulated migration distance
HeLa 43(tr336)-GFP cells showed significantly increased accumulated migration distances compared to HeLa CTL and HeLa 43NT-GFP cells, whereas HeLa 43(tr298)-GFP cells showed lower migration distances, comparable to HeLa CTL and HeLa 43NT-GFP cells, respectively. Data are represented as means + SEM (n = 5 independent cell cultures), (*) $p < 0.001$ vs. HeLa CTL and HeLa43NT-GFP.

The results of the other parameters as euclidian distance, shift of center of mass, velocity, and directionality were comparable to the results of the accumulated migration distances (data not shown). Migration of HeLa 43(tr336)-GFP cells was significantly enhanced compared to HeLa 43(tr298)-GFP cells, HeLa 43NT-GFP cells and HeLa CTL cells. Values for HeLa 43(tr298)-GFP cells were comparable to HeLa 43NT-GFP and HeLa CTL cells.

The sequence aa 299 – 336 of the C-terminal tail of Cx43 is therefore presumably required for the migration enhancing effect of Cx43.

3 Further restriction of the migration mediating part of Cx43

3.1 Generation and expression of a small part of the cytoplasmic tail of Cx43: Cx43(299-336)-GFP

To analyze if the sequence aa 299 – 336 of the C-terminal tail of Cx43 is required for the migration enhancing effect, a cDNA was created encoding Cx43(299-336) and cloned into the plasmid pcDNA4-GFP. HeLa cells were stably transfected and protein expression of single cell clones was analyzed by western blots using a polyclonal antibody against GFP. Cells expressing Cx43(299-336)-GFP showed a band at the predicted molecular weight of 30 kDa

(4 kDa Cx43(299-336) + 26 kDa GFP) and a second band at about 32 kDa, which might occur due to phosphorylation events (Figure III.9).

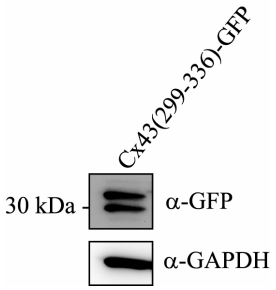

Figure III.9: Expression of Cx43(299-336)-GFP in HeLa cells
HeLa cells were stably transfected with Cx43(299-336)-GFP and protein expression of a single cell clone was analyzed by western blot using a polyclonal antibody against GFP. GAPDH was used as loading control.

Localization of Cx43(299-336)-GFP in stably transfected HeLa cells was studied using LSM. The protein was localized in the cytosol with a punctate staining indicating an accumulation in vesicular compartments (Figure III.10).

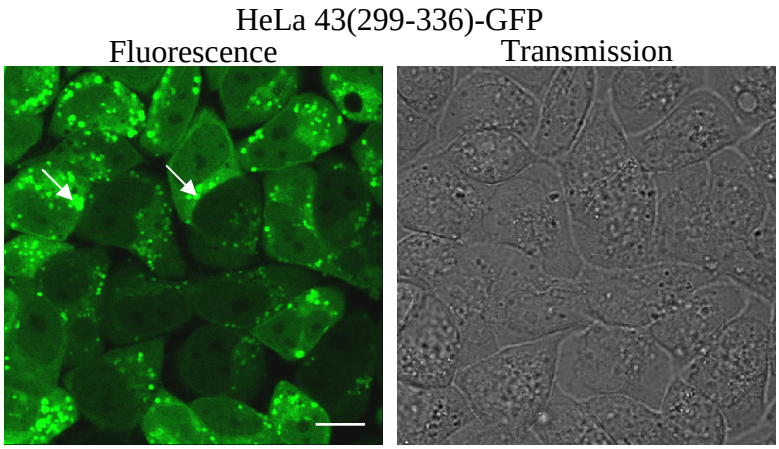

Figure III.10: Cx43(299-336)-GFP is localized in the cytosol
Fluorescence of GFP using LSM revealed cytosolic localization of Cx43(299-336)-GFP in a single cell clone of stably transfected HeLa cells, partly increased in vesicular structures (arrows). Scale bar 10 µm.

3.2 Cx43(299-336)-GFP increases cell migration of HeLa cells

Analysis of the migratory behavior of HeLa 43(299-336)-GFP cells revealed increased accumulated distances (185.89 ± 8.11 µm) compared to HeLa 43NT-GFP and HeLa CTL cells. The values were comparable to those from HeLa 43-GFP and HeLa 43(tr336)-GFP (Figure III.11).

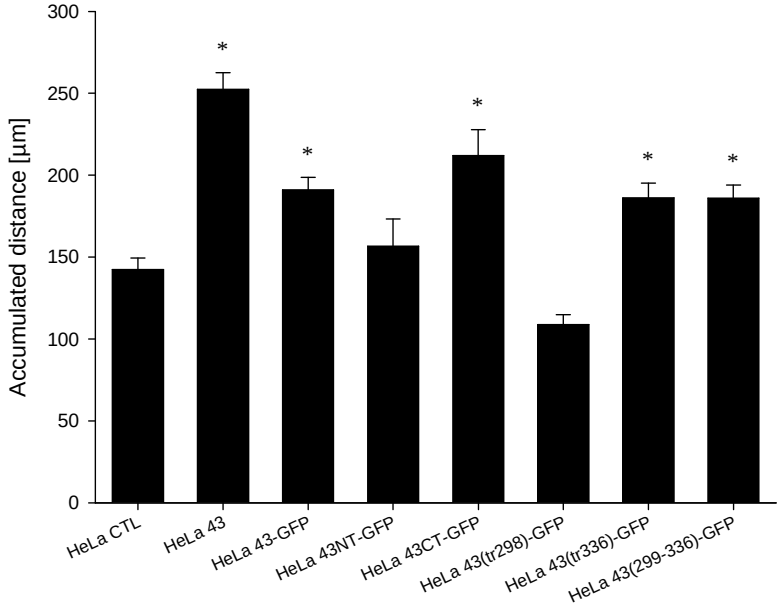

Figure III.11: HeLa 43(299-336)-GFP cells showed increased accumulated migration distances

HeLa 43(299-336)-GFP cells showed significantly increased accumulated migration distances compared to HeLa CTL and HeLa 43NT-GFP cells, similar to HeLa 43(tr336)-GFP cells. Data are represented as means + SEM (n = 5 independent cell cultures), (*) $p < 0.001$ vs. HeLa CTL and HeLa 43NT-GFP.

These results indicate that the sequence aa 299 – 336 of the C-terminal tail of Cx43 is mediating the migration enhancing effect of Cx43, which might be due to either one or several phosphorylation events taking place at this sequence or due to protein interactions. Accumulation of this sequence in vesicles might partially inhibit these events, but nevertheless the migration enhancing effect is clearly observable.

4 Analysis of protein-protein interactions of Cx43 with cortactin and NOV

Our results indicated that the migration enhancing effect of Cx43 is independent of its channel forming capacity, but mediated by the cytoplasmic C-terminal part. Moreover, the sequence responsible for the enhanced migration could be narrowed down to a small part of the cytoplasmic tail of Cx43 (aa 299 – 336). To analyze the mechanism of the migration enhancing effect of Cx43, possible protein-protein interactions were investigated. Literature searches for proteins, which have been shown to influence cell migration and also to interact with Cx43, revealed two interesting candidates: the actin-binding proteins cortactin [17 65 174] and NOV [123 110 45 48 165].

4.1 Colocalization of cortactin and the C-terminal part of Cx43 in HeLa cells

In order to find out if an interaction of cortactin with Cx43 is necessary for the migration enhancing effect, we first analyzed the localization of both proteins in migrating HeLa cells and, furthermore, identified the potential interacting region. Therefore, after serum-stimulated migration for 24 h, HeLa 43-GFP, HeLa 43NT-GFP and HeLa 43CT-GFP cells were stained with a polyclonal antibody against GFP and a monoclonal antibody against cortactin and observed by LSM. In migrating cells cortactin was mainly localized at the leading edge and in membranous protrusions. As Cx43-GFP was also localized at the leading edge and in membranous protrusions, both proteins showed colocalization in these regions (Figure III.12).

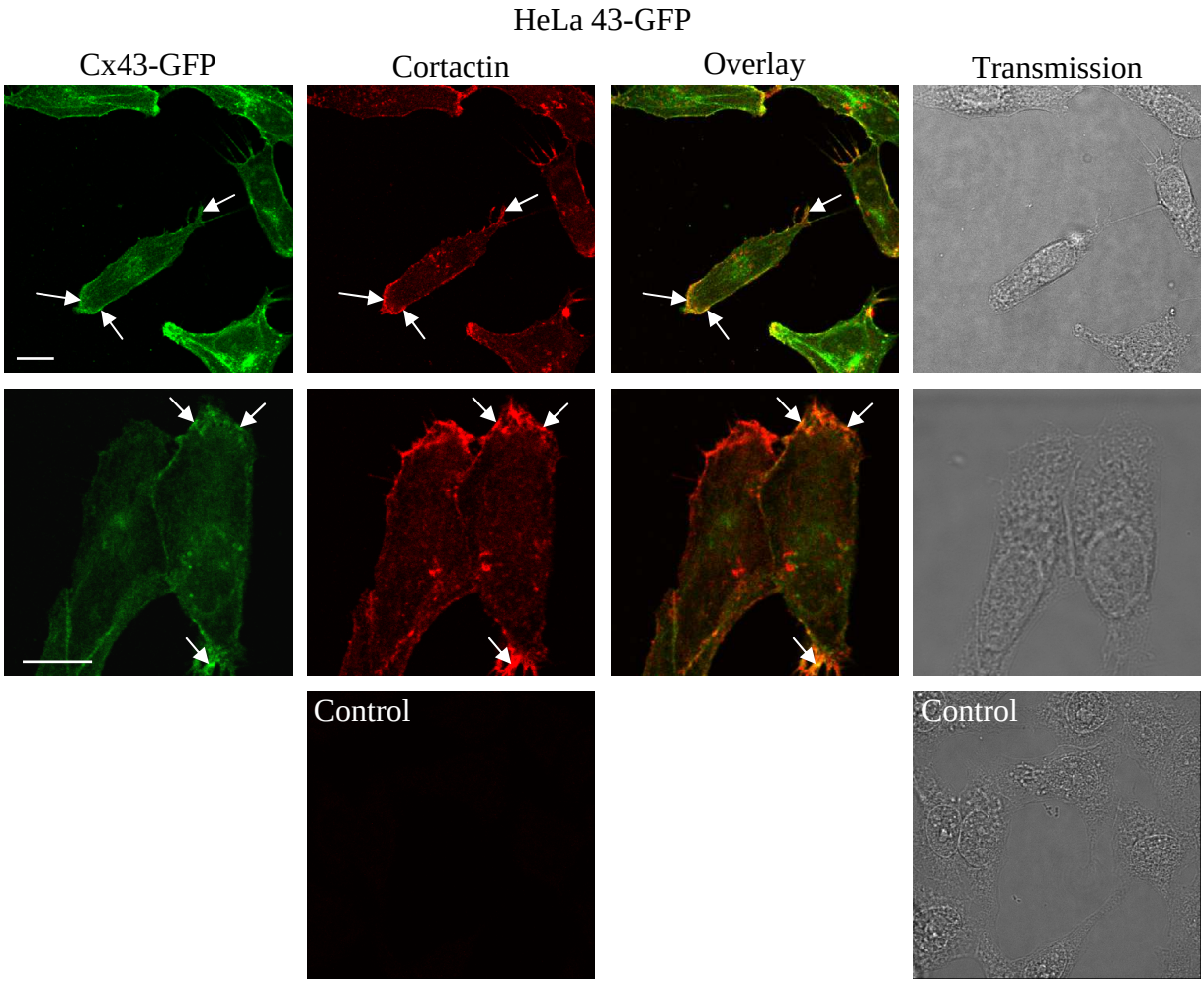

Figure III.12: Colocalization of cortactin and Cx43 in migrating HeLa 43-GFP cells
Immunofluorescence stainings using a polyclonal antibody against GFP (AF488 (green)-coupled secondary antibody) and a monoclonal cortactin antibody (AF546 (red)-coupled secondary antibody) revealed colocalization of Cx43-GFP and cortactin especially at the leading edge and in filopodia of migrating cells (arrows). Incubation with secondary antibody AF546 only (control) showed no staining (scale bars 10 µm).

In migrating HeLa 43CT-GFP cells the C-terminal part of Cx43 was not only localized in the cytosol, but also partly at the leading edge and also in filopodia. In these regions a

colocalization with cortactin was visible. As the N-terminal part of Cx43 in HeLa 43NT-GFP was localized in the membrane per se, colocalization with cortactin was also observed (Figure III.13).

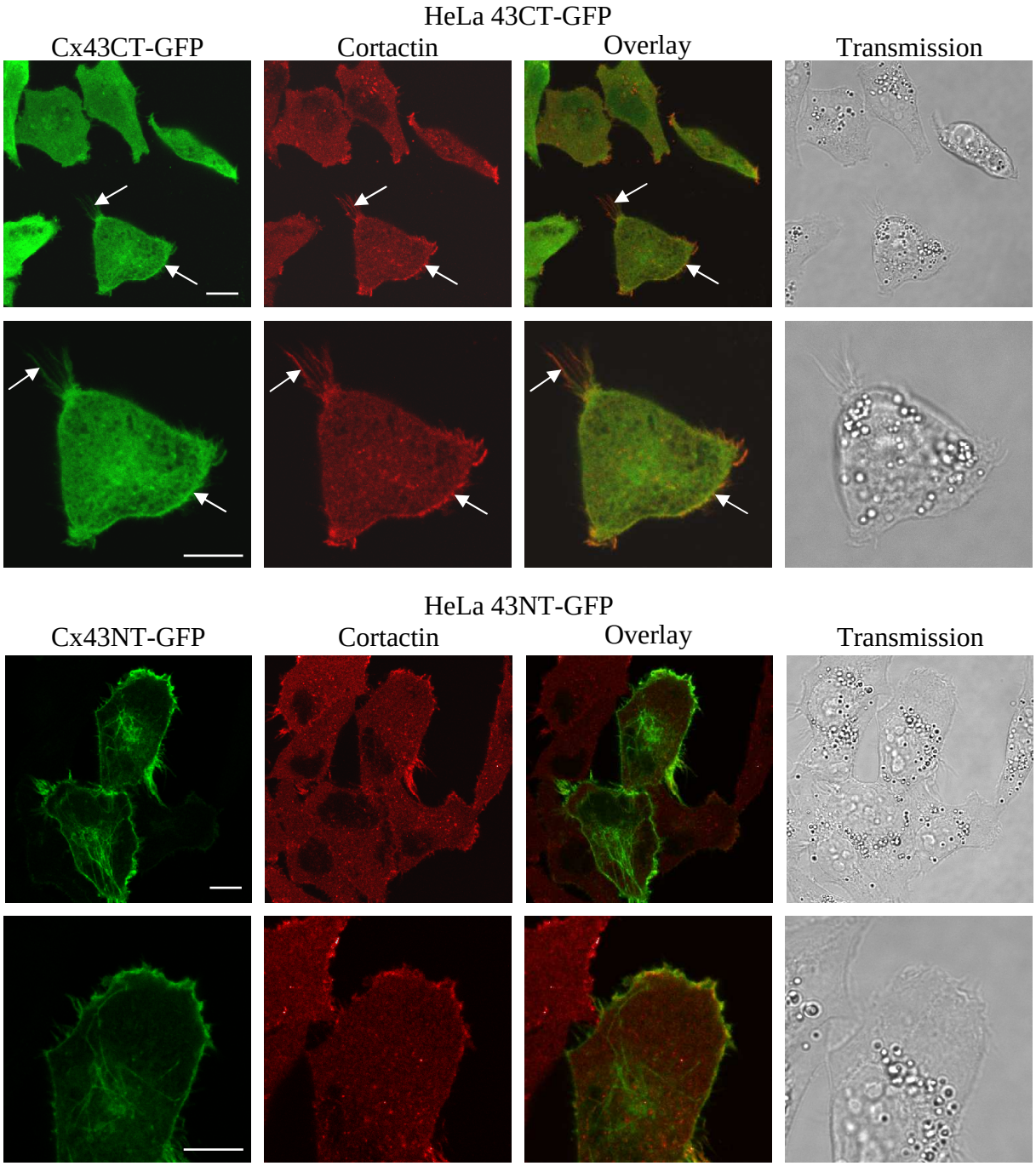

Figure III.13: Colocalization of cortactin and the N-terminal or the C-terminal part of Cx43 in migrating HeLa cells

Immunofluorescence stainings using a polyclonal antibody against GFP (AF488 (green)-coupled secondary antibody) and a monoclonal antibody against cortactin (AF546 (red)-coupled secondary antibody) revealed colocalization of the C-terminal part of Cx43GFP and cortactin, especially at the leading edge and in filopodial structures of migrating cells (arrows), whereas it was not evident if the N-terminal colocalizes with cortactin as it is localized in the membrane per se (scale bars 10 µm).

To further elucidate whether colocalization is attended by direct interaction of the proteins, immunoprecipitation studies were performed.

4.2 The C-terminal part of Cx43 and cortactin are part of a complex

The immunofluorescence stainings had shown colocalization of full length Cx43-GFP with cortactin, but it remained unclear which part of Cx43 colocalized with cortactin. Therefore, immunoprecipitation studies were performed using cell lysates of HeLa 43, HeLa 43NT-GFP and HeLa 43CT-GFP cells which were incubated with a monoclonal antibody against cortactin and analyzed by western blots using polyclonal antibodies against Cx43 and GFP. Interaction of cortactin could be demonstrated with full length Cx43 (band at 43 kDa) and the C-terminal part (band at 41 kDa) but not with the N-terminal part of Cx43. Immunoprecipitation of the same cell lysates with a polyclonal antibody against Cx43 and subsequent western blot analysis using a monoclonal antibody against cortactin revealed the same results (Figure III.14).

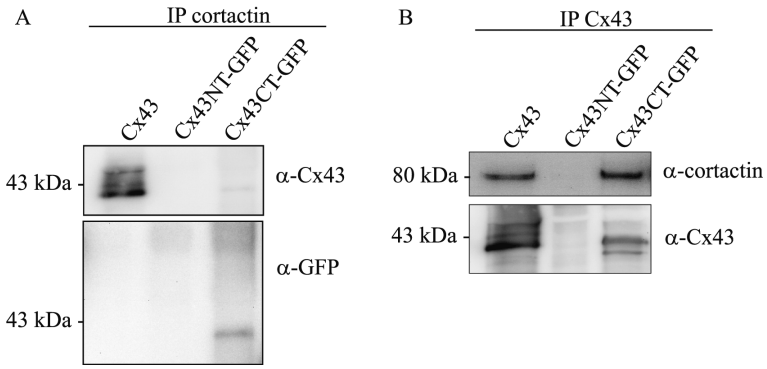

Figure III.14: The C-terminal part of Cx43 interacts with cortactin
(A) Immunoprecipitation of cell lysates with cortactin antibody followed by western blots with an antibody against Cx43 showed interaction with Cx43, especially with the C-terminal part, whereas the N-terminal part did not show a band after subsequent incubation with an antibody against GFP. (B) Immunoprecipitation of cell lysates with a polyclonal antibody against Cx43 and subsequent western blot analysis using antibodies against cortactin or Cx43 showed the same results (representative western blot of five independent experiments).

Next, we wanted to investigate which part of the C-terminus interacts with cortactin. Therefore, immunoprecipitation studies were performed for the C-terminus truncated proteins Cx43(tr298)-GFP and Cx43(tr336)-GFP. Immunoprecipitation of cell lysates with a monoclonal antibody against cortactin followed by western blot studies using a polyclonal antibody against GFP showed an interaction of Cx43(tr298)-GFP (band at 60 kDa) as well as of Cx43(tr336)-GFP (band at 64 kDa) with cortactin (Figure III.15). Thus, the interaction of cortactin with Cx43 probably takes place at the sequence aa 257 – 298 of the C-terminal part.

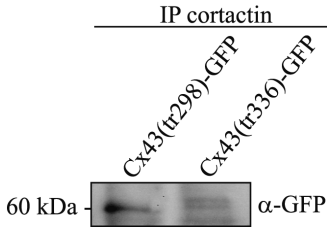

Figure III.15: Both C-terminus truncated Cx43 proteins interact with cortactin
Immunoprecipitation of cell lysates with a monoclonal antibody against cortactin followed by western blot detection using a polyclonal antibody against GFP revealed that Cx43(tr298)-GFP as well as Cx43(tr336)-GFP interacts with cortactin (representative western blot of five independent experiments).

4.3 The C-terminal part of Cx43 and NOV are part of a complex

We further wanted to investigate which part of Cx43 interacts with NOV. Therefore, cell lysates of HeLa CTL, HeLa 43, HeLa 43NT-GFP, HeLa 43CT-GFP, HeLa 43(tr298)-GFP and HeLa 43(tr336)-GFP cells were prepared and immunoprecipitation studies were performed using a polyclonal antibody against NOV. Subsequent western blot analysis with a polyclonal antibody against GFP to detect the GFP-coupled proteins revealed that the C-terminal part and not the N-terminal part of Cx43 interacted with NOV (Figure III.16; band at 41 kDa). Moreover, both C-terminus truncated proteins Cx43(tr298)-GFP and Cx43(tr336)-GFP showed an interaction with NOV (Figure III.16; bands at 60 and 64 kDa).

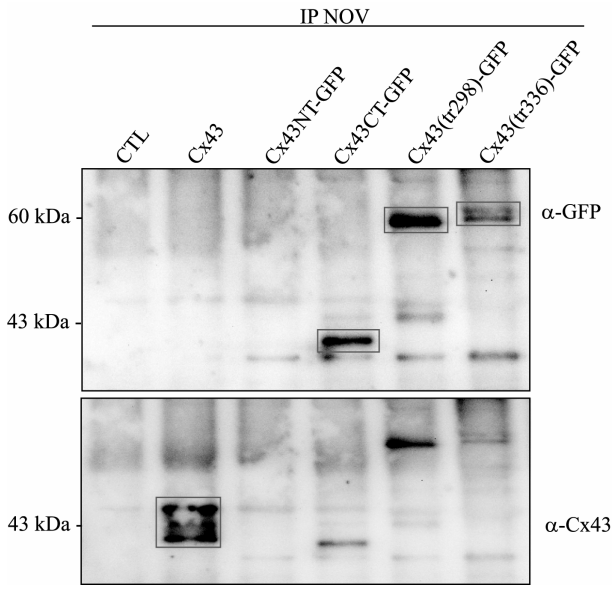

Figure III.16: Interaction of the C-terminal part of Cx43 with NOV
Immunoprecipitation with a polyclonal antibody against NOV of cell lysates followed by western blot detection using a polyclonal antibody against GFP revealed that Cx43CT-GFP, Cx43(tr298)-GFP as well as Cx43(tr336)-GFP interacted with NOV (black boxes in the upper blot), whereas the N-terminal part and the empty vector did not. The subsequent incubation of the membrane with a polyclonal antibody against Cx43 showed interaction of Cx43 with NOV (black box in the lower blot; representative western blot of five independent experiments).

Cell lysates of HeLa CTL served as controls and showed no interaction with NOV. The interaction of NOV with full length Cx43 was detected with a polyclonal antibody against Cx43 (Figure III.16; band at 43 kDa).

These results led to the conclusion that cortactin as well as NOV bound to the C-terminal part of Cx43. Moreover, both proteins interacted with both C-terminus truncated proteins of Cx43, Cx43(tr298)-GFP and Cx43(tr336)-GFP, indicating a protein binding of cortactin and NOV to Cx43 at the sequence aa 257 – 298.

5 Influence of Cx43 on the actin cytoskeleton

5.1 Cx43 and Cx43CT-GFP increase filopodia formation in migrating cells

Migration of cells requires a dynamic regulation of the actin cytoskeleton. Therefore, the effect of Cx43 expression on the actin cytoskeleton in migrating HeLa cells was investigated. After serum-stimulated migration for 24 h using cell culture inserts, the actin cytoskeleton of HeLa 43, HeLa 43-GFP, HeLa 43NT-GFP, HeLa 43CT-GFP and HeLa CTL cells was stained with phalloidin (Figure III.17). For a better visualization of the actin filament structures the maximal projections of the taken images were analyzed. It was noticeable that HeLa 43, HeLa 43-GFP and HeLa 43CT-GFP cells exhibited higher amounts of cellular protrusions, namely filopodia, compared to HeLa 43NT-GFP and HeLa CTL cells, whereas lamellipodia and stress fiber formation showed no obvious differences.

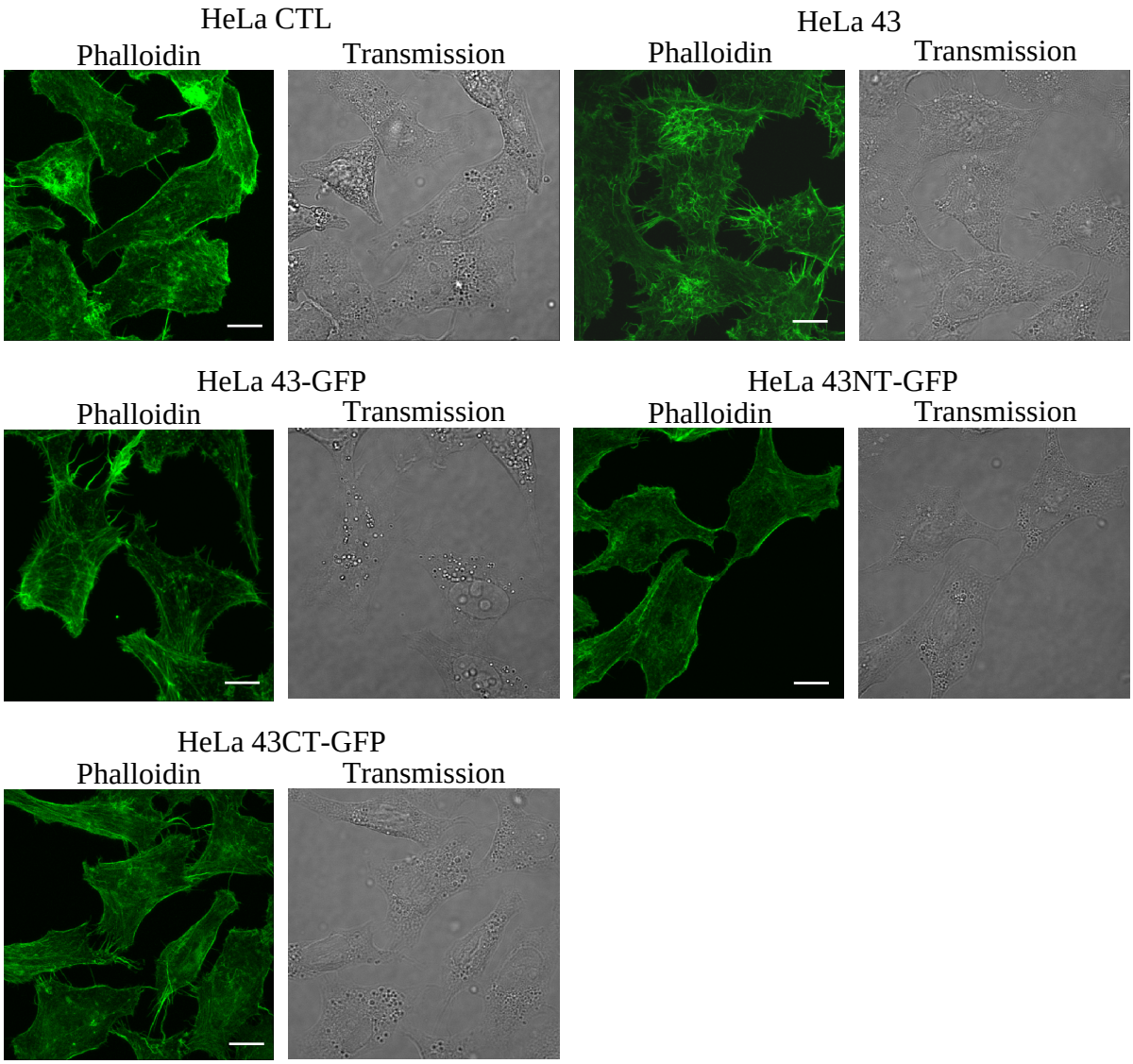

Figure III.17: Filopodia formation of migrating HeLa cells expressing Cx43 and truncated Cx43 proteins

HeLa 43, HeLa 43-GFP, HeLa 43NT-GFP, HeLa 43CT-GFP and HeLa CTL cells were stained with phalloidin-AF488 after serum-stimulated migration for 24 h. HeLa 43, HeLa 43-GFP and HeLa 43CT-GFP cells showed higher amounts of filopodia compared to HeLa CTL and HeLa 43NT-GFP cells (representative images of four independent experiments are displayed, scale bars 10 µm).

Therefore, amount and length of filopodia per single cell of randomly chosen cells without direct neighbour cells were evaluated. HeLa 43, HeLa 43-GFP and HeLa 43CT-GFP cells showed significantly longer filopodia per single cell compared to HeLa 43NT-GFP cells (length of filopodia (mean ± SEM): HeLa 43: 4.46 ± 0.57 µm, HeLa 43-GFP: 4.67 ± 0.1 µm, HeLa 43CT-GFP: 5.41 ± 0.87 µm and HeLa 43NT-GFP: 3.78 ± 0.8 µm), but not significantly longer compared to HeLa CTL cells (3.96 ± 0.71 µm; figure III.18).

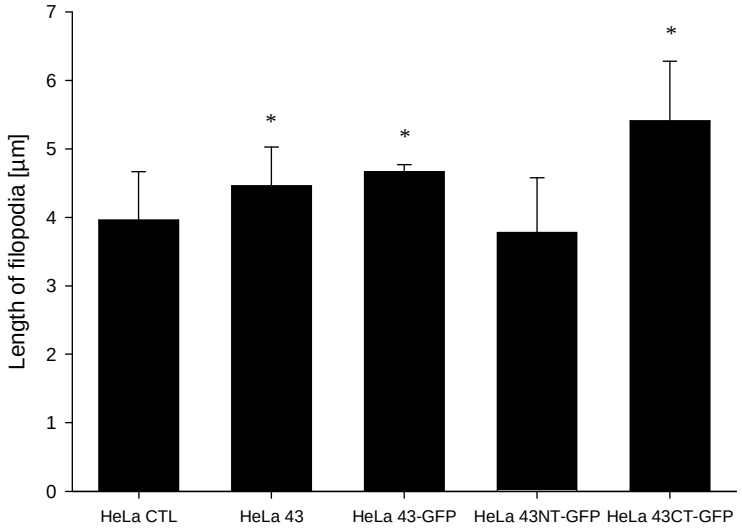

Figure III.18: Length of filopodia of migrating HeLa cells expressing Cx43 and truncated Cx43 proteins

Analysis of the length of individual filopodia per cell revealed that HeLa 43, HeLa 43-GFP and HeLa 43CT-GFP cells showed significantly longer filopodia compared to HeLa 43NT-GFP cells. Data are represented as means + SEM (n = 4 independent experiments, 14 randomly selected cells/experiment were analyzed), (*) $p < 0.001$ vs. HeLa 43NT-GFP.

Regarding the amount of filopodia, HeLa 43, HeLa 43-GFP and HeLa 43CT-GFP cells showed significantly more filopodia per cell compared to HeLa CTL and HeLa 43NT-GFP cells (quantity of filopodia per cell (mean ± SEM): HeLa 43: 30 ± 7, HeLa 43-GFP: 25 ± 5, HeLa 43CT-GFP: 21 ± 4, HeLa CTL: 12 ± 3, HeLa 43NT-GFP: 13 ± 4; figure III.19).

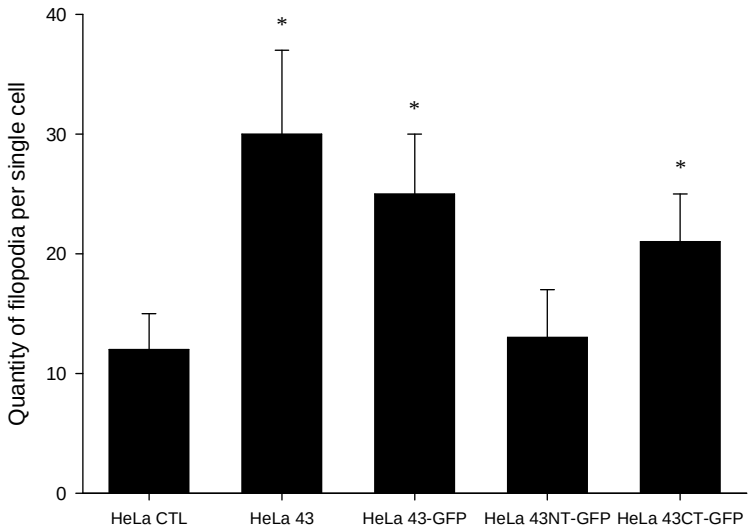

Figure III.19: Quantity of filopodia of migrating HeLa cells expressing Cx43 and truncated Cx43 proteins

Analysis of the quantity of individual filopodia per cell revealed that HeLa 43, HeLa 43-GFP and HeLa 43CT-GFP cells showed significantly more filopodia per cell compared to HeLa 43NT-GFP and HeLa CTL. Data are presented as means + SEM (n = 4 independent experiments, 14 cells/experiment were analyzed), (*) $p < 0.001$ vs. HeLa CTL and HeLa 43NT-GFP.

Thus, increased migration capacity is associated with enhanced quantity of filopodia, whereas the length of each filopodia seemed not to be important for this effect and is anyway in variation because of constant assembly and disassembly of the actin structures.

5.2 Inhibition of p38 MAPK decreases filopodia formation in HeLa 43 cells

As we had shown that Cx43-mediated enhanced cell migration correlated with increased filopodia formation (chapter III.5.1) and also with higher activation of p38 MAPK [6], we therefore investigated whether the enhanced filopodia formation by Cx43 expression is also associated with activation of p38 MAPK. Thus, HeLa 43 and HeLa CTL cells were treated with the specific p38 MAPK inhibitor (SB203580) for 5 h and subsequently the actin cytoskeleton was stained with phalloidin (Figure III.20). Cells, treated with SB203580 showed less filopodia compared to untreated cells, whereas other actin structures such as lamellipodia and stress fibers did not seem to be influenced.

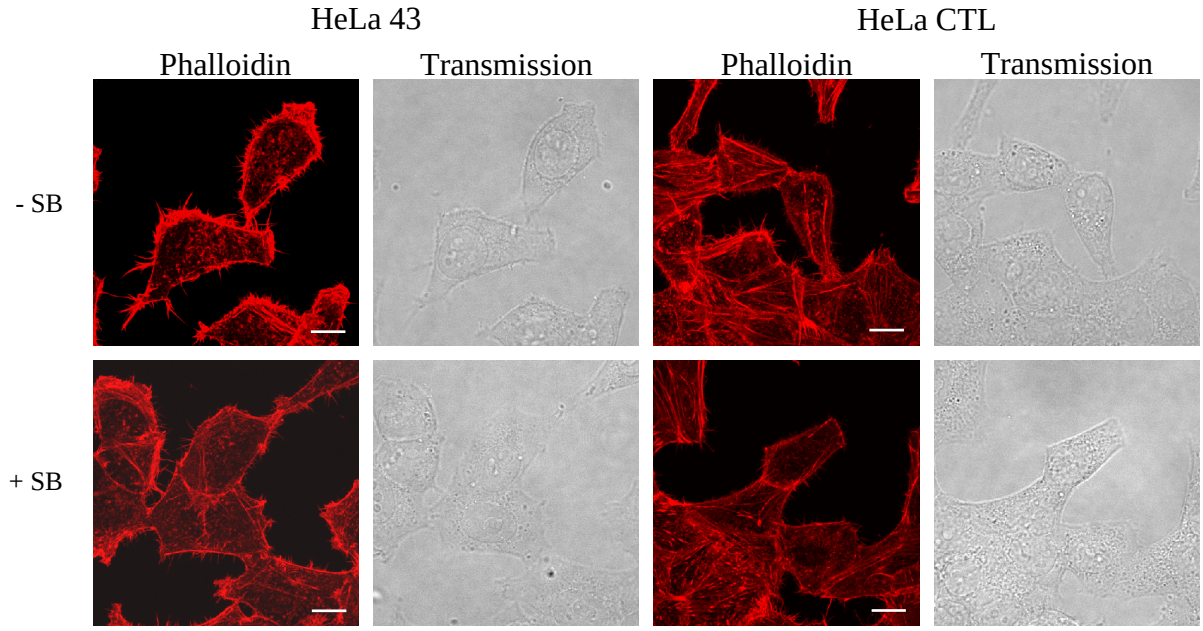

Figure III.20: Filopodia formation of HeLa cells with and without addition of p38 MAPK inhibitor

HeLa 43 and HeLa CTL cells were stained with phalloidin-AF546 after incubation with p38 MAPK inhibitor (SB203580) (+ SB) or without p38 MAPK inhibitor (- SB). After inhibition of p38 MAPK the cells showed less filopodia (representative images of seven independent experiments are displayed, scale bars 10 µm).

The amount of filopodia per single cell was quantified and the mean average of 12 cells for each cell line was calculated.

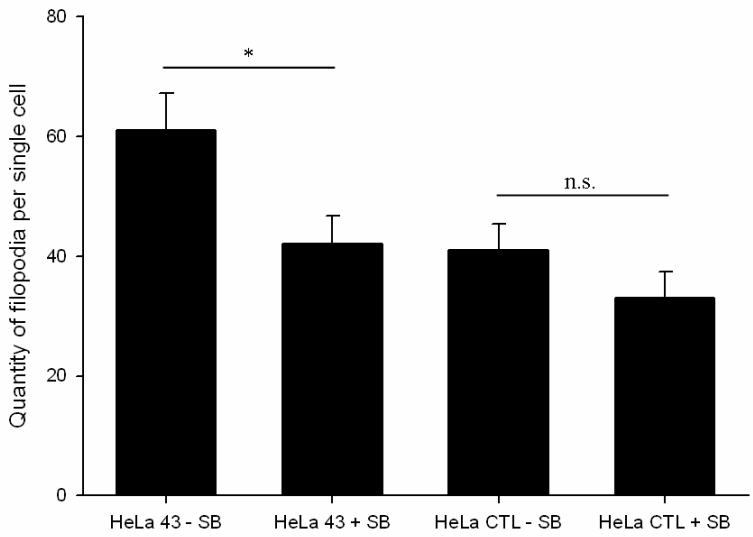

Figure III.21: Quantity of filopodia of HeLa cells with and without addition of p38 MAPK inhibitor

Analysis of the quantity of individual filopodia per cell revealed that HeLa 43 cells, treated with p38 MAPK inhibitor (SB203580) (+ SB) showed significantly less amounts of filopodia per cell compared to untreated cells, whereas for HeLa CTL cells the difference was not significant. Data are represented as means + SEM (n = 7 independent experiments, 12 cells/experiment were analyzed), (*) $p < 0.001$ vs. HeLa 43 (- SB).

HeLa 43 cells, treated with SB203580 showed significantly less amounts of filopodia per single cell compared to untreated cells, whereas for HeLa CTL cells the difference was not significant. Moreover, the amount of filopodia per cell in HeLa 43 cells after SB203580 treatment was comparable to that observed in untreated HeLa CTL cells (quantity of filopodia per single cell (mean ± SEM): HeLa 43 + SB: 61 ± 6, HeLa 43 -SB: 42 ± 5 , HeLa CTL + SB: 41 ± 4, HeLa CTL -SB: 33 ± 4; figure III.21).

5.3 Cx43(tr336)-GFP and Cx43(299-336)-GFP increase filopodia formation in migrating cells

Since the expression of the C-terminal of Cx43 influences the actin cytoskeleton by elevated formation of filopodia, we wanted to elucidate whether the migration enhancing sequence on the C-terminus of Cx43 (Cx43(299-336)) also correlates with an increased filopodia formation. Therefore, HeLa 43(tr298)-GFP, HeLa 43(tr336)-GFP and HeLa 43(299-336)-GFP cells were allowed to migrate in cell culture inserts for 24 h after stimulation with serum and the actin cytoskeleton was stained with phalloidin. It was evident that HeLa 43(tr336)-GFP and HeLa 43(299-336)-GFP cells showed higher amounts of filopodia per cell compared to HeLa 43(tr298)-GFP cells (Figure III.22), whereas other actin structures such as lamellipodia and stress fibers exhibited no obvious differences.

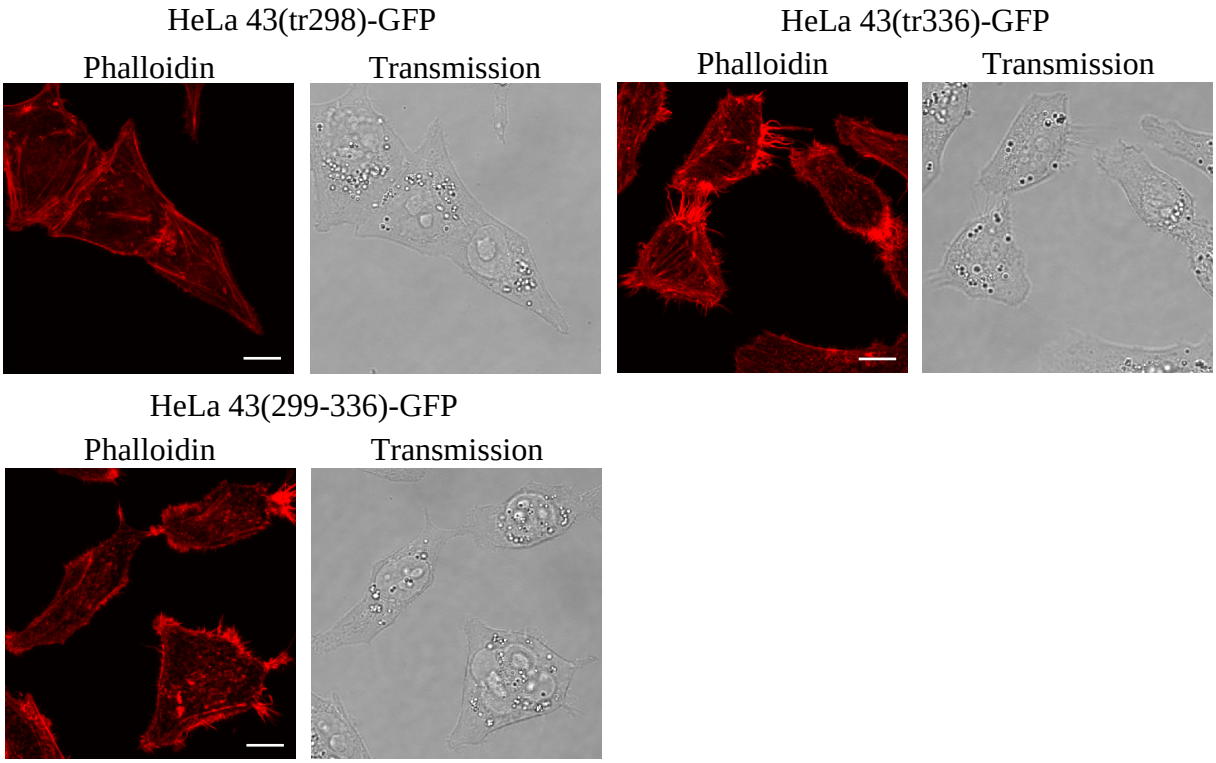

Figure III.22: Filopodia formation of migrating HeLa cells expressing C-terminus truncated Cx43 proteins

HeLa 43(tr298)-GFP, HeLa 43(tr336)-GFP and HeLa 43(299-336)-GFP cells were stained with phalloidin-AF546 after migration for 24 h. HeLa 43(tr336)-GFP and Hela 43(299-336)-GFP cells showed higher amounts of filopodia per cell compared to HeLa 43(tr298)-GFP cells (representative images of four independent experiments are displayed, scale bars 10 µm).

The amount of filopodia per cell was quantified and the mean average of 12 cells for each transfected cell line was calculated. HeLa 43(tr336)-GFP and HeLa 43(299-336)-GFP cells showed significantly higher amounts of filopodia per cell compared to HeLa 43(tr298)-GFP cells (quantity of filopodia per cell (mean ± SEM): HeLa 43(tr336)-GFP: 26 ± 5, HeLa 43(299-336)-GFP: 26 ± 5, HeLa 43(tr298)-GFP: 12 ± 3; figure III.23).

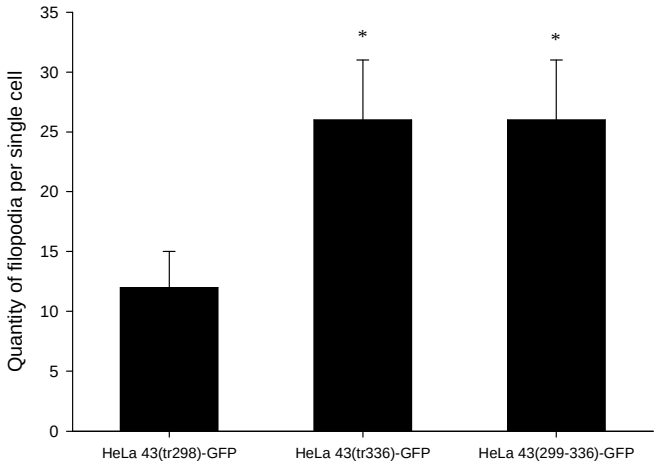

Figure III.23: Quantity of filopodia of migrating HeLa cells expressing Cx43(tr298)-GFP, Cx43(tr336)-GFP and Cx43(299-336)-GFP

Analysis of the quantity of individual filopodia per cell revealed that HeLa 43(tr336)-GFP and HeLa 43(299-336)-GFP cells showed significantly higher amounts of filopodia per cell compared to HeLa 43(tr298)-GFP cells. Data are represented as means + SEM (n = 4 independent experiments, 12 cells/experiment were analyzed), (*) $p < 0.001$ vs. HeLa 43(tr298)-GFP.

5.4 Cx43 is localized in filopodia

We could show in the previous experiments that expression of Cx43 and its C-terminal part leads to a higher formation of filopodia in migrating cells. As it has been reported that Cx43 interacts with the actin cytoskeleton [174 204], we studied whether Cx43 was localized in filopodia. For that purpose, HeLa 43 cells were allowed to migrate for 24 h after stimulation with serum and Cx43 was detected by immunostainings with an antibody against Cx43 and the actin cytoskeleton by stainings with phalloidin.

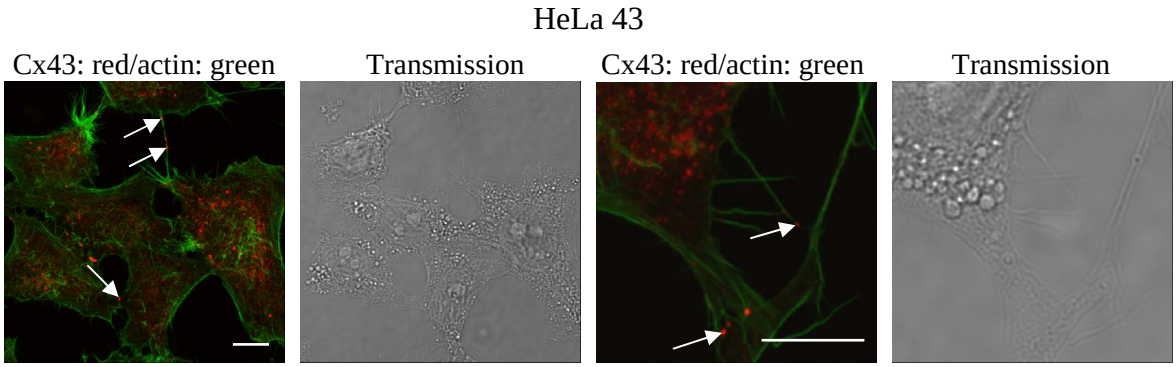

Figure III.24: Localization of Cx43 in filopodia of HeLa 43 cells

HeLa 43 cells were stained with a polyclonal antibody against Cx43 (red) and phalloidin-AF488 (green) after serum-stimulated migration for 24 h. Cx43 was localized at cell-cell contacts and partly also in filopodia (arrows) (representative images of four independent experiments are displayed, scale bars 10 µm)

Cx43 was localized at cell-cell contacts and partly also in filopodia, where it showed colocalization with the actin cytoskeleton (Figure III.24).

IV Discussion

In the present study the effect of Cx43 on serum-stimulated cell migration in the tumor cell line HeLa was studied and whether this was related to gap junction formation. Using structure function analysis we could show that Cx43 increases cell migration in HeLa cells in a gap junction independent manner and that aa 299 – 336 are required for this effect. We further observed that binding of cortactin as well as of NOV, that both regulate cell migration, takes place at aa 257 – 299. Therefore we concluded that both proteins are, at least by binding to this sequence, not involved in the migration enhancing effect of Cx43. Finally, we could demonstrate that Cx43-enhanced cell migration is associated with increased filopodia formation, an effect that requires activation of p38 MAPK.

1 Cx43 enhances cell migration in a gap junction independent manner

The current study shows that Cx43 enhances serum-stimulated migration of HeLa cells. For migration analysis cell culture inserts were used in which the cells migrated into a defined cell free gap. In this assay, simulating wound healing, the cells combined migration and proliferation to fill the gap. However, we could exclude a proliferation dependent effect of Cx43 as we used live cell imaging and tracked the cell path of single cells. We measured different migration parameters for each cell independently of the cell proliferation rate. This was a clear advantage compared to measuring the area which had been filled by migrating cells after different time points. For that analysis possible differences in the cell proliferation rate among the different cell lines would be more relevant and may lead to misinterpretations. Moreover, it has been shown that expression of Cx43 reduces cell proliferation [69 126 30 48].

A migration enhancing effect of Cx43 has been reported previously for several other cell lines, such as rat heart cells H9c2 [114], neural crest cells [68 116 204] and C6 glioma cells [4]. Likewise, downregulation of Cx43 leads to decelerated cell migration in the same cells and also in mouse embryonic fibroblasts NIH3T3 [195] as well as in endothelial progenitors cells (EPC) [6].

We could show for the first time that expression of the C-terminal tail of Cx43 alone and further expression of a small part of the C-terminal tail, namely aa 299 – 336, enhances cell migration similar to the full length Cx43 protein. The channel building part of Cx43 (Cx43NT-GFP), however, exhibited no influence on cell migration. These results clearly demonstrate that the migration enhancing effect of Cx43 is gap junction independent and thus

confirms previous migration analysis in our lab using modified Boyden chambers [6]. In these chambers the cells migrate through small pores and thus are not able to form gap junctions during migration. Results of those experiments showed that migration of HeLa cells expressing Cx43 was increased compared to HeLa cells transfected with the empty vector [6], suggesting a gap junction independent effect of Cx43 on cell migration. This fact is also confirmed by previous studies showing that Cx43 enhances cell migration independently of its channel forming capacity [127] [4]. Since the channel is not required, adhesion processes or exchange of signaling molecules can most likely be excluded as mechanisms for enhancing cell migration. The C-terminal tail of Cx43 is naturally localized in the cytosol but adjacent to the cell membrane where the N-terminal part is embedded. In the present study HeLa cells were stably transfected with the C-terminal part of Cx43 which was localized in the cytosol over the whole cell as the protein was overexpressed. The same localization pattern was observed for the small part of Cx43 (aa 299 – 336) tagged with GFP, which was also able to show a similar migration enhancing effect as the full length Cx43 tagged with GFP. Consequently, a membrane bound C-terminal part is not required for the migration enhancing effect of Cx43. There are two possibilities why the C-terminal tail could exhibit a similar effect on cell migration as the full length Cx43 protein even though the localization was different than naturally. Firstly, it could be possible that, as the protein was overexpressed in the transfected cells, there was an adequate amount of the C-terminal part localized close to the membrane similar to expression of the full-length Cx43 protein. Secondly, the C-terminal part may act as a site of protein-protein interactions or as a potential part of a signalosome complex that is localized in the cytoplasm, but does not require localization near the membrane to cause enhanced cell migration. The C-terminus of Cx43 may also directly or indirectly, via another protein, interact with the actin cytoskeleton. This interaction takes place in the cytosol and, as demonstrated in the present study, is also possible with a solely expressed C-terminus of Cx43.

That expression of the C-terminal part of Cx43 alone is sufficient to cause similar effects as the full length Cx43 protein has been shown with regard to growth inhibition. Thus, expression of the C-terminus (aa 257 – 382) in Neuro2A [126], in HeLa [30] and in HEK293 [31] cells, which all do not express Cx43 in their wild-type forms, exhibited similar growth inhibition as the full length Cx43 protein, which implicates that the channel function of Cx43 is not required for this effect.

Various cytoskeletal proteins have been shown to interact with Cx43. For example, Xu et al. observed colocalization of full length Cx43 with α-actinin and drebrin in cardiac neural crest

cells [204]. Butkevich et al. detected binding of Cx43 to drebrin in pull-down assays using the C-terminal part of Cx43 (aa 243 – 382) tagged with glutathione S-transferase (GST) and membrane fractions of mouse brain homogenate [20]. Thus, this binding clearly takes place at the C-terminus of Cx43. Furthermore, Cx43 shows interaction with the actin-binding proteins cortactin [174] and NOV [123 45 48], which could also be confirmed in the present study by immunoprecipitation experiments using whole cell lysates and could further be specified to the C-terminal part of Cx43. Therefore, the binding to cortactin and NOV is still possible though the C-terminal tail is localized in the cytosol but is not membrane-bound.

Moreover, adhesion proteins, such as E-cadherin [46], N-cadherin [205] or Zonula occludens-1 (ZO-1) [70] colocalize with Cx43. N-cadherin interacts with Cx43 at its C-terminal part (aa 227 – 382) [195] and downregulation of either N-cadherin or Cx43 leads to reduced cell motility in NIH3T3 cells [195].

All these proteins are important in the control of cell migration and Cx43 might contribute to this process by either directly binding to those proteins or by indirect binding as part of a signalosome complex. Moreover, Cx43 may also directly regulate the actin cytoskeleton leading to enhanced cell migration.

However, there exist a few studies, e.g. by Oliveira et al. and Elias et al. determining that the migration enhancing effect of Cx43 is dependent on the gap junction channel. Thus, Oliveira et al. presented that after addition of the gap junction blocker carbenoxolon cell migration of C6 glioma cells was decreased when seeded in coculture experiments with astrocytes, but increased when seeded alone on collagen IV [137]. The authors interpret these results in a way that homocellular GJC between glioma cells supports intercellular adhesion, whereas hetereocellular GJC between glioma cells and astrocytes facilitates tumor cell migration [137]. Hence, this study intended to analyze cellular communication between different cell types, namely glioma cells and astrocytes, and its consequences during tumor formation. Elias et al. revealed that the adhesive properties of gap junction channels, but not the function as an aqueous channel are required for neuronal migration [38]. Thus, both studies used other cell lines and methods than we used and focused on the adhesive properties of the Cx43 channel. Of note, there are a few studies which indicate that Cx43 decreases cell migration as downregulation of Cx43 results in faster wound closure in skin lesions [153] and increased cell growth and migration in the breast carcinoma cell line Hs578T [163]. These results imply either a cell-specific role of Cx43 during cell migration or differences regarding stimulatory pathways of migration as in the present study serum-stimulated cell migration was

investigated and inhibitory effects of Cx43 on cell migration were mainly determined without addition of migration stimulating factors [153].

2 Influences of the GFP-tag on Cx43 expression pattern, cell coupling and migration

The truncated Cx43 proteins generated in the present study were tagged with GFP, because this allows studying protein expression and localization in cells without staining [25]. It has been shown that the protein behavior seemed not to be altered by the GFP-tag [59 190 142]. Cx43 tagged with GFP has also been used in HeLa cells to visualize the structure and assembly of gap junctions in living cells [43 102].

HeLa cells were used in the present study as they have been shown to express no connexins, due to epigenetic gene silencing by DNA methylation [82 81] and thus are deficient in gap junctional communication [37]. Moreover, the cells were suitable to be transfected with Cx43 and the truncated Cx43 proteins. To determine that Cx43NT-GFP was comparable to full length Cx43 in the ability to form functional gap junction channels, cell coupling was analyzed by the transfer of the fluorescent dye calcein from HeLa 43 donor cells to HeLa 43NT-GFP acceptor cells. In these measurements, HeLa cells expressing Cx43NT-GFP or Cx43-GFP showed functional cell coupling (43 and 29 %, respectively), albeit to a lesser degree compared to HeLa cells expressing wild-type Cx43 (64 %). Truncation of the C-terminal part or the GFP-tag might be the reason for this phenomenon. Maass et al. showed that truncation of the C-terminus (at aa 258) of Cx43 leads to functional gap junction channels, but the channel size is increased and the number of channels is reduced, indicating that the C-terminal part regulates number and size of gap junction channels [118], which are both important for the cell coupling rate. In previous studies gap junction channels of Cx43, tagged with GFP at the C-terminus, exhibited slower gating transitions between fully open and closed states compared to wild-type Cx43 [19 18], which might lead to decreased cell coupling. However, another study revealed that fusion of GFP to the C-terminal part of Cx43 did not influence cell coupling [78], whereas fusion of GFP to the N-terminus of Cx43 resulted in non-functional gap junction channels [102]. As mentioned above, we used the GFP-tag for expression and localization studies of Cx43 protein and the truncated Cx43 proteins within the cell. The GFP-tagged proteins, containing the transmembrane domains, were localized in the whole cell membrane, whereas wild-type Cx43 was mainly found in the cell membrane at cell-cell contact regions. This phenomenon was also described by Hunter et al., who demonstrated that fusion of the GFP-tag to the C-terminus of Cx43 resulted in “sheet-like” gap junctions and

supposed that the different appearance of the gap junction channels might be due to the fact that binding of ZO-1, which is involved in gap junction assembly, to the C-terminus is sterically inhibited by the GFP-tag [71]. Thus, we suppose that fusion of GFP may impair cell coupling to some extent, but, nevertheless, our results clearly show that the N-terminal part of Cx43 (Cx43NT-GFP) used in this study is able to form functional gap junction channels, at least regarding to the passage of the dye utilized here.

Fusion of GFP might also be the reason for the fact that migration of HeLa cells expressing Cx43-GFP was slightly less compared to wild-type Cx43. As mentioned above, fusion of GFP to Cx43 has been shown to influence binding affinity to certain proteins such as ZO-1 [52]. However, another study showed that overexpression of untagged Cx43 in C6 glioma cells led to similar increases in cell migration as overexpression of Cx43 tagged with GFP [4], indicating that binding of ZO-1 is not associated with enhanced cell migration. If the GFP-tag influences migration of HeLa cells, the generated protein Cx43-GFP is the correct control and, compared to this, the truncated proteins Cx43CT-GFP, Cx43(tr336)-GFP and Cx43(299-336)-GFP exhibited similar migration enhancement, leading to the conclusion that the aa 299 – 336 on the C-terminus are indeed required for the migration enhancing effect of Cx43.

3 Cx43 interacts with cortactin

Cortactin has been described as an actin-binding protein, enriched in cellular protrusions of migrating cells [202] [194] and is able to enhance cell migration [17] [100]. Moreover, it interacts with Cx43 [174] and thus may link Cx43 to the actin cytoskeleton. Using immunofluorescence staining we could confirm in the current study that cortactin colocalizes with Cx43 at the leading edge and in filopodia of migrating HeLa cells expressing Cx43-GFP. Furthermore, we demonstrated that the C-terminal part of Cx43 colocalizes with cortactin at the leading edge and also in filopodia of migrating HeLa cells. In this context the cytosolic localization of the C-terminus does not seem to alter the binding to cortactin. Anyway, HeLa cells, which were stably transfected with Cx43CT-GFP, showed abundant expression of the protein in the cytosol. Thus, binding between the C-terminus of Cx43 and other interacting proteins should be possible, although the C-terminus is not membrane-bound as it is naturally the case. In the present study we showed for the first time that cortactin binds to aa 257 – 299 of Cx43 using immunoprecipitation studies. Cortactin is associated with branched lamellipodia and invadopodia. It can initiate and stabilize new branched filaments [193] by activation of the neuronal N-WASP [87]. Concerning the localization of cortactin in filopodia it has been observed that cortactin is localized in filopodial tips of neuronal growth cones in Aplysia

californica (sea slug) [32] and also in lamellipodia and filopodia of mouse embryonic fibroblasts [74]. However, in the mouse melanoma cell line B16F1 cortactin is excluded from filopodia [177] indicating that filopodia localization seems to be cell type dependent. We observed that cortactin is localized in filopodia of migrating HeLa cells, but the underlying mechanism and the exact function of cortactin there remain to be elucidated. Moreover, using immunoprecipitation studies, we investigated that cortactin binds to aa 257 – 299 of Cx43 as mentioned above. Interaction of cortactin and Cx43 has been examined in prior studies in murine C2C12 myoblasts [174] and also in Sertoli cells of mouse seminiferous epithelium [187] but the exact binding sequence has not been observed yet. Cortactin is involved in the process of cell migration, as it enhances cell migration [17 65] as well as tumor invasion [28]. Likewise, downregulation of cortactin results in decreased cell migration, for example, in fibroblasts [100]. In our study both truncated proteins, Cx43(tr298)-GFP, which had shown diminished cell migration, and Cx43(tr336)-GFP, which had shown enhanced cell migration in HeLa cells, exhibited binding to cortactin. This binding site therefore is presumably not involved in the mechanism of enhanced cell migration. However, we cannot exclude that there exists an additional binding site at aa 299 – 336 on the C-terminal tail of Cx43 that might lead to the migration enhancing effect or that binding of the whole C-terminus to cortactin is required for the effect of increased cell migration by Cx43.

4 Cx43 interacts with NOV

NOV influences cell migration [110 7] and cell growth [145 147]. It either acts intracellularly e.g. by upregulating different MMPs [110 7] or remodeling of the actin cytoskeleton [165] or is secreted, e.g. after stimulation of the cells with growth factors or transforming oncogenes [13], where it can bind to certain integrins [112]. Moreover, it shows intracellular interaction with Cx43 and links Cx43 to the actin cytoskeleton [45 48]. As this interaction might be one reason for Cx43 enhancing cell migration, we studied binding of NOV to Cx43 and whether this interaction influences cell migration in HeLa cells.

Immunoprecipitation studies in the present work revealed that Cx43 interacts with NOV at the C-terminal part and more precisely at aa 257 – 298 of Cx43. It has already been observed by immunoprecipitation studies that NOV binds to the C-terminus (aa 257 – 382) of Cx43 in Jeg3 cells [48] and in C6 glioma cells [45], which was further specified to aa 280 – 360 of Cx43 using an immunoprecipitation competition assay with different C-terminus deletion mutants in breast cancer cells (Hs578T) [165]. We were able to identify the binding sequence of NOV at the C-terminal part of Cx43 more closely to aa 257 – 298 of Cx43. This sequence contains

two Src binding domains (SH2 at aa 265 and SH3 at aa 274 – 283) [50] and thus Src might form a protein complex, in which NOV and possibly also cortactin are involved. However, there might also exist an additional binding site for NOV at aa 299 – 336 of Cx43 that could cause a migration enhancing effect, indicating that both binding sites are required. This can be assumed because of a study using differently C-terminus-truncated Cx43 proteins (aa 1 – 257, aa 1 – 264, aa 1 – 273, and aa 1 – 374) which all bind to NOV in immunoprecipitation and FRET studies in human embryonic kidney epithelial cells (293T), but only the truncated version aa 1 – 374 of Cx43 and the full length Cx43 protein showed the growth inhibition effect of Cx43 [49]. These results indicate that binding of the full length C-terminus to NOV is required for this effect which might be analogous to the migration enhancing effect.

5 Cx43 influences the actin cytoskeleton

The present study demonstrates that enhanced serum-stimulated cell migration in HeLa cells due to expression of the C-terminal part of Cx43 and, specifically, that the expression of aa 299 – 336 of Cx43 is associated with increased filopodia formation per single cell. Indeed, we could show that Cx43 is localized in filopodia of migrating HeLa cells. These results suggest that Cx43 might influence the actin cytoskeleton. This effect has also been reported in neural crest cells [204] and in epicardial cells [155] as in these cells the stress fibers are normally aligned in the direction of migration, whereas downregulation of Cx43 leads to stress fibers that show no obvious orientation [204 155]. Yet, we did not observe such changes in stress fiber alignment comparing HeLa cells expressing Cx43 and control cells. Colocalization of full length Cx43 with the actin cytoskeleton in filopodia was observed recently in LN18 glioma cells which endogenously express low levels of Cx43 [29]. The same study also showed that the C-terminal part of Cx43 influences the actin cytoskeleton as cells expressing full length Cx43 or the C-terminus of Cx43 exhibited numerous actin-rich filopodia that were not visible in cells expressing the N-terminal part [29]. These results also are in agreement with our results that Cx43 leads to an enhanced filopodia formation. Filopodia are involved in cell migration and can function as antennae for cells which use them for sensing their environment, leading to increased directionality during cell migration [122]. Moreover, invasive cancer cells show abundant filopodia formation [186]. Thus, increased filopodia formation by Cx43 may be one aspect leading to the enhanced cell migration found in Cx43 expressing cells.

6 Inhibition of p38 MAPK influences the actin cytoskeleton

The present study shows that inhibition of p38 MAPK leads to significantly reduced formation of filopodia in cells expressing Cx43 down to the level observed in untreated empty vector transfected cells. These results suggest that activation of p38 MAPK is involved in Cx43 mediated filopodia formation. Recently, we could show that addition of the migration-stimulus serum induced the activation of p38 MAPK in HeLa cells [6]. This activation was increased in HeLa cells expressing Cx43 or the C-terminal part of Cx43, which both also showed enhanced cell migration, compared to cells expressing the N-terminal part of Cx43 or empty vector transfected cells. Thus, expression of full length Cx43 or the C-terminal part of Cx43 in HeLa cells correlated with an enhanced phosphorylation of p38 MAPK in response to the migration stimulus [6]. Furthermore, we demonstrated that inhibition of p38 MAPK suppressed serum-stimulated migration in those cells to the basal migration levels observed in untreated empty vector transfected cells [6]. Influences of p38 MAPK on the actin cytoskeleton have been determined in various cell types. Thus, inhibition of p38 MAPK by the inhibitor SB202190 led to impaired formation of actin stress fibers in TGF-β stimulated mouse mammary epithelial cells (NMuMG) [3] and blocked actin polymerization and reorganization in PDGF stimulated mouse smooth muscle cells [39]. Lately, in murine myoblasts (C2C12) it has been observed that inhibition of p38 MAPK prevents the interaction between Cx43 and F-actin [174], indicating that activation of p38 MAPK plays a role in this context. We could confirm these results in the present study by demonstrating that inhibition of p38 MAPK led to decreased filopodia formation. Thus, activation of p38 MAPK is involved in Cx43 mediated influences on the actin cytoskeleton.

7 Future prospects

In the present work we determined that the migration enhancing effect of Cx43 is gap junction independent and thus might be due to Cx43 functioning as an adapter protein or as a part of a signalosome complex. In addition, we showed that a sequence on the C-terminus between aa 299 – 336 of Cx43 is necessary for this process. To further elucidate whether this sequence is sufficient and required for the migration enhancing effect, additional migration analysis studies with Cx43 mutants lacking or containing mutations in this sequence could be performed.

Moreover, we presented that Cx43 influences the actin cytoskeleton, leading to increased filopodia formation. This implies that one or several proteins bind to Cx43 and thus act as linker proteins to the actin cytoskeleton and/or Cx43 interacts directly with the actin

cytoskeleton. Both actin-binding proteins cortactin and NOV bind to aa 257 – 298 on the C-terminal part of Cx43. Therefore, this binding does not seem to influence cell migration in HeLa cells, but it has to be elucidated whether there is an additional binding site for cortactin and/or NOV that might be involved in the migration enhancing effect of Cx43. However, one or both of these proteins could link Cx43 to the actin cytoskeleton. Moreover, other actin-binding proteins which have been shown to interact with Cx43, such as α-actinin, ezrin, IQGAP or drebrin [204] could be involved in the migration enhancing effect of Cx43 and associated filopodia formation. For example, drebrin is localized in lamellipodia and filopodia [143 144] and might also be involved in the formation of podosomes in non-neuronal cells [119]. These results imply an effect of drebrin on the actin cytoskeleton that may therefore link Cx43 to the actin cytoskeleton as well. New protein candidates could be analyzed by further immunoprecipitation studies with the truncated proteins and detected by SDS-PAGE, coomassie staining and mass spectrometry or by other pull-down assays.

Besides interaction of Cx43 with certain proteins, activation of p38 MAPK could be another possible mechanism for the enhanced cell migration by Cx43. As mentioned above we recently showed that inhibition of p38 MAPK resulted in diminished cell migration in Cx43 expressing HeLa cells down to the migration levels observed in untreated empty vector transfected cells [6]. In the current study we present that inhibition of p38 MAPK leads to reduced formation of filopodia in cells expressing Cx43 down to the level observed in untreated empty vector transfected cells. These findings suggest that enhanced cell migration and increased filopodia formation by Cx43 is associated with the activation of p38 MAPK. However, this needs to be further elucidated and whether this mechanism also applies for the truncated Cx43 proteins.

The influences of Cx43 on the actin cytoskeleton have to be further clarified, for example whether Cx43 either increases assembly of filopodia, possibly by participation in the filopodial tip complex, or diminishes the disassembly of filopodia by stabilizing existing filopodia. Both processes would result in a higher amount of filopodia per single cell which might lead to increased cell migration as filopodia are involved in cell motility and enhanced directional cell migration [122]. Thus, increased filopodia formation due to Cx43 expression might be one reason for enhanced cell migration.

Several physiological and pathophysiological processes characterized by enhanced cell migration such as wound healing and atherosclerosis, are linked with increased expression of Cx43 in endothelial [95 94] and smooth muscle cells [149]. Especially atherosclerosis is a major cause of death in western societies [94 23 24]. During the process of atherosclerosis several cells,

including dysfunctional endothelium, macrophages, T lymphocytes, and smooth muscle cells, migrate into the vessel wall and consequently contribute to the formation of an atherosclerotic plaque [94 23 24]. Understanding the underlying mechanisms is important for antagonizing this migration action. With the present study we could contribute some aspects to the mechanism of enhanced cell migration due to Cx43 expression. Thus, it relies on the C-terminal tail of Cx43 and the sequence aa 299 – 336 on the C-terminus plays an important role in this context. Moreover, cytoskeletal modifications and activation of p38 MAPK are associated with enhanced cell migration by Cx43.

V Summary

The gap junction protein Cx43 is widely expressed in mammalian [10 9 191 199 101 83] and non-mammalian cells [184]. Besides its role in forming gap junctions, which allow the direct exchange between adjacent cells of molecules up to a molecular weight of 1.8 kDa [91 83], it also displays functions as an adapter protein. In fact, various proteins bind to its cytoplasmic C-terminal part [50], including actin-binding proteins, such as α-actinin [204] and drebrin [20], adhesion proteins, such as E-cadherin [46], N-cadherin [64] or ZO-1 [70]; and proteins influencing proliferation and migration such as NOV [123 45 48] and cortactin [174]. Furthermore, Cx43 has been shown to influence several cellular processes including cell migration [4 204] and proliferation [30 31 138]. Accordingly, expression of Cx43 is increased during processes associated with enhanced cell migration such as wound healing [95], angiogenesis [189 111], atherosclerosis [94] and vascular neointima formation [149].

In the present study we analyzed the potential influences of Cx43 and some truncated proteins of Cx43 on serum-stimulated cell migration and associated cytoskeletal modifications in HeLa cells, which do not express connexins in their wild-type form. Using cell culture inserts in which the cells migrate into a cell free gap, we observed that the migration enhancing effect of Cx43 is gap junction independent and that the sequence aa 299 – 336 on the C-terminus of Cx43 is required for this effect. Moreover, we could show that binding of two actin-binding proteins, which also have been associated with enhanced cell migration, namely cortactin and NOV, takes place at aa 257 – 299 of Cx43. Therefore, this binding alone is presumably not involved in the migration enhancing effect of Cx43. The present study revealed further that the migration enhancing effect of aa 299 – 336 of Cx43 is associated with increased filopodia formation leading to a higher quantity of filopodia per cell. This could be one reason for enhanced cell migration due to Cx43 expression as filopodia are involved in cell migration and cancer cell invasion [56 122]. Moreover, Cx43 mediated increased filopodia formation is associated with the activation of p38 MAPK.

In summary, the enhanced cell migration by Cx43 is gap junction independent and relies on the sequence aa 299 – 336 on the C-terminus of Cx43. Moreover, it is associated with increased filopodia formation and activation of p38 MAPK.

VI References

1 Ammer, A. G. & Weed, S. A., *Cortactin branches out: roles in regulating protrusive actin dynamics*, Cell Motil Cytoskeleton (2008), 65 (9), 687-707

2 Araya, R. et al., *Expression of connexins during differentiation and regeneration of skeletal muscle: functional relevance of connexin43*, J Cell Sci (2005), 118 (Pt 1), 27-37

3 Bakin, A. V., Rinehart, C., Tomlinson, A. K. & Arteaga, C. L., *p38 mitogen-activated protein kinase is required for TGFbeta-mediated fibroblastic transdifferentiation and cell migration*, J Cell Sci (2002), 115 (Pt 15), 3193-3206

4 Bates, D. C., Sin, W. C., Aftab, Q. & Naus, C. C., *Connexin43 enhances glioma invasion by a mechanism involving the carboxy terminus*, Glia (2007), 55 (15), 1554-1564

5 Beahm, D. L. et al., *Mutation of a conserved threonine in the third transmembrane helix of alpha- and beta-connexins creates a dominant-negative closed gap junction channel*, J Biol Chem (2006), 281 (12), 7994-8009

6 Behrens, J., Kameritsch, P., Wallner, S., Pohl, U. & Pogoda, K., *The carboxyl tail of Cx43 augments p38 mediated cell migration in a gap junction-independent manner*, Eur J Cell Biol (2010), 89 (11), 828-838

7 Benini, S. et al., *In Ewing's sarcoma CCN3(NOV) inhibits proliferation while promoting migration and invasion of the same cell type*, Oncogene (2005), 24 (27), 4349-4361

8 Bertani, G., *Studies on lysogenesis. I. The mode of phage liberation by lysogenic Escherichia coli*, J Bacteriol (1951), 62 (3), 293-300

9 Beyer, E. C., Kistler, J., Paul, D. L. & Goodenough, D. A., *Antisera directed against connexin43 peptides react with a 43-kD protein localized to gap junctions in myocardium and other tissues*, J Cell Biol (1989), 108 (2), 595-605

10 Beyer, E. C., Paul, D. L. & Goodenough, D. A., *Connexin43: a protein from rat heart homologous to a gap junction protein from liver*, J Cell Biol (1987), 105 (6 Pt 1), 2621-2629

11 Blanchoin, L., Amann, K. J., Higgs, H. N., Marchand, J. B., Kaiser, D. A. & Pollard, T. D., *Direct observation of dendritic actin filament networks nucleated by Arp2/3 complex and WASP/Scar proteins*, Nature (2000), 404 (6781), 1007-1011

12 Blanchoin, L. & Pollard, T. D., *Mechanism of interaction of Acanthamoeba actophorin (ADF/Cofilin) with actin filaments*, J Biol Chem (1999), 274 (22), 15538-15546

13 Bork, P., *The modular architecture of a new family of growth regulators related to connective tissue growth factor*, FEBS Lett (1993), 327 (2), 125-130

14 Brigstock, D. R., *The connective tissue growth factor/cysteine-rich 61/nephroblastoma overexpressed (CCN) family*, Endocr Rev (1999), 20 (2), 189-206

15 Brisset, A. C., Isakson, B. E. & Kwak, B. R., *Connexins in vascular physiology and pathology*, Antioxid Redox Signal (2009), 11 (2), 267-282

16 Bruzzone, R., White, T. W. & Paul, D. L., *Connections with connexins: the molecular basis of direct intercellular signaling*, Eur J Biochem (1996), 238 (1), 1-27

17 Bryce, N. S., Clark, E. S., Leysath, J. L., Currie, J. D., Webb, D. J. & Weaver, A. M., *Cortactin promotes cell motility by enhancing lamellipodial persistence*, Curr Biol (2005), 15 (14), 1276-1285

18 Bukauskas, F. F., Bukauskiene, A., Bennett, M. V. & Verselis, V. K., *Gating properties of gap junction channels assembled from connexin43 and connexin43 fused with green fluorescent protein*, Biophys J (2001), 81 (1), 137-152

19 Bukauskas, F. F. et al., *Clustering of connexin 43-enhanced green fluorescent protein gap junction channels and functional coupling in living cells*, Proc Natl Acad Sci U S A (2000), 97 (6), 2556-2561

20 Butkevich, E., Hulsmann, S., Wenzel, D., Shirao, T., Duden, R. & Majoul, I., *Drebrin is a novel connexin-43 binding partner that links gap junctions to the submembrane cytoskeleton*, Curr Biol (2004), 14 (8), 650-658

21 Carlier, M. F. et al., *Actin depolymerizing factor (ADF/cofilin) enhances the rate of filament turnover: implication in actin-based motility*, J Cell Biol (1997), 136 (6), 1307-1322

22 Caspar, D. L., Goodenough, D. A., Makowski, L. & Phillips, W. C., *Gap junction structures. I. Correlated electron microscopy and x-ray diffraction*, J Cell Biol (1977), 74 (2), 605-628

23 Chadjichristos, C. E., Derouette, J. P. & Kwak, B. R., *Connexins in atherosclerosis*, Adv Cardiol (2006), 42 255-267

24 Chadjichristos, C. E. & Kwak, B. R., *Connexins: new genes in atherosclerosis*, Ann Med (2007), 39 (6), 402-411

25 Chalfie, M., Tu, Y., Euskirchen, G., Ward, W. W. & Prasher, D. C., *Green fluorescent protein as a marker for gene expression*, Science (1994), 263 (5148), 802-805

26 Christ, G. J. et al., *Gap junctions modulate tissue contractility and alpha 1 adrenergic agonist efficacy in isolated rat aorta*, J Pharmacol Exp Ther (1993), 266 (2), 1054-1065

27 Cina, C., Maass, K., Theis, M., Willecke, K., Bechberger, J. F. & Naus, C. C., *Involvement of the cytoplasmic C-terminal domain of connexin43 in neuronal migration*, J Neurosci (2009), 29 (7), 2009-2021

28 Clark, E. S., Whigham, A. S., Yarbrough, W. G. & Weaver, A. M., *Cortactin is an essential regulator of matrix metalloproteinase secretion and extracellular matrix degradation in invadopodia*, Cancer Res (2007), 67 (9), 4227-4235

29 Crespin, S., Bechberger, J., Mesnil, M., Naus, C. C. & Sin, W. C., *The carboxy-terminal tail of connexin43 gap junction protein is sufficient to mediate cytoskeleton changes in human glioma cells*, J Cell Biochem (2010), 110 (3), 589-597

30 Dang, X., Doble, B. W. & Kardami, E., *The carboxy-tail of connexin-43 localizes to the nucleus and inhibits cell growth*, Mol Cell Biochem (2003), 242 (1-2), 35-38

31 Dang, X., Jeyaraman, M. & Kardami, E., *Regulation of connexin-43-mediated growth inhibition by a phosphorylatable amino-acid is independent of gap junction-forming ability*, Mol Cell Biochem (2006), 289 (1-2), 201-207

32 Decourt, B., Munnamalai, V., Lee, A. C., Sanchez, L. & Suter, D. M., *Cortactin colocalizes with filopodial actin and accumulates at IgCAM adhesion sites in Aplysia growth cones*, J Neurosci Res (2009), 87 (5), 1057-1068

33 Duffy, H. S. et al., *Regulation of connexin43 protein complexes by intracellular acidification*, Circ Res (2004), 94 (2), 215-222

34 Duffy, H. S. et al., *pH-dependent intramolecular binding and structure involving Cx43 cytoplasmic domains*, J Biol Chem (2002), 277 (39), 36706-36714

35 Dunham, B. et al., *Immunolocalization and expression of functional and nonfunctional cell-to-cell channels from wild-type and mutant rat heart connexin43 cDNA*, Circ Res (1992), 70 (6), 1233-1243

36 Durieu-Trautmann, O., Chaverot, N., Cazaubon, S., Strosberg, A. D. & Couraud, P. O., *Intercellular adhesion molecule 1 activation induces tyrosine phosphorylation of the cytoskeleton-associated protein cortactin in brain microvessel endothelial cells*, J Biol Chem (1994), 269 (17), 12536-12540

37 Elfgang, C. et al., *Specific permeability and selective formation of gap junction channels in connexin-transfected HeLa cells*, J Cell Biol (1995), 129 (3), 805-817

38 Elias, L. A., Wang, D. D. & Kriegstein, A. R., *Gap junction adhesion is necessary for radial migration in the neocortex*, Nature (2007), 448 (7156), 901-907
39 Esfandiarei, M., Yazdi, S. A., Gray, V., Dedhar, S. & van Breemen, C., *Integrin-linked kinase functions as a downstream signal of platelet-derived growth factor to regulate actin polymerization and vascular smooth muscle cell migration*, BMC Cell Biol (2010), 11 16
40 Evans, W. H. & Martin, P. E., *Lighting up gap junction channels in a flash*, Bioessays (2002), 24 (10), 876-880
41 Ewart, J. L. et al., *Heart and neural tube defects in transgenic mice overexpressing the Cx43 gap junction gene*, Development (1997), 124 (7), 1281-1292
42 Faix, J. & Rottner, K., *The making of filopodia*, Curr Opin Cell Biol (2006), 18 (1), 18-25
43 Falk, M. M. & Lauf, U., *High resolution, fluorescence deconvolution microscopy and tagging with the autofluorescent tracers CFP, GFP, and YFP to study the structural composition of gap junctions in living cells*, Microsc Res Tech (2001), 52 (3), 251-262
44 Fromaget, C., el Aoumari, A., Dupont, E., Briand, J. P. & Gros, D., *Changes in the expression of connexin 43, a cardiac gap junctional protein, during mouse heart development*, J Mol Cell Cardiol (1990), 22 (11), 1245-1258
45 Fu, C. T., Bechberger, J. F., Ozog, M. A., Perbal, B. & Naus, C. C., *CCN3 (NOV) interacts with connexin43 in C6 glioma cells: possible mechanism of connexin-mediated growth suppression*, J Biol Chem (2004), 279 (35), 36943-36950
46 Fujimoto, K., Nagafuchi, A., Tsukita, S., Kuraoka, A., Ohokuma, A. & Shibata, Y., *Dynamics of connexins, E-cadherin and alpha-catenin on cell membranes during gap junction formation*, J Cell Sci (1997), 110 (Pt 3) 311-322
47 Galbraith, C. G., Yamada, K. M. & Galbraith, J. A., *Polymerizing actin fibers position integrins primed to probe for adhesion sites*, Science (2007), 315 (5814), 992-995
48 Gellhaus, A. et al., *Connexin43 interacts with NOV: a possible mechanism for negative regulation of cell growth in choriocarcinoma cells*, J Biol Chem (2004), 279 (35), 36931-36942
49 Gellhaus, A., Wotzlaw, C., Otto, T., Fandrey, J. & Winterhager, E., *More insights into the CCN3/Connexin43 interaction complex and its role for signaling*, J Cell Biochem (2010), 110 (1), 129-140
50 Giepmans, B. N., *Gap junctions and connexin-interacting proteins*, Cardiovasc Res (2004), 62 (2), 233-245
51 Giepmans, B. N., *Role of connexin43-interacting proteins at gap junctions*, Adv Cardiol (2006), 42 41-56
52 Giepmans, B. N., Verlaan, I. & Moolenaar, W. H., *Connexin-43 interactions with ZO-1 and alpha- and beta-tubulin*, Cell Commun Adhes (2001), 8 (4-6), 219-223
53 Gohji, K. et al., *Serum matrix metalloproteinase-2 and its density in men with prostate cancer as a new predictor of disease extension*, Int J Cancer (1998), 79 (1), 96-101
54 Goodenough, D. A., Goliger, J. A. & Paul, D. L., *Connexins, connexons, and intercellular communication*, Annu Rev Biochem (1996), 65 475-502
55 Gros, D. B. & Jongsma, H. J., *Connexins in mammalian heart function*, Bioessays (1996), 18 (9), 719-730
56 Gupton, S. L. & Gertler, F. B., *Filopodia: the fingers that do the walking*, Sci STKE (2007), 2007 (400), re5
57 Gutstein, D. E. et al., *Conduction slowing and sudden arrhythmic death in mice with cardiac-restricted inactivation of connexin43*, Circ Res (2001), 88 (3), 333-339
58 Haddock, R. E. et al., *Endothelial coordination of cerebral vasomotion via myoendothelial gap junctions containing connexins 37 and 40*, Am J Physiol Heart Circ Physiol (2006), 291 (5), H2047-2056

59 Hanakam, F., Albrecht, R., Eckerskorn, C., Matzner, M. & Gerisch, G., *Myristoylated and non-myristoylated forms of the pH sensor protein hisactophilin II: intracellular shuttling to plasma membrane and nucleus monitored in real time by a fusion with green fluorescent protein*, EMBO J (1996), 15 (12), 2935-2943

60 Hanner, F., Sorensen, C. M., Holstein-Rathlou, N. H. & Peti-Peterdi, J., *Connexins and the kidney*, Am J Physiol Regul Integr Comp Physiol (2010), 298 (5), R1143-1155

61 Hazan, R. B., Phillips, G. R., Qiao, R. F., Norton, L. & Aaronson, S. A., *Exogenous expression of N-cadherin in breast cancer cells induces cell migration, invasion, and metastasis*, J Cell Biol (2000), 148 (4), 779-790

62 Head, J. A. et al., *Cortactin tyrosine phosphorylation requires Rac1 activity and association with the cortical actin cytoskeleton*, Mol Biol Cell (2003), 14 (8), 3216-3229

63 Hedges, J. C. et al., *A role for p38(MAPK)/HSP27 pathway in smooth muscle cell migration*, J Biol Chem (1999), 274 (34), 24211-24219

64 Hertig, C. M., Butz, S., Koch, S., Eppenberger-Eberhardt, M., Kemler, R. & Eppenberger, H. M., *N-cadherin in adult rat cardiomyocytes in culture. II. Spatio-temporal appearance of proteins involved in cell-cell contact and communication. Formation of two distinct N-cadherin/catenin complexes*, J Cell Sci (1996), 109 (Pt 1) 11-20

65 Hill, A. et al., *Cortactin underpins CD44-promoted invasion and adhesion of breast cancer cells to bone marrow endothelial cells*, Oncogene (2006), 25 (45), 6079-6091

66 Hirst-Jensen, B. J., Sahoo, P., Kieken, F., Delmar, M. & Sorgen, P. L., *Characterization of the pH-dependent interaction between the gap junction protein connexin43 carboxyl terminus and cytoplasmic loop domains*, J Biol Chem (2007), 282 (8), 5801-5813

67 Huang, C., Jacobson, K. & Schaller, M. D., *MAP kinases and cell migration*, J Cell Sci (2004), 117 (Pt 20), 4619-4628

68 Huang, G. Y., Cooper, E. S., Waldo, K., Kirby, M. L., Gilula, N. B. & Lo, C. W., *Gap junction-mediated cell-cell communication modulates mouse neural crest migration*, J Cell Biol (1998), 143 (6), 1725-1734

69 Huang, R. P., Fan, Y., Hossain, M. Z., Peng, A., Zeng, Z. L. & Boynton, A. L., *Reversion of the neoplastic phenotype of human glioblastoma cells by connexin 43 (cx43)*, Cancer Res (1998), 58 (22), 5089-5096

70 Hunter, A. W. & Gourdie, R. G., *The second PDZ domain of zonula occludens-1 is dispensable for targeting to connexin 43 gap junctions*, Cell Commun Adhes (2008), 15 (1), 55-63

71 Hunter, A. W., Jourdan, J. & Gourdie, R. G., *Fusion of GFP to the carboxyl terminus of connexin43 increases gap junction size in HeLa cells*, Cell Commun Adhes (2003), 10 (4-6), 211-214

72 Isakson, B. E., Best, A. K. & Duling, B. R., *Incidence of protein on actin bridges between endothelium and smooth muscle in arterioles demonstrates heterogeneous connexin expression and phosphorylation*, Am J Physiol Heart Circ Physiol (2008), 294 (6), H2898-2904

73 Johnson, G. L. & Lapadat, R., *Mitogen-activated protein kinase pathways mediated by ERK, JNK, and p38 protein kinases*, Science (2002), 298 (5600), 1911-1912

74 Johnston, S. A., Bramble, J. P., Yeung, C. L., Mendes, P. M. & Machesky, L. M., *Arp2/3 complex activity in filopodia of spreading cells*, BMC Cell Biol (2008), 9 65

75 Joliot, V. et al., *Proviral rearrangements and overexpression of a new cellular gene (nov) in myeloblastosis-associated virus type 1-induced nephroblastomas*, Mol Cell Biol (1992), 12 (1), 10-21

76 Jongen, W. M. et al., *Regulation of connexin 43-mediated gap junctional intercellular communication by Ca2+ in mouse epidermal cells is controlled by E-cadherin*, J Cell Biol (1991), 114 (3), 545-555

77 Jordan, K., Chodock, R., Hand, A. R. & Laird, D. W., *The origin of annular junctions: a mechanism of gap junction internalization*, J Cell Sci (2001), 114 (Pt 4), 763-773

78 Jordan, K. et al., *Trafficking, assembly, and function of a connexin43-green fluorescent protein chimera in live mammalian cells*, Mol Biol Cell (1999), 10 (6), 2033-2050

79 Kanner, S. B., Reynolds, A. B., Vines, R. R. & Parsons, J. T., *Monoclonal antibodies to individual tyrosine-phosphorylated protein substrates of oncogene-encoded tyrosine kinases*, Proc Natl Acad Sci U S A (1990), 87 (9), 3328-3332

80 Kardami, E. et al., *The role of connexins in controlling cell growth and gene expression*, Prog Biophys Mol Biol (2007), 94 (1-2), 245-264

81 King, T. J., Fukushima, L. H., Donlon, T. A., Hieber, A. D., Shimabukuro, K. A. & Bertram, J. S., *Correlation between growth control, neoplastic potential and endogenous connexin43 expression in HeLa cell lines: implications for tumor progression*, Carcinogenesis (2000), 21 (2), 311-315

82 King, T. J., Fukushima, L. H., Hieber, A. D., Shimabukuro, K. A., Sakr, W. A. & Bertram, J. S., *Reduced levels of connexin43 in cervical dysplasia: inducible expression in a cervical carcinoma cell line decreases neoplastic potential with implications for tumor progression*, Carcinogenesis (2000), 21 (6), 1097-1109

83 King, T. J. & Lampe, P. D., *Temporal regulation of connexin phosphorylation in embryonic and adult tissues*, Biochim Biophys Acta (2005), 1719 (1-2), 24-35

84 Kinley, A. W. et al., *Cortactin interacts with WIP in regulating Arp2/3 activation and membrane protrusion*, Curr Biol (2003), 13 (5), 384-393

85 Klekotka, P. A., Santoro, S. A. & Zutter, M. M., *alpha 2 integrin subunit cytoplasmic domain-dependent cellular migration requires p38 MAPK*, J Biol Chem (2001), 276 (12), 9503-9511

86 Korobova, F. & Svitkina, T., *Arp2/3 complex is important for filopodia formation, growth cone motility, and neuritogenesis in neuronal cells*, Mol Biol Cell (2008), 19 (4), 1561-1574

87 Kowalski, J. R., Egile, C., Gil, S., Snapper, S. B., Li, R. & Thomas, S. M., *Cortactin regulates cell migration through activation of N-WASP*, J Cell Sci (2005), 118 (Pt 1), 79-87

88 Kress, H., Stelzer, E. H., Holzer, D., Buss, F., Griffiths, G. & Rohrbach, A., *Filopodia act as phagocytic tentacles and pull with discrete steps and a load-dependent velocity*, Proc Natl Acad Sci U S A (2007), 104 (28), 11633-11638

89 Kruger, O. et al., *Altered dye diffusion and upregulation of connexin37 in mouse aortic endothelium deficient in connexin40*, J Vasc Res (2002), 39 (2), 160-172

90 Kumar, N. M. & Gilula, N. B., *Molecular biology and genetics of gap junction channels*, Semin Cell Biol (1992), 3 (1), 3-16

91 Kumar, N. M. & Gilula, N. B., *The gap junction communication channel*, Cell (1996), 84 (3), 381-388

92 Kurtz, L. et al., *High-level connexin expression in the human juxtaglomerular apparatus*, Nephron Physiol (2010), 116 (1), p1-8

93 Kwak, B. R., Hermans, M. M., De Jonge, H. R., Lohmann, S. M., Jongsma, H. J. & Chanson, M., *Differential regulation of distinct types of gap junction channels by similar phosphorylating conditions*, Mol Biol Cell (1995), 6 (12), 1707-1719

94 Kwak, B. R., Mulhaupt, F., Veillard, N., Gros, D. B. & Mach, F., *Altered pattern of vascular connexin expression in atherosclerotic plaques*, Arterioscler Thromb Vasc Biol (2002), 22 (2), 225-230

95 Kwak, B. R., Pepper, M. S., Gros, D. B. & Meda, P., *Inhibition of endothelial wound repair by dominant negative connexin inhibitors*, Mol Biol Cell (2001), 12 (4), 831-845

96 Kwak, B. R. et al., *Effects of cGMP-dependent phosphorylation on rat and human connexin43 gap junction channels*, Pflugers Arch (1995), 430 (5), 770-778

97 Kwak, B. R., van Veen, T. A., Analbers, L. J. & Jongsma, H. J., *TPA increases conductance but decreases permeability in neonatal rat cardiomyocyte gap junction channels*, Exp Cell Res (1995), 220 (2), 456-463

98 Kwak, B. R. et al., *Reduced connexin43 expression inhibits atherosclerotic lesion formation in low-density lipoprotein receptor-deficient mice*, Circulation (2003), 107 (7), 1033-1039

99 Laemmli, U. K., *Cleavage of structural proteins during the assembly of the head of bacteriophage T4*, Nature (1970), 227 (5259), 680-685

100 Lai, F. P. et al., *Cortactin promotes migration and platelet-derived growth factor-induced actin reorganization by signaling to Rho-GTPases*, Mol Biol Cell (2009), 20 (14), 3209-3223

101 Laird, D. W., *Life cycle of connexins in health and disease*, Biochem J (2006), 394 (Pt 3), 527-543

102 Laird, D. W., Jordan, K., Thomas, T., Qin, H., Fistouris, P. & Shao, Q., *Comparative analysis and application of fluorescent protein-tagged connexins*, Microsc Res Tech (2001), 52 (3), 263-272

103 Laird, D. W., Puranam, K. L. & Revel, J. P., *Turnover and phosphorylation dynamics of connexin43 gap junction protein in cultured cardiac myocytes*, Biochem J (1991), 273(Pt 1) 67-72

104 Laird, D. W. & Revel, J. P., *Biochemical and immunochemical analysis of the arrangement of connexin43 in rat heart gap junction membranes*, J Cell Sci (1990), 97 (Pt 1) 109-117

105 Lampe, P. D., Cooper, C. D., King, T. J. & Burt, J. M., *Analysis of Connexin43 phosphorylated at S325, S328 and S330 in normoxic and ischemic heart*, J Cell Sci (2006), 119 (Pt 16), 3435-3442

106 Lampe, P. D. & Lau, A. F., *Regulation of gap junctions by phosphorylation of connexins*, Arch Biochem Biophys (2000), 384 (2), 205-215

107 Lampe, P. D. & Lau, A. F., *The effects of connexin phosphorylation on gap junctional communication*, Int J Biochem Cell Biol (2004), 36 (7), 1171-1186

108 Lampe, P. D., TenBroek, E. M., Burt, J. M., Kurata, W. E., Johnson, R. G. & Lau, A. F., *Phosphorylation of connexin43 on serine368 by protein kinase C regulates gap junctional communication*, J Cell Biol (2000), 149 (7), 1503-1512

109 Lau, L. F. & Lam, S. C., *The CCN family of angiogenic regulators: the integrin connection*, Exp Cell Res (1999), 248 (1), 44-57

110 Laurent, M. et al., *NOVH increases MMP3 expression and cell migration in glioblastoma cells via a PDGFR-alpha-dependent mechanism*, FASEB J (2003), 17 (13), 1919-1921

111 Laws, M. J. et al., *Gap junction communication between uterine stromal cells plays a critical role in pregnancy-associated neovascularization and embryo survival*, Development (2008), 135 (15), 2659-2668

112 Lin, C. G. et al., *CCN3 (NOV) is a novel angiogenic regulator of the CCN protein family*, J Biol Chem (2003), 278 (26), 24200-24208

113 Liotta, L. A., Tryggvason, K., Garbisa, S., Hart, I., Foltz, C. M. & Shafie, S., *Metastatic potential correlates with enzymatic degradation of basement membrane collagen*, Nature (1980), 284 (5751), 67-68

114 Liu, X. et al., *Increased connexin 43 expression improves the migratory and proliferative ability of H9c2 cells by Wnt-3a overexpression*, Acta Biochim Biophys Sin (Shanghai) (2007), 39 (6), 391-398

115 Lo, C. W., *The role of gap junction membrane channels in development*, J Bioenerg Biomembr (1996), 28 (4), 379-385

116 Lo, C. W., Waldo, K. L. & Kirby, M. L., *Gap junction communication and the modulation of cardiac neural crest cells*, Trends Cardiovasc Med (1999), 9 (3-4), 63-69

117 Ludwig, E., Silberstein, F. C., van Empel, J., Erfle, V., Neumann, M. & Brack-Werner, R., *Diminished rev-mediated stimulation of human immunodeficiency virus type 1 protein synthesis is a hallmark of human astrocytes*, J Virol (1999), 73 (10), 8279-8289

118 Maass, K., Shibayama, J., Chase, S. E., Willecke, K. & Delmar, M., *C-terminal truncation of connexin43 changes number, size, and localization of cardiac gap junction plaques*, Circ Res (2007), 101 (12), 1283-1291

119 Majoul, I., Shirao, T., Sekino, Y. & Duden, R., *Many faces of drebrin: from building dendritic spines and stabilizing gap junctions to shaping neurite-like cell processes*, Histochem Cell Biol (2007), 127 (4), 355-361

120 Makowski, L., Caspar, D. L., Phillips, W. C. & Goodenough, D. A., *Gap junction structures. II. Analysis of the x-ray diffraction data*, J Cell Biol (1977), 74 (2), 629-645

121 Martinerie, C. & Perbal, B., *Expression of a gene encoding a novel potential IGF binding protein in human tissues*, C R Acad Sci III (1991), 313 (8), 345-351

122 Mattila, P. K. & Lappalainen, P., *Filopodia: molecular architecture and cellular functions*, Nat Rev Mol Cell Biol (2008), 9 (6), 446-454

123 McLeod, T. L., Bechberger, J. F. & Naus, C. C., *Determination of a potential role of the CCN family of growth regulators in connexin43 transfected C6 glioma cells*, Cell Commun Adhes (2001), 8 (4-6), 441-445

124 McNiven, M. A., Kim, L., Krueger, E. W., Orth, J. D., Cao, H. & Wong, T. W., *Regulated interactions between dynamin and the actin-binding protein cortactin modulate cell shape*, J Cell Biol (2000), 151 (1), 187-198

125 Mejillano, M. R., Kojima, S., Applewhite, D. A., Gertler, F. B., Svitkina, T. M. & Borisy, G. G., *Lamellipodial versus filopodial mode of the actin nanomachinery: pivotal role of the filament barbed end*, Cell (2004), 118 (3), 363-373

126 Moorby, C. & Patel, M., *Dual functions for connexins: Cx43 regulates growth independently of gap junction formation*, Exp Cell Res (2001), 271 (2), 238-248

127 Moorby, C. D., *A connexin 43 mutant lacking the carboxyl cytoplasmic domain inhibits both growth and motility of mouse 3T3 fibroblasts*, Mol Carcinog (2000), 28 (1), 23-30

128 Morley, G. E., Taffet, S. M. & Delmar, M., *Intramolecular interactions mediate pH regulation of connexin43 channels*, Biophys J (1996), 70 (3), 1294-1302

129 Musil, L. S., Beyer, E. C. & Goodenough, D. A., *Expression of the gap junction protein connexin43 in embryonic chick lens: molecular cloning, ultrastructural localization, and post-translational phosphorylation*, J Membr Biol (1990), 116 (2), 163-175

130 Musil, L. S., Cunningham, B. A., Edelman, G. M. & Goodenough, D. A., *Differential phosphorylation of the gap junction protein connexin43 in junctional communication-competent and -deficient cell lines*, J Cell Biol (1990), 111 (5 Pt 1), 2077-2088

131 Musil, L. S. & Goodenough, D. A., *Biochemical analysis of connexin43 intracellular transport, phosphorylation, and assembly into gap junctional plaques*, J Cell Biol (1991), 115 (5), 1357-1374

132 Musil, L. S. & Goodenough, D. A., *Multisubunit assembly of an integral plasma membrane channel protein, gap junction connexin43, occurs after exit from the ER*, Cell (1993), 74 (6), 1065-1077
133 Nagy, J. I. & Rash, J. E., *Connexins and gap junctions of astrocytes and oligodendrocytes in the CNS*, Brain Res Brain Res Rev (2000), 32 (1), 29-44
134 Naus, C. C., Bechberger, J. F., Caveney, S. & Wilson, J. X., *Expression of gap junction genes in astrocytes and C6 glioma cells*, Neurosci Lett (1991), 126 (1), 33-36
135 Neijssen, J., Pang, B. & Neefjes, J., *Gap junction-mediated intercellular communication in the immune system*, Prog Biophys Mol Biol (2007), 94 (1-2), 207-218
136 Niedergang, F. & Chavrier, P., *Signaling and membrane dynamics during phagocytosis: many roads lead to the phagos(R)ome*, Curr Opin Cell Biol (2004), 16 (4), 422-428
137 Oliveira, R. et al., *Contribution of gap junctional communication between tumor cells and astroglia to the invasion of the brain parenchyma by human glioblastomas*, BMC Cell Biol (2005), 6 (1), 7
138 Omori, Y. & Yamasaki, H., *Mutated connexin43 proteins inhibit rat glioma cell growth suppression mediated by wild-type connexin43 in a dominant-negative manner*, Int J Cancer (1998), 78 (4), 446-453
139 Oviedo-Orta, E. & Howard Evans, W., *Gap junctions and connexin-mediated communication in the immune system*, Biochim Biophys Acta (2004), 1662 (1-2), 102-112
140 Partridge, M. A. & Marcantonio, E. E., *Initiation of attachment and generation of mature focal adhesions by integrin-containing filopodia in cell spreading*, Mol Biol Cell (2006), 17 (10), 4237-4248
141 Paznekas, W. A. et al., *Connexin 43 (GJA1) mutations cause the pleiotropic phenotype of oculodentodigital dysplasia*, Am J Hum Genet (2003), 72 (2), 408-418
142 Pedraza, L., Fidler, L., Staugaitis, S. M. & Colman, D. R., *The active transport of myelin basic protein into the nucleus suggests a regulatory role in myelination*, Neuron (1997), 18 (4), 579-589
143 Peitsch, W. K. et al., *Drebrin is a widespread actin-associating protein enriched at junctional plaques, defining a specific microfilament anchorage system in polar epithelial cells*, Eur J Cell Biol (1999), 78 (11), 767-778
144 Peitsch, W. K. et al., *Drebrin, an actin-binding, cell-type characteristic protein: induction and localization in epithelial skin tumors and cultured keratinocytes*, J Invest Dermatol (2005), 125 (4), 761-774
145 Perbal, B., *Nuclear localisation of NOVH protein: a potential role for NOV in the regulation of gene expression*, Mol Pathol (1999), 52 (2), 84-91
146 Perbal, B., *NOV (nephroblastoma overexpressed) and the CCN family of genes: structural and functional issues*, Mol Pathol (2001), 54 (2), 57-79
147 Perbal, B., *The CCN3 (NOV) cell growth regulator: a new tool for molecular medicine*, Expert Rev Mol Diagn (2003), 3 (5), 597-604
148 Perbal, B., *CCN proteins: multifunctional signalling regulators*, Lancet (2004), 363 (9402), 62-64
149 Plenz, G. et al., *Upregulation of connexin43 gap junctions between neointimal smooth muscle cells*, Eur J Cell Biol (2004), 83 (10), 521-530
150 Pollard, T. D., Blanchoin, L. & Mullins, R. D., *Molecular mechanisms controlling actin filament dynamics in nonmuscle cells*, Annu Rev Biophys Biomol Struct (2000), 29 545-576
151 Pollard, T. D., Blanchoin, L. & Mullins, R. D., *Actin dynamics*, J Cell Sci (2001), 114 (Pt 1), 3-4

152 Puranam, K. L., Laird, D. W. & Revel, J. P., *Trapping an intermediate form of connexin43 in the Golgi*, Exp Cell Res (1993), 206 (1), 85-92
153 Qiu, C. et al., *Targeting connexin43 expression accelerates the rate of wound repair*, Curr Biol (2003), 13 (19), 1697-1703
154 Reaume, A. G. et al., *Cardiac malformation in neonatal mice lacking connexin43*, Science (1995), 267 (5205), 1831-1834
155 Rhee, D. Y., Zhao, X. Q., Francis, R. J., Huang, G. Y., Mably, J. D. & Lo, C. W., *Connexin 43 regulates epicardial cell polarity and migration in coronary vascular development*, Development (2009), 136 (18), 3185-3193
156 Richards, T. S., Dunn, C. A., Carter, W. G., Usui, M. L., Olerud, J. E. & Lampe, P. D., *Protein kinase C spatially and temporally regulates gap junctional communication during human wound repair via phosphorylation of connexin43 on serine368*, J Cell Biol (2004), 167 (3), 555-562
157 Ridley, A. J. et al., *Cell migration: integrating signals from front to back*, Science (2003), 302 (5651), 1704-1709
158 Roomi, M. W., Monterrey, J. C., Kalinovsky, T., Rath, M. & Niedzwiecki, A., *In vitro modulation of MMP-2 and MMP-9 in human cervical and ovarian cancer cell lines by cytokines, inducers and inhibitors*, Oncol Rep (2010), 23 (3), 605-614
159 Rose, B., Mehta, P. P. & Loewenstein, W. R., *Gap-junction protein gene suppresses tumorigenicity*, Carcinogenesis (1993), 14 (5), 1073-1075
160 Schirenbeck, A., Arasada, R., Bretschneider, T., Stradal, T. E., Schleicher, M. & Faix, J., *The bundling activity of vasodilator-stimulated phosphoprotein is required for filopodium formation*, Proc Natl Acad Sci U S A (2006), 103 (20), 7694-7699
161 Seki, K. & Komuro, T., *Immunocytochemical demonstration of the gap junction proteins connexin 43 and connexin 45 in the musculature of the rat small intestine*, Cell Tissue Res (2001), 306 (3), 417-422
162 Severs, N. J., *Pathophysiology of gap junctions in heart disease*, J Cardiovasc Electrophysiol (1994), 5 (5), 462-475
163 Shao, Q., Wang, H., McLachlan, E., Veitch, G. I. & Laird, D. W., *Down-regulation of Cx43 by retroviral delivery of small interfering RNA promotes an aggressive breast cancer cell phenotype*, Cancer Res (2005), 65 (7), 2705-2711
164 Sharma, G. D., He, J. & Bazan, H. E., *p38 and ERK1/2 coordinate cellular migration and proliferation in epithelial wound healing: evidence of cross-talk activation between MAP kinase cascades*, J Biol Chem (2003), 278 (24), 21989-21997
165 Sin, W. C., Tse, M., Planque, N., Perbal, B., Lampe, P. D. & Naus, C. C., *Matricellular protein CCN3 (NOV) regulates actin cytoskeleton reorganization*, J Biol Chem (2009), 284 (43), 29935-29944
166 Sohl, G. & Willecke, K., *An update on connexin genes and their nomenclature in mouse and man*, Cell Commun Adhes (2003), 10 (4-6), 173-180
167 Solan, J. L. & Lampe, P. D., *Connexin phosphorylation as a regulatory event linked to gap junction channel assembly*, Biochim Biophys Acta (2005), 1711 (2), 154-163
168 Solan, J. L. & Lampe, P. D., *Connexin43 phosphorylation: structural changes and biological effects*, Biochem J (2009), 419 (2), 261-272
169 Solan, J. L., Marquez-Rosado, L., Sorgen, P. L., Thornton, P. J., Gafken, P. R. & Lampe, P. D., *Phosphorylation at S365 is a gatekeeper event that changes the structure of Cx43 and prevents down-regulation by PKC*, J Cell Biol (2007), 179 (6), 1301-1309
170 Sorgen, P. L. et al., *Sequence-specific resonance assignment of the carboxyl terminal domain of Connexin43*, J Biomol NMR (2002), 23 (3), 245-246
171 Sorgen, P. L., Duffy, H. S., Spray, D. C. & Delmar, M., *pH-dependent dimerization of the carboxyl terminal domain of Cx43*, Biophys J (2004), 87 (1), 574-581

172 Spray, D. C. & Bennett, M. V., *Physiology and pharmacology of gap junctions*, Annu Rev Physiol (1985), 47 281-303
173 Spray, D. C., White, R. L., Mazet, F. & Bennett, M. V., *Regulation of gap junctional conductance*, Am J Physiol (1985), 248 (6 Pt 2), H753-764
174 Squecco, R. et al., *Sphingosine 1-phosphate induces myoblast differentiation through Cx43 protein expression: a role for a gap junction-dependent and -independent function*, Mol Biol Cell (2006), 17 (11), 4896-4910
175 Stauber, R. H. et al., *Development and applications of enhanced green fluorescent protein mutants*, Biotechniques (1998), 24 (3), 462-466, 468-471
176 Steffen, A. et al., *Filopodia formation in the absence of functional WAVE- and Arp2/3-complexes*, Mol Biol Cell (2006), 17 (6), 2581-2591
177 Svitkina, T. M. et al., *Mechanism of filopodia initiation by reorganization of a dendritic network*, J Cell Biol (2003), 160 (3), 409-421
178 Tang, M. X., Redemann, C. T. & Szoka, F. C., Jr., *In vitro gene delivery by degraded polyamidoamine dendrimers*, Bioconjug Chem (1996), 7 (6), 703-714
179 Traub, O., Look, J., Dermietzel, R., Brummer, F., Hulser, D. & Willecke, K., *Comparative characterization of the 21-kD and 26-kD gap junction proteins in murine liver and cultured hepatocytes*, J Cell Biol (1989), 108 (3), 1039-1051
180 Trovato-Salinaro, A. et al., *Regulation of connexin gene expression during skeletal muscle regeneration in the adult rat*, Am J Physiol Cell Physiol (2009), 296 (3), C593-606
181 Unwin, P. N. & Zampighi, G., *Structure of the junction between communicating cells*, Nature (1980), 283 (5747), 545-549
182 Valiunas, V., Beyer, E. C. & Brink, P. R., *Cardiac gap junction channels show quantitative differences in selectivity*, Circ Res (2002), 91 (2), 104-111
183 Valiunas, V. et al., *Connexin-specific cell-to-cell transfer of short interfering RNA by gap junctions*, J Physiol (2005), 568 (Pt 2), 459-468
184 van der Heyden, M. A., Roeleveld, L., Peterson, J. & Destree, O. H., *Connexin43 expression during Xenopus development*, Mech Dev (2001), 108 (1-2), 217-220
185 van der Heyden, M. A., van Eijk, M., Wilders, R., de Bakker, J. M. & Opthof, T., *Connexin43 orthologues in vertebrates: phylogeny from fish to man*, Dev Genes Evol (2004), 214 (5), 261-266
186 Vignjevic, D. et al., *Fascin, a novel target of beta-catenin-TCF signaling, is expressed at the invasive front of human colon cancer*, Cancer Res (2007), 67 (14), 6844-6853
187 Vitale, M. L., Akpovi, C. D. & Pelletier, R. M., *Cortactin/tyrosine-phosphorylated cortactin interaction with connexin 43 in mouse seminiferous tubules*, Microsc Res Tech (2009), 72 (11), 856-867
188 Vonna, L., Wiedemann, A., Aepfelbacher, M. & Sackmann, E., *Micromechanics of filopodia mediated capture of pathogens by macrophages*, Eur Biophys J (2007), 36 (2), 145-151
189 Walker, D. L., Vacha, S. J., Kirby, M. L. & Lo, C. W., *Connexin43 deficiency causes dysregulation of coronary vasculogenesis*, Dev Biol (2005), 284 (2), 479-498
190 Wang, H. G., Rapp, U. R. & Reed, J. C., *Bcl-2 targets the protein kinase Raf-1 to mitochondria*, Cell (1996), 87 (4), 629-638
191 Wang, Y. F. & Daniel, E. E., *Gap junctions in gastrointestinal muscle contain multiple connexins*, Am J Physiol Gastrointest Liver Physiol (2001), 281 (2), G533-543
192 Weaver, A. M., Heuser, J. E., Karginov, A. V., Lee, W. L., Parsons, J. T. & Cooper, J. A., *Interaction of cortactin and N-WASp with Arp2/3 complex*, Curr Biol (2002), 12 (15), 1270-1278

193 Weaver, A. M. et al., *Cortactin promotes and stabilizes Arp2/3-induced actin filament network formation*, Curr Biol (2001), 11 (5), 370-374
194 Weed, S. A. et al., *Cortactin localization to sites of actin assembly in lamellipodia requires interactions with F-actin and the Arp2/3 complex*, J Cell Biol (2000), 151 (1), 29-40
195 Wei, C. J., Francis, R., Xu, X. & Lo, C. W., *Connexin43 associated with an N-cadherin-containing multiprotein complex is required for gap junction formation in NIH3T3 cells*, J Biol Chem (2005), 280 (20), 19925-19936
196 Welch, M. D. & Mullins, R. D., *Cellular control of actin nucleation*, Annu Rev Cell Dev Biol (2002), 18 247-288
197 White, T. W. & Paul, D. L., *Genetic diseases and gene knockouts reveal diverse connexin functions*, Annu Rev Physiol (1999), 61 283-310
198 White, T. W., Paul, D. L., Goodenough, D. A. & Bruzzone, R., *Functional analysis of selective interactions among rodent connexins*, Mol Biol Cell (1995), 6 (4), 459-470
199 Willecke, K. et al., *Structural and functional diversity of connexin genes in the mouse and human genome*, Biol Chem (2002), 383 (5), 725-737
200 Willecke, K., Hennemann, H., Dahl, E., Jungbluth, S. & Heynkes, R., *The diversity of connexin genes encoding gap junctional proteins*, Eur J Cell Biol (1991), 56 (1), 1-7
201 Wu, H. & Montone, K. T., *Cortactin localization in actin-containing adult and fetal tissues*, J Histochem Cytochem (1998), 46 (10), 1189-1191
202 Wu, H. & Parsons, J. T., *Cortactin, an 80/85-kilodalton pp60src substrate, is a filamentous actin-binding protein enriched in the cell cortex*, J Cell Biol (1993), 120 (6), 1417-1426
203 Wu, H., Reynolds, A. B., Kanner, S. B., Vines, R. R. & Parsons, J. T., *Identification and characterization of a novel cytoskeleton-associated pp60src substrate*, Mol Cell Biol (1991), 11 (10), 5113-5124
204 Xu, X., Francis, R., Wei, C. J., Linask, K. L. & Lo, C. W., *Connexin 43-mediated modulation of polarized cell movement and the directional migration of cardiac neural crest cells*, Development (2006), 133 (18), 3629-3639
205 Xu, X. et al., *Modulation of mouse neural crest cell motility by N-cadherin and connexin 43 gap junctions*, J Cell Biol (2001), 154 (1), 217-230
206 Xu, X. et al., *N-cadherin and Cx43alpha1 gap junctions modulates mouse neural crest cell motility via distinct pathways*, Cell Commun Adhes (2001), 8 (4-6), 321-324
207 Ya, J. et al., *Heart defects in connexin43-deficient mice*, Circ Res (1998), 82 (3), 360-366
208 Yeager, M., Unger, V. M. & Falk, M. M., *Synthesis, assembly and structure of gap junction intercellular channels*, Curr Opin Struct Biol (1998), 8 (4), 517-524
209 Zengel, P. et al., *Multimodal therapy for synergic inhibition of tumour cell invasion and tumour-induced angiogenesis*, BMC Cancer (2010), 10 92
210 Zhu, D., Caveney, S., Kidder, G. M. & Naus, C. C., *Transfection of C6 glioma cells with connexin 43 cDNA: analysis of expression, intercellular coupling, and cell proliferation*, Proc Natl Acad Sci U S A (1991), 88 (5), 1883-1887

VII Appendix

1 Abbreviations

A	Alanine
aa	Amino acid
Abi1	Abl interactor 1
ADF	Actin depolimerization factor
AF	Alexa-Fluor
Ala	Alanine
AM	Acetoxymethylester
Amp	Ampicillin
APS	Ammoniumpersulfate
Aqua dem.	Aqua demineralisata
Arp	Actin-related protein
Asn	Asparagine
Asp	Asparagine acid
ATP	Adenosine triphosphate
bp	Base pair
BSA	Bovine serum albumine
C	Celsius
Ca^{2+}	Calcium ions
cAMP	Cyclic AMP (Adenosinmonophosphate)
cDNA	Complementary Deoxyribonucleic acid
CK1	Casein kinase 1
Cx43	Connexin 43 full length protein (aa 1 – 382)
Cx43(298)-GFP	Connexin 43 truncated protein (aa 1 – 298), GFP-tagged
Cx43(336)-GFP	Connexin 43 truncated protein (aa 1 – 336), GFP-tagged
Cx43(299-336)-GFP	Connexin 43 truncated protein (aa 299 – 336), GFP-tagged
Cx43CT-GFP	Connexin 43 C-terminal part (aa 257 – 382), GFP-tagged
Cx43-GFP	Connexin 43 full length protein (aa 1 – 382), GFP-tagged
Cx43-NP	Connexin 43 non-phosphorylated
Cx43NT-GFP	Connexin 43 N-terminal part (aa 1 – 257), GFP-tagged
Cx43-P1	Connexin 43 phosphorylated once
Cx43-P2	Connexin 43 phosphorylated twice

DMEM	Dulbecco's modified Eagle medium
DMSO	Dimethylsulfoxide
DNA	Deoxyribonucleic acid
dNTPs	Deoxynucleoside triphosphates
dsDNA	Double-stranded DNA
ECL	Enhanced chemiluminescence
ECM	Extracellular matrix
EDTA	Ethylenediaminetetraacetic acid
e.g.	For example
EGF	Endothelial growth factor
ELISA	Enzyme-linked sorbent assay
Ena/VASP	Enabled/vasodilator-stimulated phosphoprotein
ER	Endoplasmic reticulum
FACS	Fluorescent activated cell sorting
FCS	Fetal calf serum
FGF	Fibroblast growth factor
FRET	Fluorescence resonance energy transfer
GAPDH	Glyceraldehyde-3-phosphate dehydrogenase
GFP	Green fluorescent protein
Gln	Glutamine
Gly	Glycine
GJC	Gap junctional communication
GST	Glutathione S-transferase
GTP	Guanosine triphosphate
h	Hour
HeLa	Henrietta Lacks
HGF	Hepatocyte growth factor
His	Histidine
HRP	Horseradish peroxidase
HUVEC	Human umbilical vein endothelial cells
IL-1β	Interleukin-1β
IP_3	Inosintriphosphat
IRSp53	Insulin-receptor substrate p53
K^+	Potassium ions

kDa	Kilodalton
LB	Lysogeny broth
LSM	Laser scanning microscopy
Lys	Lysine
mA	Milliampere
MAPK	Mitogen-activated protein kinase
MAV-1	Myeloblastosis-associated virus type 1
mDia2	Mammalian Diaphanous-related formin 2
Min	Minute
MMP	Matrix metalloproteinase
MT1-MMP	Membrane type-1 matrix metalloproteinase
Na^+	Sodium ions
Nap1	Nck-associated protein 1
NBCS	Newborn calf serum
NM	Nanometer
NOV	Nephroblastoma overexpressed
NPF	Nucleation-promoting factor
NTA	N-terminal acidic
N-WASP	Neuronal Wiscott Aldrich syndrome protein
P	Proline
PAGE	Polyacrylamide gel electrophoresis
PAK	p21 activated kinases
PBS	Phosphate buffered saline
PCR	Polymerase chain reaction
PDGF	Platelet derived growth factor
P_i	Inorganic phosphate
PKC1	Protein kinase C 1
PMA	Phorbol 12-myristate 13-acetate
PMT	Photomultiplier tube
pS	Picosiemens (dimesion unit of the electrical conductance)
PVDF	Polyvinylidenefluoride
r	Rat
RNA	Ribonucleic acid
rpm	Rounds per minute

sec	Second
S	Serine
Scar	Suppressor of cAMP receptor
SDS	Sodium dodecylsulfate
Ser	Serine
SH2	Src homology domain 2
SH3	Src homology domain 3
siRNA	Small interfering RNA
TBE	Tris borate EDTA
TEMED	N,N,N´,N´-tetramethylethylenediamine
TGF-β	Transforming growth factor β
Thr	Threonine
TNF-α	Tumor necrosis factor α
TPA	12-O-tetradeconylphorbol-13-acetate
U	Units
V	Volts
VEGF	Vascular endothelial growth factor
WASP	Wiscott Aldrich syndrome protein
WAVE	WASP family Verprolin-homologous protein
WB	Western blot
WIP	WASP-interacting protein
wt	Wild-type
Y	Tyrosine
ZO-1	Zonula occludens-1
µ	Micro

2 Curriculum vitae

Personal data

Name:	Juliane Viktoria Behrens
Nationality:	German
Date of Birth:	December 22nd, 1978 in Wesel

Publications

Original publications

1. Behrens J., Kameritsch P., Wallner S., Pohl U., Pogoda K., *The carboxyl tail of Cx43 augments p38 mediated cell migration in a gap junction-independent manner*, Eur J Cell Biol (2010) Nov, 89(11), 828-838

2. Berge U., Behrens J., Rattan S.I., *Sugar-induced premature aging and altered differentiation in human epidermal keratinocytes*, Ann NY Acad Sci (2007) Apr, 1100, 524-529

Poster presentations

1. Juliane Behrens, Ulrich Pohl and Kristin Pogoda
   Walter-Brendel-Centre of Experimental Medicine, Munich, Germany
   The C-terminal part of connexin 43 enhances filopodia formation and cell migration in HeLa cells
   International Meeting of the German Society for Cell Biology (DGZ) on Actin Dynamics September 15th to 18th, 2010, Jena, Germany

2. Juliane Behrens, Ulrich Pohl and Kristin Pogoda
   Walter-Brendel-Centre of Experimental Medicine, Munich, Germany
   Connexin 43 enhances migration of HeLa cells in a gap junction independent manner
   FEPS Congress (Physiology meeting organized by The Slovenian Physiological Society, The Austrian Physiological Society, and The Federation of European Physiological Societies), November 12th to 15th, 2009, Ljubljana, Slovenia

3. Juliane Behrens, Ulrich Pohl and Kristin Pogoda
   Walter-Brendel-Centre of Experimental Medicine, Munich, Germany
   The C-terminal part of Cx43 enhances migration of HeLa cells
   Joint Meeting of the GfMVB (Gesellschaft für Mikrozirkulation und Vaskuläre Biologie) and the Swiss Society for Microcirculation (SSM), October 8th to 10th, 2009, Bern, Switzerland

4. Juliane Behrens, Ulrich Pohl and Kristin Pogoda
   Walter-Brendel-Centre of Experimental Medicine, Munich, Germany
   Expression of Cx43 C-terminal part enhances migration of HeLa cells
   DPG Congress, March 22th to 25th, 2009, Giessen, Germany

3 Acknowledgements

I would like to express my thanks to Prof. Dr. Ulrich Pohl for giving me the opportunity doing the present doctoral thesis at his laboratories in the Walter-Brendel-Centre of Experimental Medicine (WBex) in Munich and for his great scientific support during this time.

Moreover, I thank Prof. Dr. Zahler for supervising me as an external Ph.D. student of the institute for chemistry and pharmacy and thus enabling the doctorate of natural science.

Sincere thanks go to Dr. Kristin Pogoda for her support during the time of my thesis, for sharing scientific and experimental knowledge and for critically reading my manuscript.

Thanks to Kasia Stefanowski and Dorothee Gössel for helping me in the lab and technical assistance, Silvia Münzing for printing posters and Ulrike Wilhelm-Forster for cloning of the constructs Cx43NT-GFP, Cx43CT-GFP and Cx43-GFP.

Moreover, I would like to thank my colleagues Juliane Hellfritsch, Dr. Theres Hennig, Stefan Wallner, Angela Ritter, Julian Kirsch and Fabian Kellner for pleasant talks during lunch and for having fun together at special events in the evening, such as having a drink after work or visiting the “Oktoberfest”.

Thanks to my friends in Munich and at home in NRW for relaxing talks after work and coffees and trips on weekends.

Finally, I thank my parents very much for giving me the opportunity to study and their encouragement for doing this thesis and I thank them and also my sister and brother for always supporting and helping me in every way.